SMC Bulletin

A Publication of the Society for Materials Chemistry

Volume 5 No. 3 December 2014

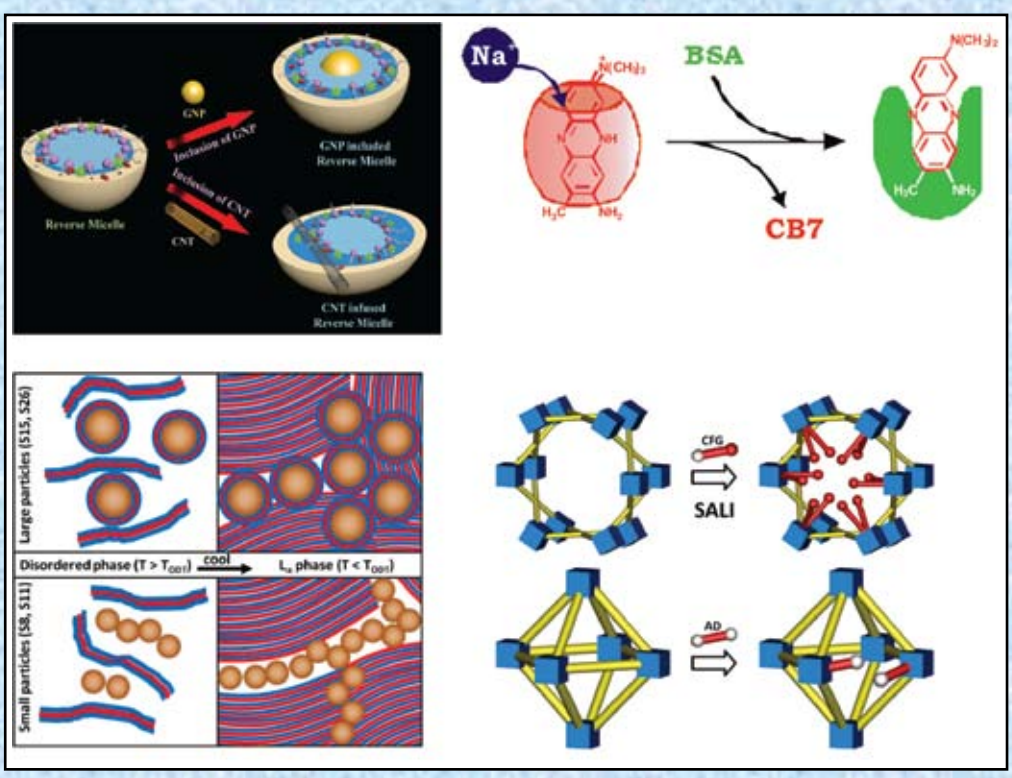

SOCIETY FOR MATERIALS CHEMISTRY

Society for Materials Chemistry

Society for Materials Chemistry was mooted in 2007 with following aims and objectives:

(a) to help the advancement, dissemination and application of the knowledge in the field of materials chemistry,

(b) to promote active interaction among all material scientists, bodies, institutions and industries interested in achieving the advancement, dissemination and application of the knowledge of materials chemistry,

(c) to disseminate information in the field of materials chemistry by publication of bulletins, reports, newsletters, journals.

(d) to provide a common platform to young researchers and active scientists by arranging seminars, lectures, workshops, conferences on current research topics in the area of materials chemistry,

(e) to provide financial and other assistance to needy deserving researchers for participation to present their work in symposia, conference, etc.

(f) to provide an incentive by way of cash awards to researchers for best thesis, best paper published in journal/national/international conferences for the advancement of materials chemistry,

(g) to undertake and execute all other acts as mentioned in the constitution of SMC.

Executive Committee

Contact address
Society for Materials Chemistry
C/o Chemistry Division
Bhabha Atomic Research Centre, Trombay, Mumbai, 400 085, India
Tel: +91-22-25592001, E-mail: socmatchem@gmail.com

SMC Bulletin

A Publication of the Society for Materials Chemistry

Volume 5 **No. 3** **December 2014**

SOCIETY FOR MATERIALS CHEMISTRY

SMC Bulletin

Vol. 5 **No. 3** **December 2014**

Guest Editors

Dr. Sandip Dey
Chemistry Division
Bhabha Atomic Research Centre,
Trombay, Mumbai 400085
e-mail: dsandip@barc.gov.in

Dr. P. A. Hassan
Chemistry Division
Bhabha Atomic Research Centre,
Trombay, Mumbai 400085
e-mail: hassan@barc.gov.in

Editorial Board

Published by
Society for Materials Chemistry
C/o. Chemistry Division
Bhabha Atomic Research Centre, Trombay, Mumbai, 400 085
E-mail: socmatchem@gmail.com,
Tel: +91-22-25592001

Guest Editorial

Dr. Sandip Dey

Dr. P. A. Hassan

It is with great pleasure we present this thematic issue on "Supramolecular Materials" to the readers of SMC Bulletin. Supramolecular Chemistry makes use of weak non-covalent interactions between small molecules to create well organised hierarchical architectures. The new macroscopic entities formed by the programmed assembly of these building blocks offer unique physico-chemical properties, otherwise not found in the individual molecules. The interplay of various non-covalent forces offers attractive strategies for the design of new materials with tailed properties. This has stimulated extensive research in this area, during the last decade, with a view to tailor material properties.

In this issue, we bring together a few selected contributions from experts in this field to share our readers some of the exciting developments in the chemistry of supramolecular materials. The roles of complementary interactions in the design of new molecular solids with desired properties are discussed in the article on crystal engineering. Synthesis and applications of functionalised metal organic frameworks, host guest assemblies of cavity shaped molecules that possess fascinating applications in sensing, drug delivery and photofunctional devices, surfactant mediated organization of large colloidal particles into macroscopic, porous assemblies etc are some of the emerging new areas in supramolecular science. Theoretical modelling of supramolecular association using atomistic molecular dynamics and dissipative particle dynamics were also discussed. Application of suprmolecular hydrogels in biocatalysis, biomedicine and as nanostructured electrolyte matrix for dye sensitised solar cells etc opens new vistas in materials synthesis.

We would like to put on record our sincere appreciation to all authors for their excellent work, and thank them for sparing their valuable time to provide well structured articles for consideration in this special issue. We hope that readers will enjoy this issue and find it highly useful and stimulating with new ideas for future research on molecular recognition and supramolecular chemistry.

(Sandip Dey and P. A. Hassan)

From the desks of the President and Secretary

Dr.Sisir K Sarkar
President

Dr. P. A. Hassan
Secretary

From the desks of the President and Secretary

Dear Fellow members and Readers,

Greetings from the Executive Council of SMC.

It gives us immense pleasure to thank all our members for successfully holding the 5th DAE-BRNS Interdisciplinary Symposium on Materials Chemistry (ISMC-2014), the most important activity of the society during December 9-13, 2014. Now we are back in our tradition on publication of thematic bulletin and the present issue is based on "Supramolecular Materials".

Supramolecular chemistry is the domain of chemistry beyond that of molecules and focuses on the chemical systems made up of a discrete number of assembled molecular subunits or components. While traditional chemistry focuses on the covalent bond, supramolecular chemistry examines the weaker and reversible noncovalent interactions between molecules.

The importance of supramolecular chemistry was established by the 1987 Nobel Prize for Chemistry, which was awarded to Donald J. Cram, Jean-Marie Lehn, and Charles J. Pedersen. The past decade has seen dramatic developments with supramolecular chemistry leaving its roots in classical host guest chemistry and expanding into exciting areas of materials chemistry and nanoscience with many real and potential applications. The study of non-covalent interactions is crucial to understanding many biological systems which are becoming the latest motivation for research in this field. Now it is witnessing a spectacular growth at the triple meeting point of chemistry with biology and physics.

It is simply not possible to capture all the advances and aspects of the scientific challenges in a single issue, but we believe the present issue comes very timely and it opens perspectives to the creative imagination of all participants in our common adventure. We would like to very warmly congratulate and thank the two guest editors and the six contributors alike for this precious gift to the science of chemistry.

As you may be aware UNESCO has adopted a resolution declaring 2015 to be the International Year of Light (IYL 2015). The importance of raising global awareness about how light-based technologies can promote sustainable development and provide solutions to global challenges in energy, education, agriculture, health care and security. We are planning to organize a workshop (NWMC-2015) on Optical Materials in our workshop series this year to celebrate IYL-2015. We also request our members to send their valued proposals for this celebration.

At the end we wish to express our gratitude to each and every member for their unstinted support and cooperation in the rapid growth of the society as we currently achieved the magnificent thousand membership mark.

Dr. Sisir K Sarkar
President

Dr. P.A.Hassan
Secretary

CONTENTS

Supramolecular Interactions in Crystal Engineering

Goutam Kumar Kole
Chemistry Division, Bhabha Atomic Research Centre, Mumbai – 400085, India
Email: goutamk@barc.gov.in; Tel: +91 22 2559 2943; Fax: +91 022 2550 5151.

Crystal Engineering

The phrase '*crystal engineering*' was first coined by Pepinsky in 1955 and it began its journey as a subject in the late 1960s from the research work by Schmidt in the context of their fundamental research to understand the solid state packing patterns of various organic compounds and their photoreactivity in the solid state.[1] The definition of *crystal engineering* was later provided by Desiraju in 1989 as "*the understanding of intermolecular interactions in the context of crystal packing and in the utilisation of such understanding in the design of new solids with desired physical and chemical properties*".[2] The subject deals with the ideas and techniques from supramolecular chemistry, X-ray crystallography, materials science and solid state chemistry. Crystal engineering talks about the assembly of molecules rather than the molecule itself. A crystal is a periodic assembly of molecules held together by weak interamolecular interactions, alternatively known as supramolecular interactions. Crystal engineering teaches us how to anchor the molecules, utilizing the weak supramolecular interaction, in an assembly exactly the way we want.

Supramolecular Interaction

The periodic arrangement of the molecules in a crystal is held by intermolecular or non-covalent interactions. Various types of supramolecular interactions that we encounter in a crystal are hydrogen bonding of various types, π···π stacking, halogen bonding, van der Waal interactions etc. The metallophilic interactions (aurophilic, Au···Au and aregentophilic, Ag···Ag) often play important role in molecular arrangement in inorganic complexes. In most of the cases, these interactions are anisotropic, i.e. they occur along a particular direction. The energies involved in such interactions lie in the range of 0.6 - 20 Kcal/mol. Although weak in nature, the resultant effect of a large number of these interactions can play a decisive role in crystal packing. This is often referred to the *Gulliver effect*.[3] It can be understood from a common observation at our houses that a lizard can hang on any vertical surface and even from a ceiling. There are thousands of toe hairs present at the foot-pad of lizard. The molecules of the toe hairs make van der Waal interaction with the molecules of the surface. Although, each single interaction is weak, it becomes strong enough collectively and is able to suspend itself without any difficulty.

Hydrogen Bonding as a Supramolecular Interaction

Among all the directional supramolecular interactions, hydrogen bonding is the most important one. This weak bonding is responsible for many abnormalities known in chemistry including anomalous behaviour of water. When a hydrogen atom is covalently bonded to a strongly electronegative element (X) the bond becomes dipolar and the fractional positive charge enables it to drag electron density from a negatively polarized atom (A) forming a weak bond known as hydrogen bond.[3] The strength of hydrogen bonding depends on electronegativity of the X element in X-H···A. The group X-H is called proton donor or electron acceptor and A is called proton acceptor or electron donor. The X-H bonds with reverse polarity (such as in metal hydrides) can also form such directional interaction. Although, each hydrogen atom can form only one covalent bond, it is capable of forming multiple hydrogen bonds with multiple electronegative elements. In a simple hydrogen bond, the donor interacts with one acceptor and termed as two-centred hydrogen bond. When the donor interacts with two and/ three acceptors, the bondings are called as 'bifurcated' and trifurcated' respectively as described in Figure 1.[4] The geometry of hydrogen bonding is very important in constructing

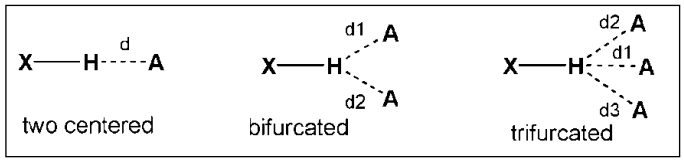

Figure 1: Types of hydrogen bonding.

functional molecular solids. It often forms infinite chains or arrays which are represented by graph set notation.

Graph Set Notation

A set of molecules that are hydrogen bonded to one another by repetition of different types of hydrogen

bonding patterns in the structure of interest, is known as a motif. The Motifs that are involved in intermolecular hydrogen bonding are generally characterized by one of four designators which indicate whether the motif is finite or infinite and cyclic or not. The designator **C** stands for a chain, **R** stands for a ring, **D** stands for dimer or other finite set and **S** stands for an intramolecular hydrogen bond. The number of the hydrogen bond donor and acceptors are represented as subscript and superscript respectively. The number specified in parentheses indicates the size or degree of the motif (the number of atoms in the repeating unit).[5] The examples of graph set notation of some common hydrogen bonded motifs are illustrated in Figure 2.

Supramolecular Synthons

Desiraju developed the concept of 'supramolecular synthon' in crystal engineering by adopting the concept 'synthon' by Corey in molecular synthesis. To synthesize a specific supramolecular entity with desired properties, the self assemblies of molecular fragments and their geometrical pattern are very crucial. The directional supramolecular interactions can be utilized to achieve the designed arrangement of functional groups in the molecular skeleton which is called supramolecular synthons. Therefore 'supramolecular synthons' was defined as "*...structural units within molecules which can be formed and or assembled by known or conceivable synthetic operations involving intermolecular interactions*". Supramolecular synthons play the same role in supramolecular synthesis as synthons do in molecular synthesis.[6] Therefore the concept of supramolecular synthon (Figure 3) is very helpful for the designed synthesis of various types of molecular solids with desired properties.

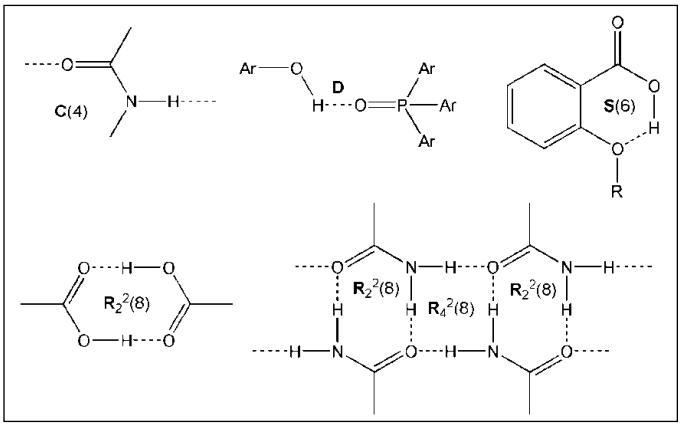

Figure 2: Examples of graph set notation for hydrogen bonding

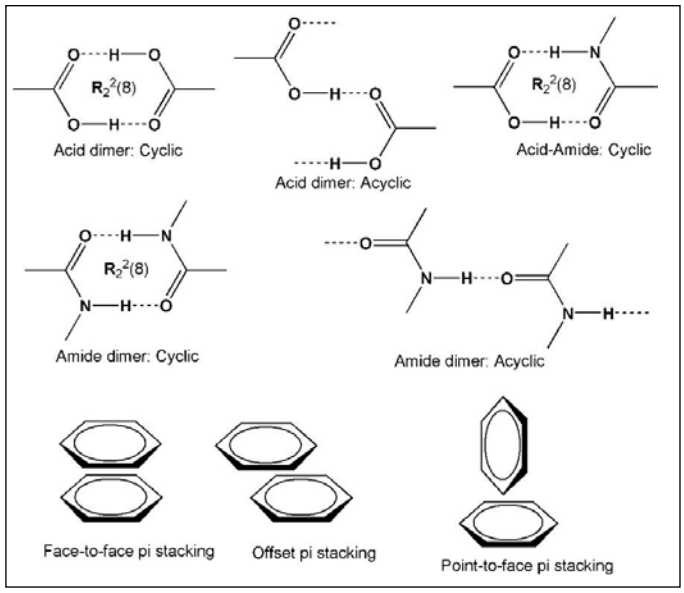

Figure 3: Example of various types of supramolecular synthons

Co-crystal and Molecular Salts

The designed synthesis of a co-crystal or molecular salt or a particular polymorph with desired physical and chemical properties is the ultimate goal of a crystal engineer. A multi-component crystal in which the components that are solid at ambient condition coexist in definite stiochiometric amounts through supramolecular interactions is known as co-crystal.[7] When different molecules with complementary functional groups construct hydrogen bonding that are energetically more favourable than those between like molecules of each component, then the formation of a co-crystal is favoured. Supramolecular synthons like carboxylic acid-pyridine, carboxylic acid-amide, and alcohol-pyridine generally

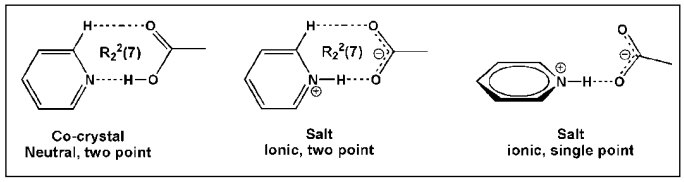

Figure 4: Position of hydrogen in co-crystal and salt of pyridine-acid system

favour the formation of co-crystals. Depending upon the acidity or basicity (pKa values) of the reacting molecules in the co-crystal, proton transfer often takes place that results in the formation of a molecular salt. Generally, it is observed that a reaction between a acid and a base is expected to form a salt when ΔpKa value [pKa(base) - pKa(acid)] is greater than 3, though there are many exceptions to this

assumption.[7] The co-crystals or molecular salts have wide range of applications in pharmaceutical science.

Pharmaceutical Co-crystal

Pharmaceutical co-crystals consist of the drug (the active pharmaceutical ingredient, API) and an auxiliary compound known as co-former. The co-formers are chosen by identifying the complementary hydrogen bonding sites in the API and the co-former. Upon co-crystallization, the co-former often enhances the physicochemical properties like dissolution properties, suspension stability, pharmacokinetics, etc, as per the need of the drug in our body. For example, co-crystal of caffeine with oxalic acid provides better stability of caffeine towards humidity that can be stored for several weeks. In case of paracetamol, the form-I crumbles upon compaction (tableting). Co-crystallization of paracetamol with oxalic acid and theophylline provide better mechanical property that helps in easy compaction. Mechanical properties of molecular crystals depend on the supramolecular interaction and crystal packing.[8]

Polymorphism

Polymorphism is the phenomenon where a solid chemical substance exists in many different crystalline forms, which have different physical and sometimes different chemical properties. When an element occurs in many different forms, the phenomenon is called allotropy (e.g. graphite and diamond). The concept of polymorphism is similar to allotropy. The difference between these terms is that the allotropy is used only for elements, whereas the polymorphism is used for compounds. Polymorphism occurs as the result of alternative possibility of crystal packing during crystallization of a compound. When polymorphism occurs for the existence of two different conformers of the same molecule is known as conformational polymorphism. Pseudopolymorphism or solvomorphism is the phenomenon where difference in crystal packing appears from the presence of solvent molecule in the lattice. Since polymorphs are different crystalline forms, polymorphism is entirely a solid state phenomenon. The polymorphs of a compound are generally called as α, β, γ... or, A, B, C... or I, II, III... depending on the order of their discovery.[3]

Millions of molecules aggregate to form a crystal. If there are energetically viable alternate pathways, molecules may choose any of these pathways during crystallization which leads to the formation of different polymorphs. The formation of polymorphs is difficult to control as the process involves kinetically competitive nucleation and crystal growth processes. The aggregate present in higher concentration will form the nucleus that grows further to give a particular polymorph. Sometimes, a metastable polymorph can transform into another stable form depending on the difference of their free energies and condition. However, many lesser stable kinetic polymorphs do not transform into thermodynamic forms or the transformation is extremely slow. For example, diamond never transforms into graphite.

Factors that favour the formation of a particular polymorph are many including lattice energies, conformations, hydrogen bonding, packing arrangements, temperature, pressure, solvents, etc. Among all these, the principal factor is the intermolecular interactions, i.e.

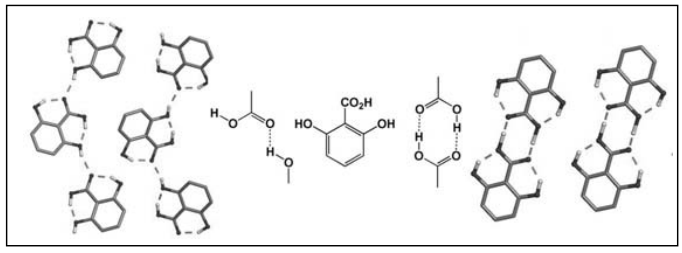

Figure 5: The different patterns of supramolecular interactions in two polymorphs of 2,6-dihydroxybenzoic acid.

supramolecular synthons. For example, let us consider two polymorphic forms of 2,6-dihydroxybenzoic acid. In form-I, the carboxyl hydrogen atom is intramolecularly hydrogen bonded to an oxygen atom of neighboring OH group, whose H atom is intermolecularly hydrogen bonded to the carbonyl oxygen atom of another carboxylic acid group. On the other hand, the hydrogen bonding pattern in the other polymorphic form (II) is different. The carboxylic acid groups form the conventional dimer arrangement and both the ortho-substituted OH groups form intramolecular

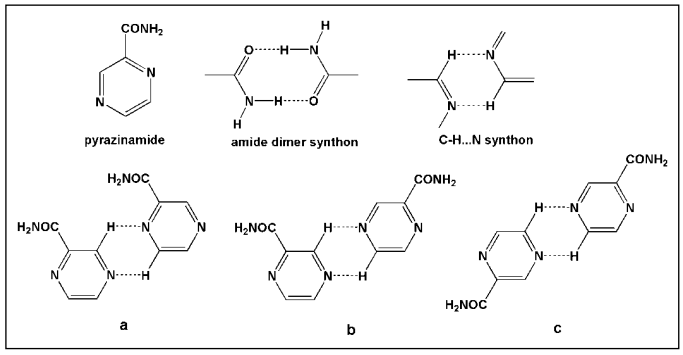

Figure 6: Observed patterns of interaction in three polymorphs of pyrazinamide.

hydrogen bonds with two oxygen atoms of the carboxylic acid group (Figure 5).[3]

The hydrogen bonding patterns found in the polymorphic forms of pyrazinamide (a well known anti-tuberculosis drug) are very interesting. The major hydrogen bonding pattern in all the polymorphs is the conventional amide dimer. The minor pattern is the C-H···N dimer formed between the heterocyclic N-atoms and aromatic C-H groups, also found in all the polymorphs. The difference in crystal packing arises in choosing the C-H bond among three distinct C-H bonds present in different location in the molecule (a, b, c in Figure 6). There are three possibilities and each of them occurs separately in the polymorphs of pyrazinamide.[3]

Properties of Polymorphs

Although, the chemical composition of the polymorphs is unique, different physical and chemical properties are observed depending on the difference in their crystal packing. The distinct properties that we generally observe for various polymorphs are colour, mechanical properties, chemical reactivity and reactivity of drugs in biological system. The compound 2-(4-anisyl)-1,4-benzoquinone is known to exhibit two polymorphic forms having red and yellow colours. The anisyl ring acts as a donor whereas the quinoid ring functions as the acceptor. In the yellow form, the molecules stack in DDD.. AAA.. fashion whereas in the red form the molecules stack in DADADA... fashion. Similarly, 5-methyl-2-[(2-nitrophenyl)amino]-3-thiophenecarbonitrile or ROY has several polymorphs having distinct colours including red, orange, yellow, orange-red, etc.[3]

Crystals of several organic compounds including 1,3,5-trichlorobenzene, 3,4-dichlorophenol, 2-(methylthio) nicotinic acid, pyrazinamide, etc are known to be bent under mechanical force. Bending in organic crystals occurs when the packing is anisotropic, i.e. the strong and weak interaction patterns occur in nearly perpendicular direction. This bending is different from bending of plasticine, clay or even slab of metal. Pyrazinamide exists in four polymorphic forms and only the α-form can be bent. The bending face is (100) which is the thickest face. The thin face is not the bending face, in this case. The strong hydrogen bonding pattern (amide dimer) is stacked along (001) axis. The weak N-H···N, C-H···O, C-H···N hydrogen bondings are along other two orthogonal directions. The bending occurs through weak C-H···N hydrogen bonding. Organic crystals having comparable intermolecular interactions in all direction are harder to bend. The mechanical properties of crystals are very important in pharmaceutical industry. Soft crystals become pasty, whereas the hard crystals become granular upon grinding, and can be handled more easily.[3]

Polymorphism in Pharmaceutics

Polymorphism has huge impact in pharmaceutical industry. Ritonovir, the HIV drug introduced by Abbott is polymorphic. The kinetic polymorph, form-I was pharmaceutically active; whereas the more stable conformational polymorph, form-II was pharmaceutically inactive. After commercialization of form-I of this drug under the trade name Norvir, it was found that desired form-I had converted to undesired form-II. Then Abbott had to withdraw all the capsules from the market which had serious implications in its business. The form-I of Ritonovir is often quoted as disappearing polymorph. Polymorphism has huge impact in the legal field as each polymorph of a drug can demand separate patent protection. It is well known fact that there was a long legal battle between Glaxo Smith Kline and Novopharm

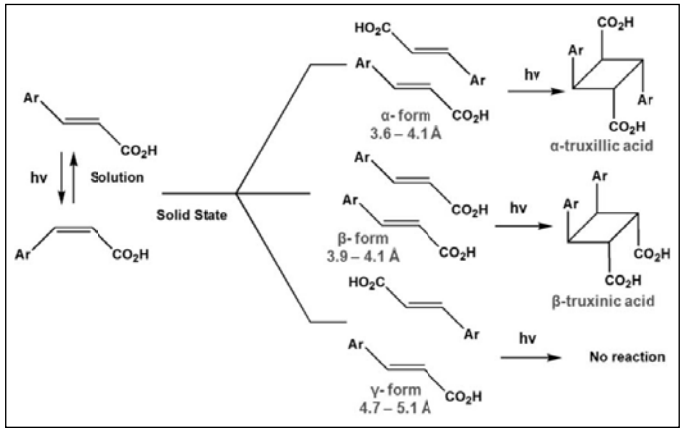

Figure 7: Solid state and solution phase photoreactivity of polymorphic trans-2-ethoxycinnamic acid

(generic company) on the issue of patent of two polymorphs of Ranitidine (trade name Zantac by Glaxo) and right to commercialize.[3]

Solid State Photoreactivity

The reactivity of solid is essentially different from the reactivity of molecules in liquid or gaseous phase. The formation of product in the solid state is driven by the ordered arrangement of the reacting molecules that lack long range molecular movement. The reactions in the solid state that occur with a minimum amount of atomic or molecular movement are called topochemical

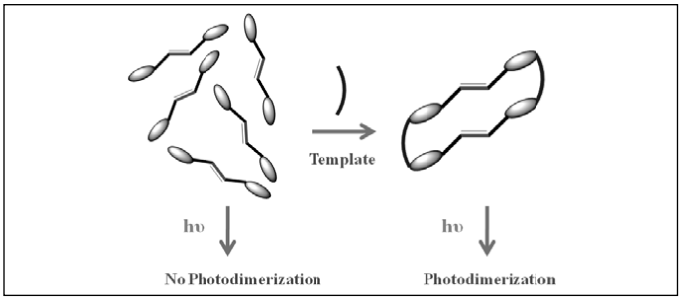

Figure 8: Crystal Engineering for template driven preorganisation of C=C bonds

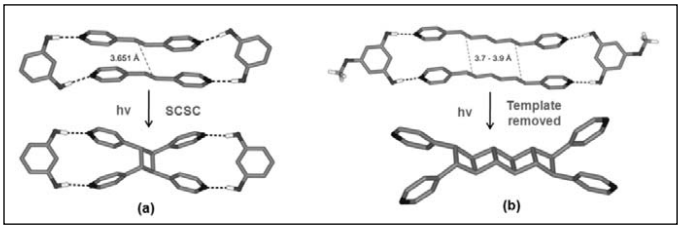

Figure 9: Template controlled alignments of C=C bonds in various types of hydrogen bonded co-crystals

reactions. There are many advantages of reactions in the solid state namely, stereoselectivity i.e. formation of one particular isomer of the product among its many possible isomers, high yield (usually quantitative) and access to products that are inaccessible otherwise from reaction in solution phase. The solid state photoreactivity of *trans*-2-ethoxycinnamic acid, as was observed by Schmidt, is the best example to understand the matter. *Trans*-2-ethoxycinnamic acid undergoes *trans-cis* isomerisation in solution. On the other hand, three different polymorphs show different photoreactivity in the solid state. The α-form photodimerizes in *head-to-tail* fashion and yields α-truxillic acid; β-form photodimerizes in *head-to-head* fashion to yield β-truxinic acid; whereas, the γ-form does not exhibit photoreactivity (Figure 7).[1]

Schmidt's Postulates and Designing Photoreactive Solids

Based on the observations on the photochemical studies and crystallographic analyses, Schmidt deduced the conditions for cycloaddition reaction to occur in the solid state. According to his postulate, the photoreactive olefins must align parallel keeping a distance of 3.5 – 4.2 Å between two C=C bonds.[1] A minimum amount of atomic or molecular movement is necessary during reaction and the stereochemistry of the dimer depends on the contact geometry (antiparallel/ parallel or head-to-head/ head-to-tail) of nearest neighbouring double bonds.

Now, when the stacking of C=C bonds of organic olefins occurs naturally in their crystals, solid state photoreactivity is observed. But when the C=C bonds of olefins are not stacked parallel naturally, crystal engineering modifications are needed to transform photostable crystals into photoreactive crystals. Therefore, the challenge in this type of design relies in anchoring the C=C bonds into parallel arrangement maintaining a proper distance between them. Crystal engineering principles have been employed utilising directional nature of supramolecular interactions (e.g. hydrogen bonding) to control the self-assembly of olefins to yield photoreactive solids. The process is known as preorganisation and the molecule which serves the purpose is known as template (Figure 8). By exploiting the hydrogen bonding ability of the olefins, the templates are selected having complementary functional groups. For example, *trans*-1,2-bis(4′-pyridyl)ethylene is a hydrogen bond acceptor and can be preorganised in the co-crystal with resorcinol having hydrogen bond donor phenolic functionality.[9] Extensive work has been reported in this field and it is worth to mention that the synthesis of laderane was successfully achieved in a single step which is otherwise very difficult to synthesize in conventional synthetic route (Figure 9).[9] The idea of template controlled solid state photoreactivity has also been extended to preorganise many olefins in various types of supramolecular assemblies like hydrogen bonded co-crystals, organic salts and coordination compounds to generate functional cyclobutane derivatives.[10]

Conclusion

Crystal Engineering is relatively a newer subject and is rapidly growing. It imparts huge interest to the scientific communities in both the academics and industries. Intermolecular interactions like hydrogen bonding, π··π stacking, cation··π, etc have been known even before the subject area received due regular. However, understanding the complementary interactions and utilizing them in terms of supramolecular synthons and to design new molecular solids with desired physical and chemical properties are taught us by crystal engineering. Designed syntheses of new molecular architectures like diamondoid, herringbone, honeycomb, chicken-wire networks have created a new dimension in structural chemistry. Modern researches in polymorphism, pharmaceutical co-crystals, etc have constructed the bridge between academics to industry. The nuts-and-bolts of crystal engineering entirely rely on the complete understanding of intermolecular interactions.

References

1. G. M. J. Schmidt, *Pure Appl. Chem.*, 1971, **27**, 647-678
2. G. R. Desiraju, Crystal engineering: the design of organic solids. Elsevier: 1989.

3. G. R. Desiraju, J. J. Vittal, A. Ramanan, Crystal Engineering: A Text Book. World Scientific Publishing: 2011.
4. T. Steiner, *Angew. Chemie Int. Ed.,* 2002, **41**, 48-76.
5. M. C. Etter, *Acc. Chem. Res.,* 1990, **23**, 120-126.
6. G. R. Desiraju, *Angew. Chemie Int. Ed.,* 1995, **34**, 2311-2327.
7. S. L. Childs, G. P. Stahly, A. Park, *Mol. Pharmaceutics* 2007, **4**, 323-338.
8. (a) A. V. Trask, *Mol. Pharmaceutics* 2007, **4**, 301-309; (b) N. Shan, M. J. Zaworotko, *Drug Disc. Today,* 2008, **13**, 440-446.
9. L. R. MacGillivray, *J. Org. Chem.,* 2008, **73**, 3311-3317.
10. G. K. Kole, *Crystal Engineering Studies on Molecuar Salts and Silver(I) Coordination Polymers for [2+2] Cycloaddition Reaction in the Solid State*, Ph.D Thesis, National University of Singapore, 2011.

Dr. Kole *received B.Sc in Chemistry from University of Calcutta in 2005 and M.Sc from Indian Institute of Technology (IIT) Madras in 2007. He carried out his doctoral research in crystal engineering under supervision of Prof. J. J. Vittal at the National University of Singapore. After a short postdoctoral stint at the same group, he joined the Institute for Materials Research and Engineering (IMRE) in Singapore as a Scientist in 2012. He joined the Bhabha Atomic Research Centre as a Scientific Officer in 2014 through K. S. Krishnan Research Associateship scheme. His current research interests include crystal engineering, supramolecular chemistry, coordination polymers, chemistry of chalcogens (S, Se), chemistry of silver and gold etc.*

Metal Organic Frameworks (MOFs) through Building Block Replacement

Amit Pratap Singh
Department of Applied Science, National Institute of Technology Delhi
Delhi-110040 (India)
Email: apsingh@nitdelhi.ac.in

Abstract

Metal organic frameworks (MOFs), also termed as porous coordination polymers (PCPs) are the hybrid porous materials with many potential applications such as gas adsorption, separation, host–guest chemistry, optics, magnetism, catalysis and photoluminescence. The properties of these materials is mainly depend upon the presence of chemical functionality either at the organic linkers and/or at the metal nodes. However, the properties of theses material can be tuned using post-synthesis modification (PSM) without disrupting the metal–linker bonds. Even the attractive approach that go beyond PSM are herein termed *building block replacement* (BBR) which includes (i) transmetalation (ii) solvent-assisted linker exchange (SALE) and (iii) non-bridging ligand replacement. These single step or tandem BBR processes involve exchanging various key structural components of the MOFs, resulting a protoMOF structures (where a parent MOF used as a template) to design MOFs composed of new components and functionality. In present review article, the influence of building block replacement on the stability and properties of MOFs will be discussed, and some insights into their mechanistic aspects are provided. Moreover, the future perspectives of these techniques providing a preview that how these can lead to various unexplored areas of MOF chemistry are also discussed.

1. Introduction

During the past two decades, metal organic frameworks (MOFs) have become probably the most studied family of materials because of their almost infinite variations in structure and composition. However, the use of their full synthetic potential might be further improved and post-synthetic modification, that is modification of the solid after synthesis, is a powerful tool to achieve that aim. The post-synthesis modification (PSM) process were extensively reviewed by Cohen[1,2] and by Burrows,[3] effectively removes the potential for functional-group interference during MOF assembly. PSM involves heterogeneous chemical reactions to functionalize preassembled MOF structures *via*: *(i) modification of linkers* including (a) covalent modification (or elaboration), (b) deprotection of linker functionality (including demetalation), and (c) electron addition (reduction) and concomitant incorporation of charge compensating ions. *(ii) modification of metal-containing nodes* including (a) incorporation of non-framework or pendant ligands *via* dative bonding to coordinately unsaturated metal sites,[1-4] (b) alkyl or silyl grafting to oxygen atoms in metal-oxide nodes,[5,6] and (c) attachment of metal ions or complexes at node oxygen sites *via* atomic layer deposition (ALD) or *via* reaction with organometallic species in dry solutions.[7,8]

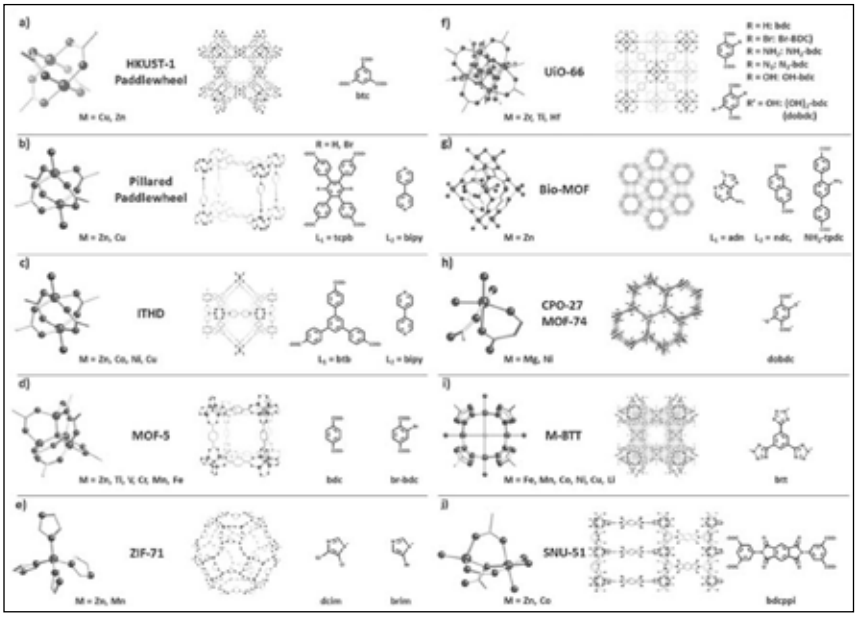

Figure 1: Lattice structures (middle) and corresponding SBUs (metal nodes (left), and organic linkers (right)) of some of the MOFs discussed in this review. (Atom definition: blue – metal, red– oxygen, purple – nitrogen, grey – carbon, green – chlorine).

Outside these extensively studied PSM approaches, various conceptually different post-synthesis routes are now emerging. *Building block replacement* (BBR) involves replacement of key structural components of the MOF including (i) transmetalation at nodes or within linkers.

(ii) solvent- assisted linker exchange (SALE) (iii) non-bridging ligand replacement. Some of the examples of BBR processes in MOFs are shown in Fig. 1. BBR is intriguing given that it opens up a very broad strategy for the synthesis of iso-structural MOFs that in turn should enable functional MOF chemistry.

The transmetalation[9] provides a route to incorporate desired metal ions that are difficult to incorporate *via de novo* synthesis, replacement of non-bridging charge balancing ligands represents an efficient way to engender new functional chemistry. Whereas the solvent assisted linker exchange, (SALE),[10-12] often offers complete exchange of one organic linker for another possessing new functionality. In general, BBR reactions offer the changes in heterogeneous, linker/ligand, or metal ion exchange, *via* breaking and remaking chemical bonds within the parent MOF.

Finally, in many cases it is relatively easy to find more mild conditions for BBR than the solvothermal conditions typically required for direct syntheses of MOFs. In BBR reactions often work well with reactant concentrations that are too low for effective direct synthesis. Thus BBR can be especially useful when desired linkers or non-bridging ligands are expensive, delicate, or inherently incompatible with typical conditions for direct MOF synthesis.

2. Transmetalation

In this process of post- synthesis modifications of MOF the building blocks the building block replacement take place through the transmetalation.[9] Also known as ''metal metathesis''[13] or ''metal-ion exchange'',[14] transmetalation entails partial or complete replacement of the metal nodes (or sometimes extra-framework metal moieties) of a MOF by a reaction with a metal precursor (in most cases a solution of a metal salt) in a single crystal-to-single crystal fashion. The emergence of this synthetic pathway in MOFs has been relatively recent.

2.1 Metal node engineering

2.1.1 Obtaining compounds that are unattainable *de novo*.

Perhaps the most straightforward and obvious aspect of transmetalation is its ability to generate MOFs featuring metals that are challenging to obtain for specific compounds through conventional syntheses. This is especially relevant in the case when a new structurally or functionally interesting MOF topology is synthesized with a given metal node. Attempts to diversify a specific MOF by adapting an established synthetic pathway to other metal ions are not always successful, since the variation in size, geometric restriction on the preferred coordination sphere and electronic properties of the different metal ions may interfere with the MOF structure assembly. For instance, Prasad *et al.* prepared {[Zn_2 (bdcppi) $(DMF)_3$].6DMF.4H_2O} (SNU-51), a Zn^{2+} based MOF of PtS topology (Fig. 1k); however, when they employed Cu^{2+}, under similar synthetic conditions the resulting product crystallized in the NbO topology {[Cu_2(bdcppi) $(DMF)_2$].10DMF.2H_2O}.[15] In an attempt to prepare Cu-SNU-51, the authors employed transmetalation by soaking Zn-SNU-51 in a methanolic $Cu(NO_3)_2$ solution. While powder X-ray diffraction (PXRD) established that the parent and daughter materials are structurally similar and no new phase was formed, the authors ruled out the recrystallization following a dissolution process based on the fact that the transmetalation rate was fast (27%, 44% and 75% conversion in 10, 30 and 120 minutes respectively) as followed *via* ICP analysis. It is important to note that more information regarding the rates of single crystal-to-single crystal transmetalation as well as dissolution followed by recrystallization are needed to establish the true nature of these processes. The authors also found that no transmetalation occurred when they attempted transmetalation of Cu^{2+} with Zn^{2+} on the Cu^{2+} exchanged Cu-SNU-51. Likewise, in the presence of various other transition metal ions, such as Co^{2+}, Ni^{2+}, and Cd^{2+}, the Zn^{2+} based SNU-51 only transmetalated with Cu^{2+} in a solvent-dependent manner indicating that *thermodynamic stability of the daughter framework is a key driver for transmetalation, where solvent governs other crucial aspects including solubility, coordinating ability and the effective solvation shell of a metal ion*.

2.2 Introducing new chemical functionality in MOFs *via* transmetalation

2.2.1 Synthesis of redox-active MOFs and catalysis.

MOFs endowed with redox-active properties could prove valuable for both chemical and electrochemical catalysis. However, decorating MOFs with redox-active metals is not an easy task due to the vulnerability of cations in lower oxidation states towards oxidation during *de novo* synthesis. Sub-stoichiometric transmetalation allowed Brozek *et al.* to produce seven MOF-5 (Fig. 1d) analogues featuring Ti^{3+}, V^{2+}, V^{3+}, Cr^{2+}, Cr^{3+}, Mn^{2+} and Fe^{2+} ions (Fig.2).[16] Using $NOBF_4$, the authors successfully oxidized Cr^{2+} to Cr^{3+} in Cr-MOF-5. An innersphere oxidation of Fe^{2+} to Fe^{3+} in Fe-MOF-5 by coordinated NO was demonstrated to highlight the redox activity of the transmetalated products.

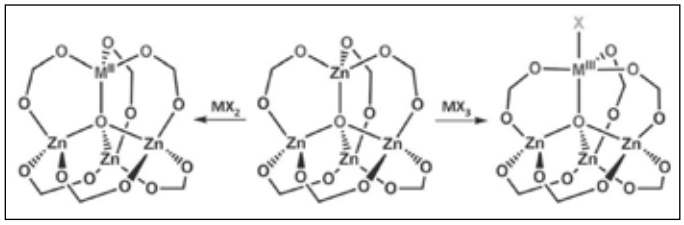

Figure 2: Partial transmetalation in Zn4O node within MOF-5.

Transmetalation offers an attractive strategy for the incorporation of catalytically active metal centers in MOF linkers. The synthesis of catalytic MOFs featuring salen-[17] or porphyrin- based[18] linkers has particularly benefitted from this approach. Shultz *et al.* were able to expand a family of M-salen-containing pillared-paddlewheel MSO-MOF materials [Zn_2(tcpb)(salen)] by a stepwise replacement of Mn^{3+} in the salen linker with Co^{2+}, Zn^{2+}, Cr^{2+}, Cu^{2+}, Ni^{2+} or Mn^{2+} (Fig. 3a) resulting in a series of potential catalysts.[17] Similarly, Zhang *etal.* applied transmetalation to their ''ship-in-a-bottle'' material porph@MOM-10, a [meso tetra(N-methyl-4-pyridyl) porphine tetratosylate] encapsulated in the {$Cd_6(bpt)_4Cl_4(H_2O)_4$} framework, which contains catalytically inactive Cd^{2+} ions both in its nodes and in the porphyrin moiety.[18] Replacement of Cd^{2+} throughout the material with Mn^{2+} afforded a product (Fig. 3b) that could catalyze the epoxidation of *trans*-stilbene with 75% conversion (compared to only 7% conversion provided by the original Cd^{2+} containing porph@MOM-10). Notably, the Mn^{2+} analogue proved inaccessible *de novo*.

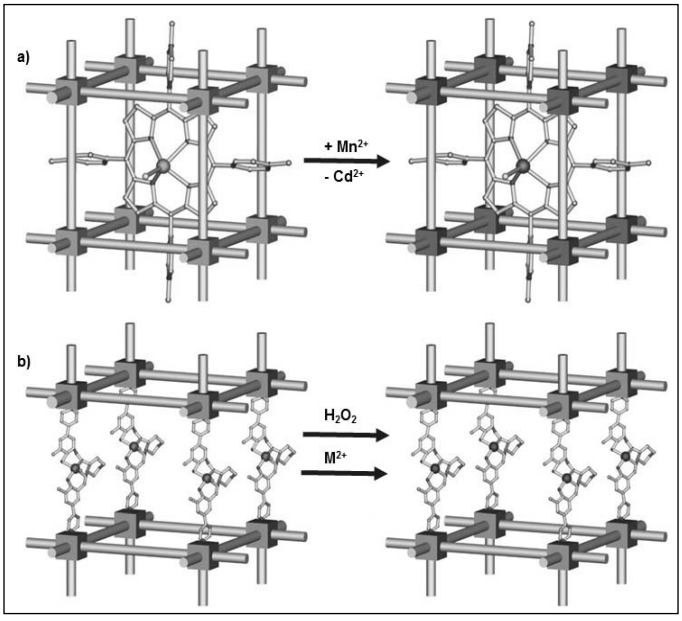

Figure 3: Transmetalation in (a) porph@MOM-10, and (b) MSO-MOF. Note that for the panel (b), the metalation was carried out after the demetalation of the parent MOF in a sequential manner.

3. Solvent-assisted linker exchange

The PSM is often effective for circumventing problems associated with direct MOF preparation, replacement of linkers is another viable strategy. It has variously been termed ''stepwise synthesis'',''bridging linker replacement'',''post-synthetic exchange'', isomorphous ligand replacement, and stepwise ligand exchange.[19-21] We prefer the term ''SALE''[10-12,19-21] as it highlights the importance of the solvent during linker exchange. Conceptually SALE occurs at the solid–solution interface; a parent MOF is placed in a solution containing a second linker and a daughter MOF retaining the parent MOF topology is obtained.

3.1 Pore engineering

3.1.1 Controlling pore volume.

Burnett *et al.* first demonstrated that SALE could be utilized to engineer the pore dimensions of a MOF.[19] Starting from 2-D (PPF-18) and 3-D (PPF-20) pillared-paddlewheel structures (consisting of Zn_2(tcpp) 2-D layers periodically linked with dpni pillars; see Fig. 1b for a related structure), Burnett *et al.* completely exchanged the 15.4 Å dpni pillars of PPF-18 and PPF-20 with 7.0 Å bipy pillars in a DEF–EtOH solution at 80 °C. The resultant frameworks, PPF-27 and PPF-4, have significantly smaller pores when examined by single crystal X-ray diffraction (*e.g.*, *c* = 87.59 to 54.89 Å for PPF-20 to PPF-4).[19] A handful of additional papers utilizing MOFs of varying topologies (see Fig. 1 for example) have confirmed that SALE does in fact occur in the presence of linkers whose dimensions are smaller and/or of similar size to the linkers of the parent MOF.[22-24]

One might suspect smaller pore volumes to be readily obtainable *via* SALE, the diffusion of smaller linkers should be facile into pores of larger dimension. In contrast, SALE of longer linkers might be significantly more difficult given presumably slower diffusion as well as the necessity for significant structural changes within the framework upon exchange. Recently however, Karagiaridi *et al.* demonstrated that linkers of increasing length could be introduced into the pillared-paddlewheel MOF, SALEM-5 [Zn_2(Br-tcpb)(dped)], *via* SALE (Fig. 4).[11] SALEM-5 contains layers of Br-tcpb linker and the 9 Å dped pillars which could be replaced by dipyridyl pillars of 11 Å tmbbp (SALEM-6), 14 Å nbp (SALEM-7) and 17 Å tmbebp (SALEM-8) (Fig. 4). In the most striking example (*i.e.*, SALEM-5 with dped pillar to SALEM-8 with tmbebp pillar), the *c*-axis of the resultant unit cell expands from 17.75 to 23.50 Å. Likewise, Rosi and co-workers demonstrated that SALE of longer linkers is possible in MOFs containing carboxylate linkers, specifically during the transformation of Bio-MOF-101 (Fig. 1g), which consists of the zinc-adeninate clusters

($Zn_8(adn)_4O_2$ $^{8+}$ periodically linked with ndc linker), to Bio-MOF-103 ($Zn_8(adn)_4O_2^{8+}$ periodically linked with NH_2-tpdc linker). In this series the unit cell was increased from 62.04 to 82.25 Å. Notably, most MOFs with increased pore volume could not be prepared *de novo*.

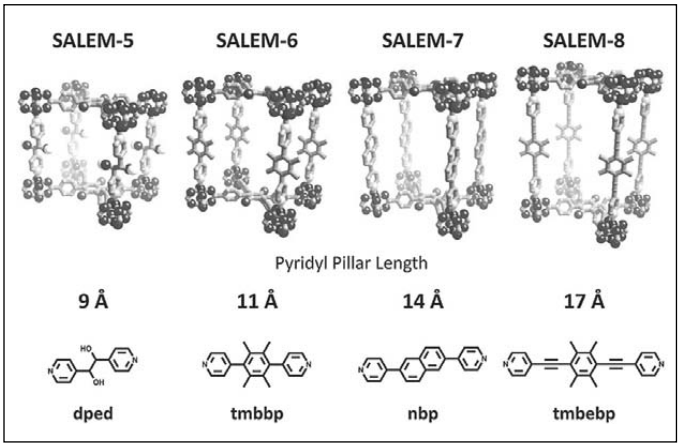

Figure 4: Increasing pore sizes in an isoreticular series of pillared-paddlewheel MOFs synthesized via SALE. The value in Å represents the length of the dipyridyl linkers utilized for SALE on the parent MOF SALEM-5.

Framework catenation can also drastically change (diminish) MOF pore volumes. Bury *et al.* found that SALE could be used to access the non-catenated version of an otherwise catenated material. The SALE starting point was the non-catenated pillared-paddlewheel compound DO-MOF [Zn_2(tcpb)(dped); see Fig. 1b for a related structure].[25,26] DO-MOF contains 2-D sheets of the zinc-coordinated tetracarboxylate linker, tcpb, separated by the dipyridyl pillar, dped. In contrast, the tcpb linker with dipyridyl bipy and abp pillars yields two-fold catenated structures.

However, DO-MOF, under SALE conditions with bipy and abp replaces the dped pillars and yields the non-catenated MOFs containing bipy and abp ligands. Control over catenation was confirmed *via* thermogravimetric analysis as well as structural modelling *via* powder X-ray diffraction (PXRD). This study delineates an interesting alternative avenue to prepare non- catenated MOFs from those that exhibit catenation.

3.1.2 Controlling pore environment.

The pore environment can also be readily controlled and modified *via* SALE. Kim *et al.* demonstrated that the bdc linker of UiO-66 [$M_6O_4(OH)_4(bdc)_6$] could be exchanged with NH_2-bdc, Br-bdc, N_3-bdc, OH-bdc, and $(OH)_2$-bdc (see Fig. 1f).[21] These exchanges could be observed both at the single particle level using aerosol time-of-flight mass spectrometry (ATOFMS) and on the bulk sample *via* ^{1}H NMR. ^{1}H NMR demonstrated that exchange ratios between 9 and 76% could be achieved depending on the solvent, temperature, and time of the reaction utilized. Interestingly, SALE can also occur between the preformed NH_2-bdc and Br-bdc MOF derivatives (*i.e.*, in a solid–solution–solid transformation). These results suggest that one of the MOFs must dissolve to some extent for linker incorporation to occur.

Karagiaridi *et al.* also demonstrated that pore functionality could be readily controlled in another highly sought after class of MOFs, namely zeolitic imidazolate frameworks (ZIFs).[10] The eim linkers in {Cd(eim)$_2$} (CdIF-4), a ZIF possessing RHO topology and Cd^{2+} nodes, could be exchanged for nim and mim linkers to form {Cd(nim)$_2$} (CdIF-9), and {Cd(mim)$_2$} (SALEM-1) respectively. The SALE reactions that occur between CdIF-4, CdIF-9 and SALEM-1 are summarized in Fig. 5. Importantly the studies from Kim *et al.*, as well as Karagiaridi *et al.*, demonstrate that some of the most robust MOF structures known are indeed amenable to SALE.

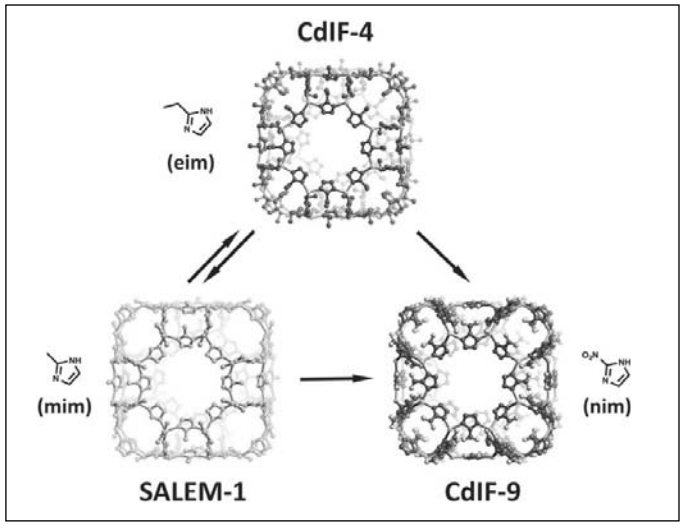

Figure 5: Pore environment modification through SALE in ZIFs.

4. Non-bridging ligand replacement

The MOF nodes can be composed of single metal ions; they can also be comprised of discrete metal-containing clusters (see Fig. 1 for examples). These metal-cluster containing nodes offer an opportunity to introduce a battery of new functionality through the replacement of charge balancing non-bridging ligands. Whereas typical metal node functionalization utilizes dative bonding to coordinatively unsaturated metal sites,[27-29] non-bridging ligand replacement relies on either acid–base or ligand exchange chemistry between the existing anionic ligand on the MOF node and the

incoming anionic ligand. The result is the introduction of functional groups as charge compensating and strongly bound moieties to the MOF node *via* ionic bonding. Like SALE, non-bridging ligand replacement is expected to be governed by many of the factors that govern SALE including solvent selection, diffusion, and pK_a of the conjugate acids.

This idea was recently realized when Deria *et al.* reported a new BBR technique called solvent-assisted ligand incorporation (SALI) for Zr-MOFs. The authors reported the efficient incorporation of carboxylate-based organic functional groups (CFGs) into the mesoporous MOF, NU-1000 (Fig. 6a), consisting of $[Zr_6(\mu_3\text{-}OH)_8(\text{-}OH)_8]^{8+}$ nodes and TBAPy linkers.[30] The incorporation of new carboxylate based functionalities (CFGs) *via* SALI is encompassed by two boundary compositions of the Zr_6-node – $[Zr_6(OH)_{16}(RCOO)_8]$ before functionalization, and $[Zr_6(O)_4\text{-}(OH)_4(RCOO)_8(R'COO)_4]$ – after the SALI process, which is governed by an acid–base equilibrium between the carboxylic acid moiety of the incoming ligand (R'COOH) and a pair of hydroxyl ligands of the node (forming a water molecule as a by-product). Notably, carboxylates (R'COO-) of weaker conjugate acids were found to be efficiently supplanted by those of stronger conjugate acids. Thus the distinctive feature of SALI, from a SALE reaction perspective, is that it does not involve replacement of a bridging linker, but instead a charge compensating and non-bridging ligand (e.g. hydroxide or a carboxylate ligand). The authors incorporated perfluoroalkane functionality within the mesoporous channels of NU-1000 by utilizing perfluoroalkyl carboxylic acids of varying chain length (–CF_3,–C_3F_7, –C_7F_{15} and –C_9F_{19}). The resulting materials showed increased Q_{st} values for CO_2 and slightly less affinity for water vapor. Notably, this technique not only proved to be versatile, tolerates many functionalities, but is also shown to yield new materials that are robust and effective for secondary functionalization at the SALI-incorporated moiety.[31]

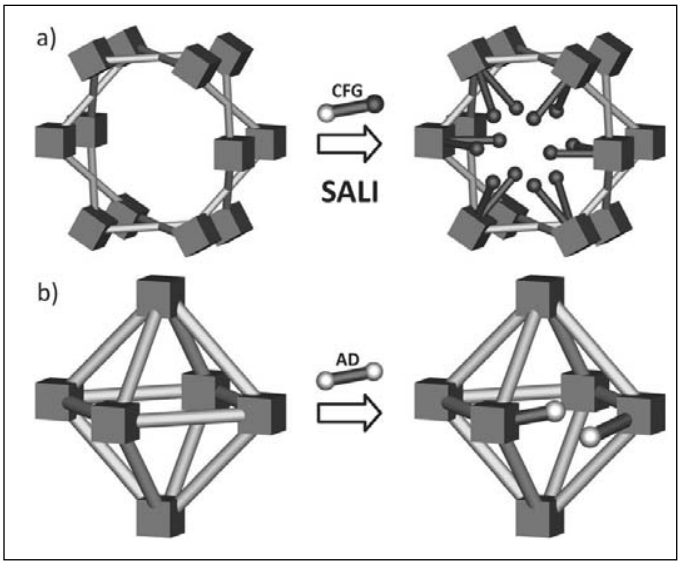

Figure 6: Schematic representation of (a) solvent-assisted linker incorporation (SALI) with CFGs and (b) linker replacement with alkanedioic acids in various Zr-MOFs

In view of their high thermal, mechanical, and chemical stability,[32] UiO-66-type materials constitute a similarly intriguing class of MOFs compounds, considering a comprehensive picture regarding the stability and reactivity of this group of MOF materials. For instance, it was demonstrated by Wu *et al.*[33] and subsequently Katz *et al.*[34] that depending on the synthetic conditions the UiO-66 framework (see Fig. 1f) may lack one or more structural elements (*i.e.*, they may exhibit the missing linker phenomenon) without losing its integrity and topology; such systems can facilitate non-bridging ligand exchange. In a recent study, Suh and coworkers employed a slightly modified SALE approach to exchange the bdc linkers in UiO-66 material for various flexible alkanedioic acids (AD).[35] As a result the authors obtained a series of modified UiO-66-ADn derivatives (Fig. 6b; ADn is defined as HOOC–$(CH_2)_n$–COOH, where n = 4, 6, 8, and 10). In contrast to a conventional SALE process, during the post-synthetic linker exchange, a single ditopic terephthalate linker (bdc) was replaced by two flexible ditopic alkanedioate ligands, leading to UiO-66 derivatives functionalized with pendant carboxylic groups. Given that UiO-66 materials can possess ''missing linker''-defects (for UiO-66 consisting 12 linker nodes, a geometric surface area of 800 $m^2\ g^{-1}$ was estimated[34]), it is quite possible that a part of the AD-functionalization could proceed *via* a non-bridging hydroxyl ligand replacement (similar to that involved in SALI) in addition to the bdc linker replacement process as described by the authors. Using ideal adsorption solution theory (IAST), they demonstrated that for landfill gas separation (a 50 : 50 mixture of CO_2 and CH_4), all of the UiO- 66-ADns showed higher selectivity for CO_2 over CH_4 relative to UiO-66.

5. Outlook and future directions

In previous sections we discussed numerous examples of BBR, where only one structural element, namely the metal ions, charge-balancing ligands in the node or the organic linkers had been replaced. These examples nicely demonstrate that MOF structures are highly modular and can be altered *via* BBR. Recently presented strategies for tuning the physical and chemical properties of porous

crystalline materials emphasize a deliberate introduction of framework heterogeneity by increasing the number of constituents. Introducing a variety of building units into a single crystalline solid containing gradients of functionality may open up new opportunities for application-based MOF chemistry. This goal can be achieved, to some extent, by using *de novo* approaches – for example, incorporating multiple linkers into the same crystal containing different functional groups.[36]

Importantly, some recent examples demonstrate a high potential for the construction of multiple building block (nodes and the organic linkers) MOFs by utilizing the BBR strategy. An important exploration of BBR reactions towards multiple building block MOF structures is a stepwise replacement of linkers and metal ions in nodes within the parent framework

Cohen's work provides the first example of sequential metal and linker replacement in the same system, which nicely illustrates the synthetic potential of BBR for the introduction of functional variety into MOF scaffolds. Looking forward, another interesting possibility for BBR would be the complete conversion of a protoMOF structure into a new material with new nodes and linkers by tandem building block replacement.

Similarly, we speculate the future utility of BBR can conceptually encompass the following areas:

(i) BBR in MOF membranes: MOF membranes are regarded as interesting materials for gas separations.[37-39] However, the formation of MOF membranes is limited by synthetic obstacles (related to solvothermal MOF synthesis and preparation of a good quality membrane)[40] and the incorporation of desired functionality is also challenging. In this view, BBR in MOF membranes, especially ZIF-containing systems, could offer new possibilities for enhancing the stability and versatility of separations.

(ii) BBR in Layer-by-Layer (LbL)-grown MOF films; the LbL technique has become a promising methodology for growing MOF films, with precise control over thickness, orientation, and porosity, on various substrates.[37] BBR in combination with LbL could significantly widen the scope of the LbL approach by application of post-LbL SALE or transmetalation, leading to multi- functional MOF films that are difficult to synthesize *de novo*.

(iii) Different attachment chemistry for non-bridging, charge compensating ligand exchange (SALI): exploration of different attachment chemistry for SALI is another way forward for the synthesis of highly robust functional MOFs. This new concept could be further expanded in several directions by incorporation of various types of charged anchoring moieties (not limited to carboxylic acids) resulting in a broader scope of SALI. Utilizing this approach might lead to interesting directions such as incorporation of multiple light harvesters or redox active moieties for the construction of functional arrays or photoredox antenna systems.

Acknowledgments

The author is grateful to Department Science and Technology (DST) and Science of Science and Engineering Research Board (SERB), New Delhi for financial support.

References:

1. K. K. Tanabe and S. M. Cohen, *Chem. Soc. Rev.,* 2011, 40, 498–519.
2. S. M. Cohen, *Chem. Rev.,* 2012, 112, 970–1000.
3. A. D. Burrows, *in Metal Organic Frameworks as Heterogeneous Catalysts, ed.* F. L. i. Xamena and J. Gascon, The Royal Society of Chemistry, 2013, pp. 31–75.
4. A. M. Shultz, A. A. Sarjeant, O. K. Farha, J. T. Hupp and S. T. Nguyen, *J. Am. Chem. Soc.,* 2011, 133, 13252–13255.
5. R. Ameloot, M. Aubrey, B. M. Wiers, A. P. Go´mora-Figueroa, S. N. Patel, N. P. Balsara and J. R. Long, *Chem. – Eur. J.,* 2013, 19, 5533–5536.
6. M. Meilikhov, K. Yusenko and R. A. Fischer, *J. Am. Chem. Soc.,* 2009, 131, 9644–9645.
7. J. E. Mondloch, W. Bury, D. Fairen-Jimenez, S. Kwon, E. J. DeMarco, M. H. Weston, A. A. Sarjeant, S. T. Nguyen, P. C. Stair, R. Q. Snurr, O. K. Farha and J. T. Hupp, *J. Am. Chem. Soc.,* 2013, 135, 10294–10297.
8. C. Larabi and E. A. Quadrelli, *Eur. J. Inorg. Chem.,* 2012, 3014–3022.
9. M. Lalonde, W. Bury, O. Karagiaridi, Z. Brown, J. T. Hupp and O. K. *J. Mater. Chem. A*, 2013, 1, 5453–5468.
10. O. Karagiaridi, W. Bury, A. A. Sarjeant, C. L. Stern, O. K. Farha and J. T. Hupp, *Chem. Sci.,* 2012, 3, 3256–3260.
11. O. Karagiaridi, W. Bury, E. Tylianakis, A. A. Sarjeant, J. T. Hupp and O. K. Farha, *Chem. Mater.,* 2013, 25, 3499–3503.
12. O. Karagiaridi, M. B. Lalonde, W. Bury, A. A. Sarjeant, O. K. Farha and J. T. Hupp, *J. Am. Chem. Soc.,* 2012, 134, 18790–18796.
13. S. Das, H. Kim and K. Kim, *J. Am. Chem. Soc.*, 2009, 131, 3814–3815.
14. K. Brozek and M. Dinc˘a, *Chem. Sci.*, 2012, 3, 2110–2113.
15. T. K. Prasad, D. H. Hong and M. P. Suh, *Chem. – Eur. J.*, 2010, 16, 14043–14050.
16. K. Brozek and M. Dinc˘a, *J. Am. Chem. Soc.*, 2013, 135, 12886–12891.
17. A. M. Shultz, A. A. Sarjeant, O. K. Farha, J. T. Hupp and S. T. Nguyen, *J. Am. Chem. Soc.,* 2011, 133, 13252–13255.

18. Z. Zhang, L. Zhang, L. Wojtas, P. Nugent, M. Eddaoudi and M. J. Zaworotko, *J. Am. Chem. Soc.*, 2011, 134, 924–927.
19. J. Burnett, P. M. Barron, C. Hu and W. Choe, *J. Am. Chem. Soc.*, 2011, 133, 9984–9987.
20. S. Kim, K. W. Dawson, B. S. Gelfand, J. M. Taylor and G. K. H. Shimizu, *J. Am. Chem. Soc.*, 2013, 135, 963–966.
21. M. Kim, J. F. Cahill, H. Fei, K. A. Prather and S. M. Cohen, *J. Am. Chem. Soc.*, 2012, 134, 18082–18088.
22. M. Kim, J. F. Cahill, Y. Su, K. A. Prather and S. M. Cohen, *Chem. Sci.*, 2012, 3, 126–130.
23. M. Kondo, S. Furukawa, K. Hirai and S. Kitagawa, *Angew. Chem., Int. Ed.*, 2010, 49, 5327–5330.
24. S. Jeong, D. Kim, X. Song, M. Choi, N. Park and M. S. Lah, *Chem. Mater.*, 2013, 25, 1047–1054.
25. W. Bury, D. Fairen-Jimenez, M. B. Lalonde, R. Q. Snurr, O. K. Farha and J. T. Hupp, *Chem. Mater.*, 2013, 25, 739–744.
26. H. Fei, J. F. Cahill, K. A. Prather and S. M. Cohen, *Inorg. Chem.*, 2013, 52, 4011–4016.
27. Y. K. Hwang, D.-Y. Hong, J.-S. Chang, S. H. Jhung, Y.-K. Seo, J. Kim, A. Vimont, M. Daturi, C. Serre and G. Fe´rey, *Angew. Chem., Int. Ed.*, 2008, 47, 4144–4148.
28. T. M. McDonald, D. M. D'Alessandro, R. Krishna and J. R. Long, *Chem. Sci.*, 2011, 2, 2022–2028.
29. J. S. Seo, D. Whang, H. Lee, S. I. Jun, J. Oh, Y. J. Jeon and K. Kim, *Nature*, 2000, 404, 982–986.
30. P. Deria, J. E. Mondloch, E. Tylianakis, P. Ghosh, W. Bury, R. Q. Snurr, J. T. Hupp and O. K. Farha, *J. Am. Chem. Soc.*, 2013, 135, 16801–16804.
31. P. Deria, W. Bury, J. T. Hupp and O. K. Farha, *Chem. Commun.*, 2014, 50, 1965–1968.
32. H. Wu, T. Yildirim and W. Zhou, *J. Phys. Chem. Lett.*, 2013, 4, 925–930.
33. H. Wu, Y. S. Chua, V. Krungleviciute, M. Tyagi, P. Chen, T. Yildirim and W. Zhou, *J. Am. Chem. Soc.*, 2013, 135, 10525–10532.
34. M. J. Katz, Z. J. Brown, Y. J. Colo´n, P. W. Siu, K. A. Scheidt, R. Q. Snurr, J. T. Hupp and O. K. Farha, *Chem. Commun.*, 2013, 49, 9449–9451.
35. H. Hong and M. P. Suh, *Chem. – Eur. J.*, 2014, 20, 426–434.
36. X. Kong, H. Deng, F. Yan, J. Kim, J. A. Swisher, B. Smit, O. M. Yaghi and J. A. Reimer, *Science*, 2013, 341, 882–885.
37. B´etard and R. A. Fischer, *Chem. Rev.*, 2012, 112, 1055–1083.
38. J. Gascon and F. Kapteijn, *Angew. Chem., Int. Ed.*, 2010, 49, 1530–1532.
39. Guo, G. Zhu, I. J. Hewitt and S. Qiu, *J. Am. Chem. Soc.*, 2009, 131, 1646–1647.
40. O. Shekhah, R. Swaidan, Y. Belmabkhout, M. d. Plessis, T. Jacobs, L. J. Barbour, I. Pinnau and M. Eddaoudi, Chem. Commun., 2014, 50, 2089–2092.

Dr. Amit Pratap Singh *is working as an Assistant Professor in Chemistry at National Institute of Technology Delhi. He received his Doctoral degree in Chemistry from University of Delhi in year 2010. He has availed the prestigious German Research Foundation (DFG) fellowship for post-doctoral research at Institute of Inorganic Chemistry, University of Goettingen (Germany) for the period of 2011-2013. Dr. Singh has been awarded by INSPIRE Faculty Award in year 2013 from Government of India and joined Indian Institute of Technology Roorkee as an INSPIRE Faculty in Chemistry and continued till November 2014. Since November 2014, he is an Assistant Professor in Chemistry at National Institute of Technology Delhi (India). His research interest is design and synthesis of new porous materials with metal skeleton and their application in catalysis, chemical technology, and host-guest chemistry (molecular adsorption and molecular recognition), electrical, optical, and magnetic properties.*

Self-Assembly of Polymer Carbon Nanotube Composites and Block Co-polymers: From Multiscale Simulations

Sudip Roy* and Souvik Chakraborty
Physical Chemistry Division, National Chemical Laboratory, Dr. Homi Bhabha Road, 411008 Pune, India
** Corresponding author: s.roy@ncl.res.in, Phone: +91 20 2590 2735, Fax: 0202590 2615*

Abstract

In this article we have elucidated the use of two particle based simulation methods in different length and time scale. We have given briefly the description of atomistic molecular dynamics and dissipative particle dynamics simulation methods. Both the simulation methods are based on Newton's second law of motion, which defines the trajectory of particles as a function of time. The atomistic molecular dynamics method is used for smaller size systems i.e., nanometer scale and we can get information about properties e.g., structure, dynamics and thermodynamics. Dissipative particle dynamics simulation are useful when we target morphology of much larger systems (micrometer scale) e.g., block copolymers, polymer nanoparticle composites etc. We have applied both the methods to understand atomic level properties of polymer nanotube composites, equilibrium self-assembled morphologies offuel cell membrane made of block copolymer. We have also shown how these two simulation methods, we call them together multiscale simulations are connected and can be applied to understand self-assembly at different scales.

Introduction:

Self-assembly has become one of the crucial aspects of scientific pursuit in modern era of science and technology. It is one of the most abundant phenomena in nature and it plays utmost important part in biology and life science. Cell, the building block of life, is formed by the self-assembly of billions of lipids, proteins and other biological molecules. From molecular scale to macromolecular scale,self-assembly guides different molecular structures formed by the aggregation of tiny particles. Earlier, scientists have faced great difficulties in building devices and novel materials by excruciating and expensive manufacturing procedures. Self-assembly came to their rescue where billions of particles spontaneously come together and assemble themselves into the desired nanostructures.So, extensive research is going on to transform the process of self-assembly into an effective nano-engineering tool. In order to apply self-assembly in generating useful nanostructures having potential applications in material science, biology, polymer, electronics and engineering it is of foremost importance to understand the interaction between the self-assembling particles.The atomic/ molecular level interactions guide them to come together and team up to form large specific configurations. So in order to understand the underlying science of self-assembly and apply to build novel materials, scientists are constantly expanding their horizons of research and investigations with the help of experiments, theory, and computer simulations.

Self-assembly has paramount importance in the field of polymer science and engineering. From nanocomposites to fuel cell membrane, self-assembly of molecules guides the efficiency and effectiveness of the materials for desired applications. Polymers are long chain molecules with high molecular weight having numerous repeating units linked together via covalent bonds. The mechanical strength and stiffness coupled with light-weight property, electrical conductivity, chemical durability make polymers the most desired material in substitution of metals nowadays. Great deal of studies is going on to prepare polymeric materials with even more desired properties to cope up with increasing demand for more effective material. Materials made of pristine polymers seem struggling to achieve the target to fulfill the ongoing demand. So polymer composite materials are gaining importance because of their enhanced and improved properties with respect to the pristine polymers.[1-5]A small amount of filler can enhance the thermal, mechanical, electrical properties of polymer by manyfold.[8,9]These fillers are in nanometer to micrometer length scale with different dimensions and they include nanoparticles, nanotubes, nanorods, nanowires, clays with various chemical building blocks and different shapes. Carbon nanotube (CNT) is one of theimportant and widely used filler and when added to polymer by a small amount can improve the mechanical, thermal, and electrical properties. Due to its anisotropic shape and high aspect ratio, it is used as a potential filler to form percolating network within polymer matrix and thus can enhance electrical, thermal conducting efficiency. It has enormous mechanical strength and thus it is used to mix with pristine polymer to prepare composite with desired mechanical strength and stiffness. When CNTs are added

to polymer matrix, it has been observed experimentally that they tend to self-assemble to form bundles located within the polymer matrix. Polymers like polycarbonate, polystyrene, polyethylene and many moreare widely used and popular because of their potential applications in almost every field of manufacturing and engineering industries. Their uses comprise of electronic devices, data storage, indoor and outdoor fixtures, packaging, furniture, paint, coating, garments, and medical equipment etc. encompassing almost all necessary utilities of everyday life.[1,10] But there is a great deal of demand to produce more efficient and sustainable material to match the impending expectations. Polycarbonate is known for its versatile applications in industry. It is a light-weight polymer with considerable strength. Pure polycarbonate is a poor conductor of electricity. However, if CNT is mixed with polycarbonate, its conductivity gets increased due to the formation of percolation network by CNTs within the matrix. This property of CNT-polycarbonate composite has potential application in case of dissipating built-up charges in electronic devices used in mobiles, aircrafts, computers, and other electrical gadgets. As polycarbonate reinforced by CNT is having mechanically superior strength and stiffness it can replace heavy metallic plates used in devices and thus can reduce the manufacturing cost effectively.The dispersion pattern, morphology and network formation by nanotubes drive the efficiency of composite material for such applications. Thus to explore the mechanism and energetics of self-assembly of CNTs which lead to percolation network formation in polymer matrix is essential field of research. The dynamics and distribution of bundles of CNTs are crucial to study to get more insight in this matter. Experimentally it is observed that nanotubes self-assemble in polycarbonate matrix and at very low filler concentration (0.5-5wt %) percolation can be achieved for different multiwall CNTs.[6-7] However, no proper study of the mechanism, energetics, and dynamics of such network of CNTs was performed. Computer simulation is an efficient technique for theoretical investigation of to get deeper understanding of the physical phenomena like self-assembly of various kinds of systems. We have applied Molecular Dynamics (MD) simulation technique to explore the phenomena of bundling of nanotubes in polycarbonate matrix. To understand the local molecular level interactions playing roles in mechanism, dynamics and energetics during the process of self-assembly of CNTs we have performed all atom molecular dynamics simulation of pure polycarbonate and CNT-polycarbonate composite systems. To explore the energetics of bundling process, Umbrella Sampling technique[19,20]has been used.After studying the composite system at molecular level we were interested in exploring the morphology of CNT bundles at higher length and time scale so that we can translate the molecular level information gathered from all atom molecular dynamics simulation to mesoscopic simulation and by doing so, we could be able to understand the mechanism, dynamics, and dispersion pattern of CNT bundles at a much higher length and longer timescale where percolation network can be achieved. So through the multiscale simulation process we have studied the self-assembly of CNTs in polycarbonate matrix aiming to contribute to the understanding of such composite polymeric systems in a systematic way.

Another important field of application of self-assembly as a consequence of phase segregation of block copolymers is fuel cell membrane. Fuel cells are used as source of energy in space technology, heating devices, automation etc.[22,23]and have potential to be used as power source in automotive applications. To generate more efficient fuel cells scientific efforts have been going on experimentally and theoretically. The commonly used fuel cell membrane material is Nafion. But the main drawback of Nafion-based membrane is that it cannot operate above 100°C because of water, an integral part of such membrane, starts evaporating at 80°C and the membrane loses its usability. Phosphoric acid based fuel cell membrane has the disadvantage of being mechanically unstable. Thus alternate constituents for efficient fuel cell membrane which can show good proton conductivity in dry and heated conditions are in demand for last few years. One such technique is polymer electrolyte membrane (PEM). Poly(p-vinylbenzylphosphonic acid) (PVBPA) and its copolymers are such materials that satisfy the criteria for potential constituents for fuel cell membrane as they can work at dry condition and at high temperature. This type of polymers conducts proton in dry condition via hydrogen bond network. PVBPA copolymerized with PEEK (poly-ether-ether-ketone) is a potential candidate for PEM because while PVBPA block can conduct proton efficiently the PEEK block is able to provide necessary mechanical stability without interfering in proton conducting process. The relative volume fraction of PVBPA and PEEK guides the morphology of the block copolymer and hence the proton conductivity. As large scale phase-segregated morphologies of such block copolymers can be studied computationally by mesoscopic simulation technique, we have performed DPD simulations on PVBPA-PEEK-PVBPA like block copolymer systems with different block volume ratios, topologies and connectivity to help the synthetic chemists to synthesize block copolymers that can have better proton conducting ability due to their morphological properties.[15]

Computational Methods:

Molecular Dynamics (MD) is a computational method to study properties and behavior of molecular systems. MD can capture the configurational changes and local fluctuations at molecular level and produces detailed information about it efficiently. MD is a frequently used tool to investigate structural, dynamical, thermodynamical properties of all types of material and biological systems. The molecular dynamics simulation is guided by Newton's equation of motion (Second Law):

$$F_i = m_i a_i$$

Where F_i is the force acting on particle*i* having mass m_i, position r_i, and acceleration a_i. The force is related to the potential energy by the equation:

$$F_i = -V_i V$$

Where V is the potential energy and the force is expressed as the gradient of potential energy. By the combination of two above-mentioned equations:

$$-\frac{dV}{dr_i} = m_i a_i = m_i \frac{d^2 r_i}{dt^2}$$

Thus derivative of potential energy is related to the position and time of the particles. The potential energy is the summation of bonded and non-bonded potentials. Bonded part includes potentials resulting from bond, angle, and dihedral interactions. Non-bonded part comprises of van der Waals interaction (Lennard-Jones) and Coulombic interactions. Integration of the equation of motion provides us the trajectory of the particle where the velocities and accelerations of each particle are calculated as particles change positions with time. The time-average values of required properties can be calculated from the trajectory. Atomistic MD simulation helps us to understand the local interactions between atoms by investigating the structural, dynamical properties at molecular level. However, for our studies, not only we needed to understand the atomistic interactions well but also it was necessary to explore morphology and dynamics at higher length and timescale so that we can correlate information obtained from all atom MD simulation with that of the properties manifested by systems simulated for larger length and longer timescale. So Dissipative Particle Dynamics (DPD) simulation, a mesoscopic MD technique, has also been performed.

DPD which was put forwardby Hoogerbrugge and Koelman[11] is a mesoscopic simulation technique that is used to study mesophase separation phenomena. In DPD, the molecules are coarse-grained as interacting beads with soft repulsive interaction potential. The considerable decrease in degrees of freedoms allows to perform simulations with large system size as well as manifold increase in simulation time as compared to those in case of all-atom simulations. So morphologies formed at mesoscopic domain of length and timescale can be obtained by DPD method. In DPD, the forces acting on particle i consist of a conservative force F^C, a dissipative force F^D, and a random force F^R. The conservative force between particle i and j is given by

$$F_{ij}^C = \begin{cases} a_{ij}\left(1 - \frac{r_{ij}}{R^C}\right)\mathbf{r}_{ij}, & r_{ij} < R^C \\ 0, & r_{ij} \geq R^C \end{cases}$$

where a_{ij} is the maximum repulsion between particle i and j separated by a distance $r_{ij} = r_i - r_j$. R^C is the radius of interaction or cut-off distance. $\mathbf{r}_{ij} = r_{ij}/|r_{ij}|$. The dissipative and random force together hold the thermostat of the system. They are given by

$$F_{ij}^D = -\gamma\, \omega^D (r_{ij})\, (\mathbf{r}_{ij} \,.\, v_{ij})\, \mathbf{r}_{ij}$$

$$F_{ij}^R = \sigma\, \omega^R (r_{ij})\, \square_{ij}\, \Delta t^{-1/2} \mathbf{r}_{ij}$$

where $v_{ij} = v_i - v_j$. $\square_{ij}$is a random number with zero mean and unit variance. γ is a drag coefficient. ω^D and ω^R are weighting functions, which are also correlated to each other by the following equation.

$$\omega^D (r_{ij}) = [\omega^R (r_{ij})]^2,$$

Random (σ) and drag coefficient (γ) are connected via following equation.

$$\sigma^2 = 2\gamma k_B T$$

These forces are integrated as per Newton's second law

$$m_i\, r\square_i = \sum(F_{ij}^C + F_{ij}^D + F_{ij}^R)$$

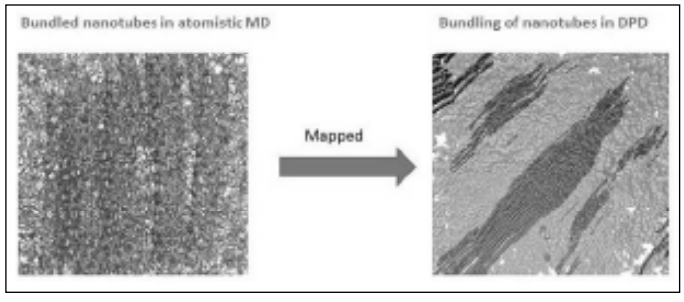

Figure 1: Percolating morphology of CNT in atomistic and mesoscopic scales

Table: BindingFreeEnergiesofCNTs(kcal/mol)

System	Parallel	Perpendicular
Monomer	-5.53	-1.72
Trimer	-39.27	-20.10

The repulsion parameter a_{ij} is linearly related to segregation parameter χ_{ij} which is the thermodynamic parameter that controls the extent of segregation between two species.[12] Using Flory-Huggins theory for solubility, segregation parameter χ_{ij} can be calculated from the thermodynamical data obtained either from atomistic MD simulation or experiments. In our study we have mapped the necessary parameters for DPD simulations from the thermodynamic information obtained by all atom MD simulations we have performed.

Results and Discussions:

Case study 1: Multiscale simulation of polycarbonate-CNT composites:

Molecular Dynamics (MD) simulations of pure monomer and trimer of amorphous polycarbonate and systems mixed with different molecular weight percentages of SWCNT have been studied with an all atom force field using MD code GROMACS 4.0.7.[16-17] The total potential energy we have used is the sum of harmonic bond angle potential, proper dihedral potential with both periodic and Ryckaert-Bellemans forms, improper dihedral potential, non-bonded interactions consisting of Lennard-Jones potential and point-charge electrostatics. Approximately 2%, 5% and 10% by molecular weight of SWCNT-monomer mixtures are prepared at temperatures 500 K, 480 K and 460 K. 2%, 5% and 10% mixtures contain 5, 10 and 15 SWCNTs, respectively. We have taken a zig-zag single walled CNT for study. For trimer, we have prepared the pure trimer system at 520 K, 500 K, 490 K, 480 K, 460 K and 440 K. Simulated annealing is performed to sample the phase space properly because of long chains of the oligomers. 2%, 5%, 10% of SWCNT-trimer mixtures are also prepared at 500 K, 480 K and 460 K in the similar way.[14] Figure 01 depicts the bundle formed by CNTs in polycarbonate matrix.

For Dissipative Particle Dynamics simulation we have calculated repulsion parameter for polycarbonate-CNT composite using Flory-Huggins theory according to the method developed by Groot and Warren.[12] From atomistic simulations of polycarbonate we have computed the Flory-Huggins parameter for DPD simulations. The relationship between Flory-Huggins parameter and repulsion parameter for polycarbonate-CNT composite is obtained as[13]

$$\chi = 0.028\ \Delta a + 0.45$$

Where χ is Flory-Huggins parameter and Δa is the repulsion between two unlike species. Now to simulate systems of 2%, 5% and 10% loading with CNTs of much higher length, a single nanotube is represented by 20 beads. Polymer is generally much longer in length than nanotube. So we have constructed the polymer with 60 beads. Repulsion parameter for similar beads is kept 25 kT and Δa is calculated as 275 kT.[13] Other parameters are kept same as mentioned above. The total system size (total number of beads) in each case (2%, 5%, 10%) is taken as one fourth of a million which is large enough to explore morphology of the components.

Results from atomistic MD simulation:

In atomistic MD simulations, to investigate the structural environment around CNT in monomer and trimer mixtures, radial distribution function (RDF) is calculated between CNT's carbons and four types of atoms of monomer and trimer: carbonyl oxygen, carbonyl carbon, bridge oxygen and aromatic carbon.[14] For 2% mixtures of both monomer and trimer, we have seen that minima of first peaks for carbonyl oxygen, bridge oxygen, carbonyl carbon and aromatic carbon are approximately at 0.45 nm, 0.65 nm, 0.70 nm and 0.70 nm, respectively. For carbonyl oxygen, second minimum is at around 0.66 nm. For carbonyl carbon, second minimum is observed at around 1.05 nm. For 5% and 10% mixtures also, these distances are almost same. The absence of sharp peaks in RDFs indicates that there are very less attractive interactions between CNT and the different chemical moieties of polycarbonate chain.

To compare the self-diffusion behavior of the monomer and the trimer in pure system and three different mixtures of CNT-monomer and CNT-trimer at three different temperatures, we have calculated diffusion coefficients from the average MSD. When we compared the diffusion coefficients of pure monomer and 2% mixture at different temperatures we have observed the increase in the diffusion constant. To compare the diffusivity of CNTs (as the number of CNT is less) we have plotted MSDs both in case of monomer and trimer matrices. In case of monomer matrices, MSD plots have shown that diffusivity of CNT decreases with increasing CNT percentage at a particular temperature. For 10% mixtures diffusivity is observed to be quite low and this fact can be attributed to the high tendency of bundle formation by the CNTs. In case of trimer matrices, the diffusivity of CNT is lower than that in monomer.

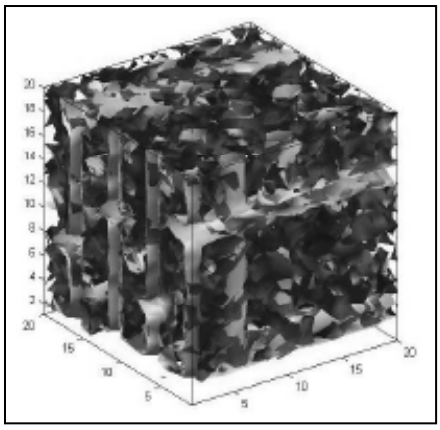

Figure 2: Percolating morphology formed by PVBPA/PEEK copolymer (model 2).

Bundle formation mechanism of nanotubes and energetics have also been studied.[14] The structural changes at CNT-monomer interface during bundle formation have been investigated. We have selected four types of atoms of monomer (carbonyl oxygen, bridge oxygen, carbonyl carbon and aromatic carbon) to see how their spatial proximity with carbon atoms of CNT changes with time. To find the energetics of the bundle formation, we have performed umbrella sampling on the CNTs in both monomer and trimer matrices. It is also interesting to investigate how the binding energy between CNTs changes if we go from monomer to trimer matrix.[14] We have taken two types of arrangements of CNTs: in one case, two CNTs are placed parallel to each other and in another one, they are placed in a perpendicular fashion. The motivation of putting CNTs in two different conformations separately is to compare the corresponding free energy changes associated with two different types of approaches: parallel approach of one CNT to other one and the perpendicular approach of one to another in the composite. The potential of mean force (PMF) curves are obtained for each of the systems by applying weighted histogram analysis method (WHAM[21]). In monomer matrix, free energy change for parallel tubes is -5.53 kcal per mole and for perpendicular tubes it is -1.72 kcal per mole. In trimer system binding energy has increased significantly. Free energy change for parallel tubes is -39.27 kcal per mole and for perpendicular tubes it is -20.10 kcal per mole. From the umbrella sampling, we can interpret the energetics associated with bundle formation mechanism for CNTs. Binding free energy is less for parallel alignment of nannotubes than perpendicular in both monomer and trimer matrices. Interestingly, binding free energy decreased significantly when matrix is changed from monomer to trimer. Interaction between CNTs and matrix plays quite significant role in energetics of bundle formation. More polymeric solvent may enhance the binding energy hence bundle formation.

Results from DPD simulations:

Dissipative Particle Dynamics (DPD) simulation has been performed to find Flory-Huggins parameters of polymer nanotube mixture consisting of higher chain length polymer and larger nanotubes using DL_MESO package[18]. DPD simulations of polymer nanocomposite also showed the bundling of nanotubes.[13] The repulsion parameter between nanotube and polymer beads has been varied to establish the relationship between the Flory-Huggins solubility parameter and repulsion parameter. We have taken the parameters from our atomistic simulation to get the DPD parameters. We have coarse-grained monomer and CNT to DPD beads and performed DPD at different excess repulsion parameters to find the relationship between Flory-Huggins parameter and excess repulsion parameter. The linear relationship is achieved. Now we have calculated nonbonded energies of monomer of polycarbonate and CNT separately from atomistic simulation. Then Hildebrand solubility parameters are calculated. Hildebrand solubility parameters give Flory-Huggins parameter for monocarbonate-CNT mixture. Using linear relationship between Flory-Huggins parameter and excess repulsion parameter, we calculated the necessary excess repulsion parameter for DPD simulation of polycarbonate-CNT composite. This way we have mapped atomistic simulation to DPD simulation for polycarbonate-CNT composite.

We have prepared three different concentrations of CNT polycarbonate composite (2%, 5% and 10%) with varying amount of CNT loadings to explore equilibrium morphology and percolation pathway. Nanotubes are found to form aggregates that are dispersed in polymer matrix in 2% and 10% mixtures.[13]In 10% mixture, percolation pathway is found to be formed (Figure 01). The dynamics of nanotubes in three different concentrations has been studied by mean square displacement. It has been observed from these mesoscale simulations that with the increase in CNT content in the matrix the diffusivity of nanotube get decreased. The bundle formation (or self aggregation of CNTs) is observed for all concentrations but the bundle size varied from lower to higher content of nanotube. To explore bundle size in different mixtures bundle size distribution is studied. Higher concentration of CNT in matrix is found to be more favorable to form larger bundles. Bundled nanotubes are found to have much slow dynamics. In 10% mixture, long striped morphology of nanotubes is observed which indicates that percolation pathway is formed.

Polymer electrolyte membrane:

To perform DPD simulation of PVBPA-PEEK-PVBPA copolymer we have coarse grained the polymer in three different ways.[15] Model 1 is $A_nC_mA_n$ like structure which represents linear triblock copolymer and where A represents PVBPA unit and C represents PEEK unit. To match with the experimental molecular weight fraction of the blocks we have considered n=6; m=2. Model 2 was built to represent a grafted copolymer with three types of beads. In this model PVBPA block is split to two structural segments: one is polystyrene backbone and the other one is methylphosphonic acid attached to styrene unit. Thus $(AB)_n$-C_2-$(AB)_n$ type topology was adopted where A represents polystyrene backbone that is connected to C, B represents pendant methylphosphonic acid bead attached to A bead. C represents PEEK block. Chain length multiplicity n is varied by3 and 6 for this model. Model 3 represents a grafted copolymer with two types of beads, symbolically $(AB)_n$ type where A represents styrene and B represents methylphosphonic acid like in model 2 but in this case we have ignored C i.e. PEEK block. Here, n is taken as 5, 10, 15 to vary chain length. The necessary repulsion parameters for DPD simulation of these models were obtained by performing atomistic MD simulations and by applying Flory-Huggins theory. Different morphologies of the polymer models were obtained by DPD simulations. In case of model 1, we have observed that PVBPA units got clustered to form percolation network which is good for proton conductivity. No such network was observed to form by PEEK beads though. In case of model 2, we have split the PVBPA block to two segments depending on the difference in polarity. Styrene backbone is apolar unit and methylphosphonic acid is the polar moiety. For longer chains, in this model, we have observed rodlike micelles formed by methylphosphonic acid and moreover, these rodlike micelles form parallel bundles and some of them are intercrossing each other perpendicularly (Figure 2). So it indicates percolation network is formed both by phosphonic acid as well as by PS/PEEK backbone. Such percolating morphology is useful to enhance the efficiency of proton conduction and simultaneously good for mechanical stability also. For model 3, where central PEEK block is ignored, we observed rodlike micelles only in case of longer chains. Shorter chains showed no ordered structures. However, the rodlike micelles formed are much less ordered and pronounced in comparison to the model 2. So the presence of central PEEK block is, apparently, a significant contributing factor to get pronounced and orderly percolation morphology.

Conclusions:

In this article we have discussed the study of self-assembly in two of our fields of research. One is the polymer composite study and the other one is the fuel cell electrolyte membrane. The outcomes of the investigations we have pursued are expected to contribute to understand the underlying science of such phenomena and help to make more advanced and efficient material in future.

By performing multiscale computer simulations we have observed the bundle formation and parallel alignment of CNTs in the matrix of polycarbonate and analyzed the mechanism, structural properties, dynamics, and energetics of this phenomenon. Different atoms of polymer present at the polymer-CNT interface play crucial role in the mechanism of bundle formation. The self-assembly of CNTs affects the dynamics of both filler and the polycarbonate matrix. From energetics of bundle formation it is observed that bundle formation is more favorable in oligomers than monomer solutions. For DPD simulations of polycarbonate-CNT composite systems, Flory-Huggins solubility parameters have been calculated to map the DPD parameters from all-atom simulations. Bundles are found to be formed in 2%, 5% and 10% mixtures by DPD simulations. The dynamics of bundling is fast as there is a significant repulsion between nanotubes and polymer matrix. Diffusivity of bundles is quite slow as they experience the effect of confinement within the matrix. Percolation morphology is found to be formed in 10% mixture.

The morphology of PVBPA/PEEK copolymer is found to be important to conduct proton in an efficient manner. The structure, topology, and connectivity of such polymer segments are crucial to determine the extent of pronouncement of the percolation network formed. With different model of copolymer the morphological patterns have been explored systematically. The contribution of each block in forming desired percolating network has been investigated to help chemists to synthesize copolymers having more efficient proton conducting ability.

References:

1. Potschke, P.; Fornes, T. D.; Paul, D. R. *Polymer* 2002, 43, 3247−3255.
2. Starr, F. W.; Knauert, S. T.; Douglas, J. F.J. Polym. Sci., Part B: *Polym. Phys.*2007, 45, 1882−1897.
3. Lozano, K.; Bonilla-Rios, J.; Barrera, E. V. *J. Appl. Polym. Sci.*2001, 80, 1162−1172.
4. Lozano, K.; Barrera, E. V.*J. Appl. Polym. Sci*.2001, 79, 125−133.
5. Subramoney, S.*Adv. Mater.*1998, 10, 1157−1171.

6. Pegel, S.; Potschke, P.; Petzold, G.; Alig, I.; Dudkin, S. M.; Lellinger, D.*Polymer*2008, 49, 974−984.
7. Potschke, P.; Pegel, S.; Villmow, T.; Stoyan, D.; Heinrich, G. *Polymer*2009, 50, 2123−2132.
8. Potschke, P.; Dudkin, S. M.; Alig, I. *Polymer* 2003, 44, 5023−5030.
9. Coleman, J. N.; Curran, S.; Dalton, A. B.; Davey, A. P.; McCarthy, B.; Blau, W.; Barklie, R. C. *Phys. Rev. B* 1998, 58, R7492−R7495.
10. Pisanova, E.Wiley *Encyclopedia of Composites; John Wiley andSons, Inc.: New York*, 2011.
11. Hoogerbrugge, P. J.; Koelman, J. M. V. A. *Europhys. Lett.*1992,19, 155.
12. Groot, R. D.; Warren, P. B.*J. Chem. Phys.* 1997, 107, 4423−4435.
13. Chakraborty, S; Choudhury, C. K.; Roy, S.*Macromolecules*2013, 46, 3631−3638.
14. Chakraborty, S.; Roy, S.*J. Phys. Chem. B*2012, 116, 3083−3091.
15. Roy, S.; Markova, D.; Kumar, A.; Klapper, M.; Müller-Plathe, F. *Macromolecules* 2009, 42, 841−848.
16. Van Der Spoel, D.; Lindahl, E.; Hess, B.; Groenhof, G. *J. Comput. Chem*. 2005, 26, 1701−1718.
17. Hess, B.; Kutzner, C.; van der Spoel, D.; Lindahl, E.*J. Chem. Theory Comput*. 2008, 4, 435−447.
18. Seaton, M. A.; Anderson, R. L.; Metz, S.; Smith, W. *Mol. Simulat*. 2013, 39, 796–821.
19. Karplus, M.; Bartels, C.*J. Phys. Chem. B* 1998, 102, 865−880.
20. Bevan, D. R.; Lemkul, J. A.*J. Phys. Chem. B* 2010, 114, 1652−1660.
21. Rosenberg, J. M.; Kumar, S.; Bouzida, D.; Swendsen, R. H.; Kollman, P. A.*J. Comput. Chem*. 1992, 13, 1011−1021.
22. Schuster, M.; Kreuer, K. D.; Steininger, H.; Maier, *J.Solid State Ionics* 2008, 179, 523.
23. Hickner, M.; Ghassemi, H.; Kim, Y. S.; Einsla, B. R.; McGrath, J. E. *Chem. ReV*. 2004, 104, 4587.

Souvik Chakraborty *is a Ph.D student under the supervision of Dr. Sudip Roy at CSIR-NCL, Pune, India. His research interests are in multiscale simulation of polymer composite materials, study of morphologies and dynamics of nanoparticles under the confinement of block-copolymer matrices, simulation of associating polymers, and adsorption study of large molecules on metal surface by quantum mechanical calculations.*

Dr. Sudip Roy *is chemist by training. He finished his PhD under the supervision of Prof. Dr. Michael Springborg from University of Saarland, Germany in 2006 in Theoretical and Computational Chemistry. He worked as a Post Doctoral Fellow at Technical University Darmstadt, Germany. In his post doctoral research he worked with Prof. Dr. Florian Mueller-Plathe and learned simulation of polymeric system using high performance computing. Since January 2009 he is leading an independent research group at National Chemical Laboratory, Pune, India. His scientific interests cover the research areas, which include, development of multiscale methods for soft matter simulation and its applications in materials, energy and biomolecules.*

Cucurbituril-based Supramolecular Assemblies and their Applications

Jyotirmayee Mohanty and Achikanath C. Bhasikuttan
Radiation & Photochemistry Division, Bhabha Atomic Research Centre,
Mumbai 400 085, India, Emails: jyotim@barc.gov.in (JM) and bkac@barc.gov.in (ACB)

Abstract

The research on the supramolecular chemistry of host-guest complexes based on noncovalent interactions involving a macrocyclic host and a guest has seen an upsurge in recent years due to their various potential applications in metal ion separation, molecular sensors, catalysis, nanomaterials, therapeutics and other stimuli-responsive systems. The noncovalent host-guest assemblies with cucurbiturils bring out spectacular modulation in the physico-chemical properties of the guest molecules such as solubility, stability, aggregation behavior, acidity constants and antibacterial activity. Efforts have also been made to give specific examples of cucurbituril-encapsulated guest assemblies and discuss their dynamic response towards external triggers and applications toward controlled uptake and release of drugs, construction of photofunctional devices, aqueous-based dye lasers, molecular architectures, gas sensors, stimuli-responsive hydrogel, chemoselective photoreactions, biological catalytic activity.

1. Introduction

Supramolecular chemistry is an interdisciplinary field of science involving the chemical, physical and biological features of molecular assemblies having greater complexity and applications than the individual molecules themselves [1]. It is the study of the structures and functions of the supermolecules that result from intermolecular binding interactions of two or more chemical entities in an organized manner [2]. While traditional chemistry focuses on the covalent bond, supramolecular chemistry examines the weaker and reversible non-covalent interactions between molecules. This class of interactions spans a wide range of binding energies and encompasses electrostatic interactions such as hydrogen bonding, dipole-dipole, ion-dipole interactions and hydrophobic interactions such as van der Waals, π-π interactions, dispersion interactions, etc. The dimensions of supramolecular assemblies can range from nanometers to micrometers. Jean-Marie Lehn aptly described supramolecular chemistry as an ''information science''; the instruction set for the creation of a large complex assembly is contained within its constituent components [1]. Nature provides the most spectacular examples of supramolecular chemistry. The enzyme-substrate complex, the DNA structure, its intricate packing and replication mechanisms, protein-protein interactions, are all examples of supramolecular chemistry at work. Supermolecules such as the octahedral iron storage vessel ferritin, for example, is assembled from many smaller repeated subunits that contain precise information for their correct integration into the larger structure [1, 3]. Supramolecular assemblies demonstrate cooperativity which affects both the stability of the cluster and the mechanism of its formation and rearrangement. Detailed mechanistic studies of supramolecular assemblies are important not only for understanding the self-assembly processes but also for designing assemblies for specific applications. For the synthetic chemist, self-assembly represents a powerful synthetic methodology in the creation of large, discrete, ordered structures from relatively simple synthons. Increasingly, the focus is on application of these macromolecular systems to other chemistry problems: selective substrate binding, trapping reactive intermediates or protecting unstable species, influencing reaction chemistry within host cavities, or creating new nanodevices.

One of the major interests in supramolecular chemistry is the design of structurally well-defined architectures with dynamic and stimulus-responsive properties. Dynamic and adaptive supramolecular materials that self-assemble from multiple components will find a range of applications in materials and medicines. A number of fundamental studies in the field of supramolecular chemistry have demonstrated that more intricate and functional materials can be engineered from noncovalent complexes by carefully combining several intermolecular interactions [4]. Chemical interactions between a protein and a drug, or a catalyst and its substrate, or a macrocyclic host and a guest, self-assembly of nanomaterials, and even some chemical reactions, are dominated by noncovalent interactions [5]. The use of a scaffold for self-assembly is a particularly interesting option, since a scaffold can guide the organization of weakly interacting molecules into well-defined self-assembled architectures [6]. These supra-molecules possess ample functionality such as catalytic, photophysical, electronic, or redox properties and are ideal building blocks for sensors, information storage

materials, and nanodevices. In the past decades, scientists have made enormous strides toward creating nanoscale assemblies and structures with aim to achieve applications ranging from targeted drug delivery to the development of functional materials [2, 7-9].

The area of host-guest chemistry encompasses the complexation by organic hosts with a range of both organic and inorganic guests, where the host-macromolecules recognize and encapsulate specific molecules, atoms or ions (guests) to form complexes [3]. In the formation of these complexes, noncovalent intermolecular interactions such as electrostatic interaction, hydrophobic interaction, hydrogen bonding, etc. are utilized to bring selectivity and specificity [3, 10]. That is, for strong host-guest complexation, the host and the guest must be capable of interacting with each other such that the respective binding sites exhibit complementary steric and/or electronic arrangements. An ideal host/guest fit leads to the added stabilization of specific complexes, whereas, a misfit between host and guest may lead to the selective destabilization of a specific assembly and therefore to a selectively enhanced reactivity [11]. Apart from the usual parameters influencing the guest specificity of open chain hosts, cyclic hosts can be further 'tuned' by variation of the macrocyclic cavity size. By this means, a mechanism for discrimination of guests on the basis of their radii may become available. Molecular sensors, synthetic enzymes, separation systems, etc. utilize the high guest selectivity of such host compounds [11].

Since the host-guest complexes are held together by comparatively weak, reversible, non-covalent interactions, the preferential affinity of these forces and the stoichiometric arrangements of the complexes bring out significant modulation in the physico-chemical properties of the guests [10]. These assemblies respond to a range of external stimuli such as light, temperature, pH or ligands and the specific control over the formation and dissociation of the assembly remains challenging as this property is very much akin to the substrate-catalyst (lock-key specificity) binding in many biological systems. These biomimetic properties make synthetic host-guest systems attractive tools for the development of therapeutics and diagnostics. Many attempts have been made over the last few decades to realize such non-covalently linked host-guest complexes using classical synthetic macrocyclic receptors such as cyclodextrins and calixarenes (described below), but limitations often arose due to the stability and solubility of the complexes formed [10]. A relatively new addition to this synthetic macrocyclic hosts is the cucurbit[*n*]uril, showing marked differences in water solubility, guest affinity as well as guest size selectivity, and binding stoichiometry. Especially, the possibility to study these fascinating macrocycles in neutral aqueous solution has attracted enormous attention since applications in many areas, including biology, are now in sight. Moreover, it has become possible to contrast the inclusion properties and binding strengths of cucurbiturils with extensively used macrocyles, such as cyclodextrins and calixarenes. In fact, use of cucurbiturils have several advantages over the other two, such as their low toxicity, high chemical stability, large complexation-induced pK_a shifts, as well as their tight, selective binding [12].

2. Cucurbituril Macrocyclic Hosts

Cucurbit[n]urils (CB*n*), initially discovered by Behrend in 1905 but fully characterized in 1981, are a relatively new class of macrocyclic receptor molecules composed of methylene-bridged glycoluril monomers having highly symmetrical hydrophobic cavities accessible through two identical highly polarizable carbonyl laced portals [13-17]. The pumpkin-shaped cucurbiturils are obtained by acid-catalyzed condensation of glycoluril with formaldehyde under controlled conditions [18-20]. Like cyclodextrins and calixarenes, different homologues of cucurbit[n]urils (commonly abbreviated as CB*n* or in some cases CB[*n*], Q[*n*], Q*n* or Cucn; *n* = 5-10, represents number of glycoluril units in the macrocycle, Fig. 1) with varying cavity and portal dimensions are known (Table 1) [13, 15-17]. Among the set of CBs, the complexation behavior of cucurbit[7]uril (CB7), has been extensively studied due to its appropriate cavity size and portal diameter comparable to the dimension (width) of most small size organic guests and also due to its substantial solublity in water as compared to the other homologues like CB5, CB6, CB8 and CB10. The water solubility of the CBn, in general, can be enhanced in the presence of salts, at low pH, or in the presence of charged guests [13, 17]. All cucurbituril homologues, except CB5, can form much stronger host/guest complexes than cyclodextrins and their binding constants range typically from 10^4 to 10^{15} M^{-1} [17, 21]. Only recently, this class of macrocycles has been shown to exhibit low *in vitro* as well as *in vivo* toxicity, thereby facilitating biologically relevant applications of these macrocycles [16, 22-24].

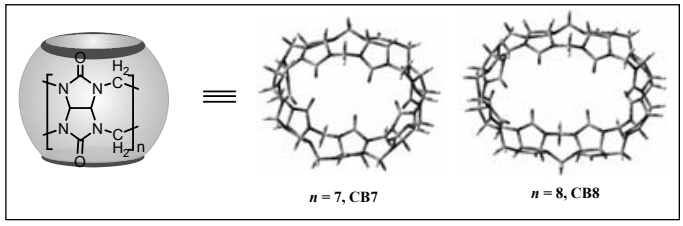

Fig. 1: *Structural formula of CBn (n = 5-10) and energy optimized structures of CB7 and CB8.*

Table 1: Structural parameters for cucurbit [*n*] uril (*n* = 5-8).

Parameters	CB5	CB6	CB7	CB8
Portal diameter (Å)	2.4	3.9	5.4	6.9
Cavity diameter (Å)	4.4	5.8	7.3	8.8
Height (Å)	9.1	9.1	9.1	9.1
Outer diameter (Å)	13.1	14.4	16.0	17.5
Cavity volume ($Å^3$)	82.0	164.0	279.0	479.0

3. Guest Binding and Molecular Recognition Properties of Cucurbiturils

Cucurbiturils have a nonpolar inner cavity which is prone to bind neutral organic residues or guests by hydrophobic interactions. The hydrophobic effect in the course of host–guest complexation is a combination of at least three effects, namely differential dispersion interactions, the desolvation of the guest, and the desolvation of the host, where the latter involves the removal of so-called high-energy water molecules [25]. The electrostatic stabilization is limited to ion-dipole interactions between the two carbonyl portals and the positively charged dyes (frequently as ammonium, iminium, or pyridinium salts) and metal ions [13-15, 17]. CBs also involve in electrostatic hydrogen bonds engaging their carbonyl portals as H-bond acceptor with suitable protonated guest molecules. In general, cucurbiturils favor the binding of cationic guests over neutral ones [10, 13, 15, 17].

Among the CB homologues, going from CB5 to CB10 and CB14, the cavity size increases gradually with a constant height (9.1 Å). Though they have similar structural features, their varying inner and portal diamensions lead to remarkable molecular recognition behavior with various organic guest molecules which are different from each other. Except the smaller homologue CB5, all the higher CB homologues encapsulate the guest molecules to form inclusion host-guest complexes with unprecedented physico-chemical properties [10, 26]. CB6 and CB7 forms stable inclusion complexes with guest molecules like diaminoalkanes, benzyl amines, adamantyl amine, methyl viologen cations, fluorescent dyes, metal ions, metal nanoparticles, etc. through complete or partial encapsulation of the guest molecules [13, 15-17, 27-29]. For example, CB7 forms 1:1 complex with organic guest molecules like coumarin 1 (C1), coumarin 481, neutral red, acridine orange, rhodamine 6G (Rh6G), Rhodamine B (RhB), cetylpyridinium chloride, etc. [15, 27, 30-34]. On the other hand, the cavity of CB8 is large enough to accommodate more than one guest molecules to form multiple/higher order host-guest complexes. It forms 1:2 host-guest complexes with two similar guests like neutral red, thioflavin T, *p*-dimethylaminobenzonitrile, etc. or 1:1:1 ternary complexes with two different guest molecules like the combination of tryptophan and neutral red [35-37]. Interestingly CB10, the relatively larger CB homologue reported, is capable of encapsulating the smallest homologue, CB5 [38] and also large chromophores like metalated tetra(N-methylpyridinium)porphyrins [39] through its large ellipsoidal cavity [15]. All the CB*n* bind to alkali and alkaline earth metal ions via their two carbonylated portals, where, most metals interact with only a fraction of the oxygen atoms at the CB*n* rim and accordingly, several cations may occupy the same portal. In the case of transition metal ions, they do not interact directly with the oxygens of the carbonyl groups of CB*n*. The binding generally takes place between the carbonyl groups and the coordinated water molecules of the metal aqua complexes [16]. Redox-active polyoxovanadate and polyoxotungstate anion clusters interact strongly with the equatorial periphery of CB6 and CB8 [40].

4. Prospects of Cucurbituril based Supra-molecular Assemblies

The effect of molecular encapsulation by macrocyclic hosts on the properties of organic guest molecules is an area of immense current interest. Extensive research activities in the recent past have documented a variety of applications such as in drug binding and delivery systems [41-43], supramolecular architectures [8, 44] and in supramolecular functional materials [33, 45-47] and in catalytic/enzymatic activities [48, 49]. All these were possible mainly due to the drastic changes in the physico-chemical properties of the involved guests on complexation with cucurbiturils and prospective applications of some of these supramolecular assemblies have been discussed in the following sections.

Organic compounds such as fluorescent dyes often face issues associated with dye aggregation, stability, medium of usage, disposal etc. Increasing the photostability of fluorescent dyes either by using additives or by structural modification is extremely essential for their technological and biological applications [50]. In general, for most of the cationic laser dyes, photostability is apparently low. In principle, this problem can be reduced by supramolecular encapsulation strategy that isolate the individual dye molecules and prevent self-aggregation or other destabilizing interactions with the surrounding environment. In the presence of cucurbiturils (CBs), the thermal stability of xanthene dyes in aqueous solution increases due to the combination of favorable effects like deaggregation, desorption and enhanced solubilization of

the dyes on their complexation with CB hosts [15, 51]. The complexation is in general accompanied with significant spectral shifts, enhanced fluorescence quantum yields and increased fluorescence lifetimes of the dyes. These added features are due to the inclusion of the dye in a less polar and low polarizability environment of CB7 cavity compared to bulk water, as well as due to structural confinement. On the other hand, these features can be exploited suitably for many potential applications involving the chromophoric guest molecules [15, 51].

4.1. Aqueous Dye Laser

Enhanced stability, increased solubility and prevention of aggregation/adsorption of organic dyes in aqueous solution are the crucial parameters for a dye laser system and is nicely demonstrated by the operation of a supramolecularly assisted aqueous dye laser system of rhodamine dyes with CB7 as the macrocyclic host additive [33, 52]. The effect of CB7 on the performance

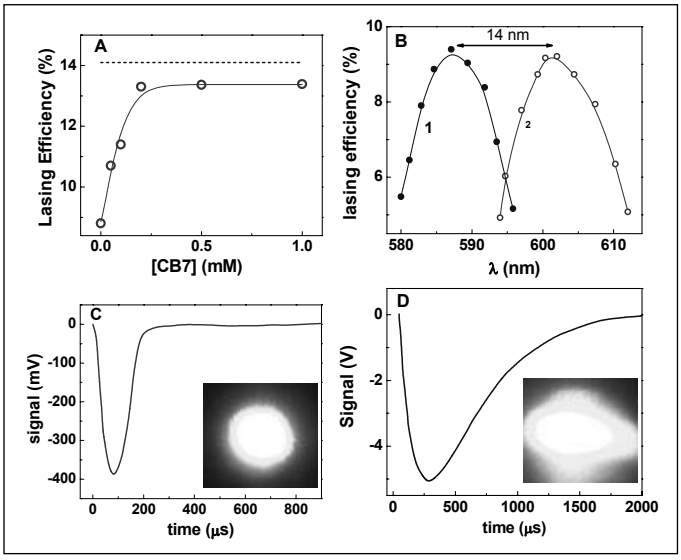

Fig. 2: (A) Dependence of the lasing efficiency of KR (200 μM) on CB7 concentration. Shown for comparison (dashed line) is the lasing efficiencies of KR in optically matched ethanol solutions. (B) Tuning curves of KR in EtOH (1) and in the presence of 200 μM CB7 (2) at a pump energy of 6.3 mJ. Thermal deflection signals of KR in water-CB7 (C) and in EtOH (D) systems. Insets of C and D show the laser beam profiles for the respective medium.

of aqueous kiton red (KR) dye solution has been investigated by both broad-band and narrow-band dye laser set-ups with respect to the practically relevant parameters like lasing efficiency, lasing stability and beam quality. Large increase in lasing efficiency is observed with addition of micromolar concentration of CB7 to the aqueous solution of kiton red dye (Fig. 2), predominantly due to the deaggregating action of CB7 on the dye [15, 33]. The resulting supramolecular dye lasers are environmentally more benign, more laboratory-safe, and less maintenance-sensitive than the presently employed dye laser systems based on organic solvents. The novel aqueous dye-CB7 systems are not only equally efficient with complementary tuning ranges, but also possess superior thermo-optic characteristics and unmatched beam profiles (Fig. 2), which should jointly enable new and revived photonic applications based on such dye lasers [15, 33].

4.2. Supramolecular pK_a Shift

The prototropic equilibrium of dyes can be significantly altered upon complexation with macrocyclic hosts due to the differential binding affinty of the host molecules towards the different prototropic forms of the dyes. This property is useful in medicinal and biological applications to achieve controlled binding and release of the active form of the drugs. Upward pK_a shifts are frequently observed for weakly basic molecules in the presence of cation-receptor or hydrogen bond-acceptor hosts, while downward pK_a shifts are expected for anion-receptor or hydrogen bond-donor host molecules, or those offering a nonpolar cavity [24].

Cucurbiturils, which act as cation receptors, preferentially stabilize the protonated form of guest molecules and therefore increase the pK_a values of the conjugate acids of amines. The effect of cucurbituril on the guest molecule is through affecting the protonation without the necessity of adjusting the pH. The binding constants of the guest molecules in their different protonation states depend on their complexation induced pK_a shifts [15, 31].

4.2.1. Salt-induced pK_a Tuning and Guest Relocation

Employing the competitive binding strategy, the pK_a value of the complexed guest shifted gradually towards that of the free guest upon increasing the concentration of the salt, confirming a tunability essentially over the entire range of pK_a of the free dye to that of CB7:dye complex. Use of supramolecular pK_a shift towards drug delivery applications has been demonstrated in a biological environment where the unprotonated dye would tend to be noncovalently bound to a protein, whereas the protonated dye prefer the CB7 host. In the presence of inorganic cations, the guest molecule (the dye, neutral red (NR) is used as a model for a drug) could be actively released from the CB7 host cavity and relocated into the hydrophobic cavity of the protein, namely BSA (Fig. 3) [41]. Therefore, presence of salts provides a simple stimulus to release the drug from the macrocyclic cavity for biological/medicinal activity.

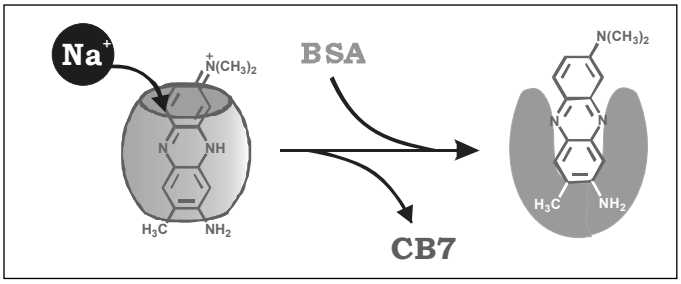

Fig.3: This scheme shows the salt-induced transfer of a dye from CB7 to BSA near pH 7.5.

4.3. Fluorescent Supramolecular Capsule and its Rupture

The formation of a novel stimulus-responsive and highly *fluorescent supramolecular nanocapsule* through the cooperative metal ion binding to the stoichiometrically selected cucurbit[7]uril-thioflavin T complex (Fig. 4A) [45] has been demonstrated. The first example of such an unusual assembly became feasible due to the stoichiometry and the structural arrangement of the host-guest complex with two CB7 portals providing strong negative charge density for the metal ions to group and seals the complex, thus rigidizing and protecting the incorporated dye. The rupture of the capsular complex was demonstrated with a strong competitive guest, 1-amantadine hydrochloride, which helped in disrupting the capsule to release the dye (Fig. 4B) [45]. By proper design criteria of the guest chromophores, the methodology can be explored for the binding and release of drug molecules and for application in on-off systems and will have immense potential as building blocks for molecular architectures displaying unique properties.

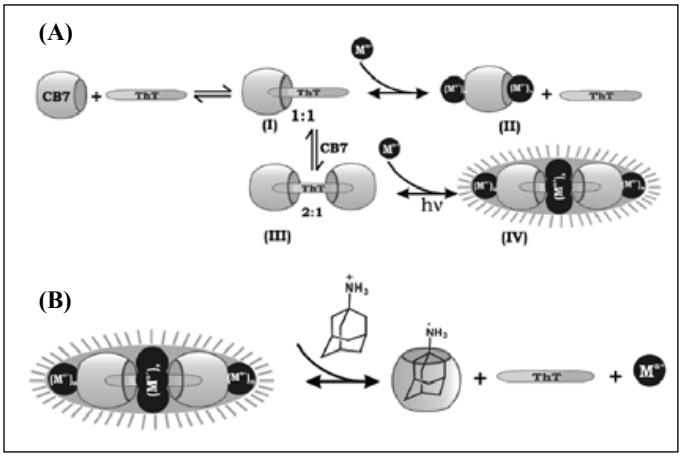

Fig. 4: (A) Proposed binding interactions in the ThT, CB7 and metal ion system leading to the highly fluorescent supramolecular capsule and (B) release mechanism of ThT from the metal ion bound supramolecular capsule by amantadine hydrochloride as the stimulant.

4.4. Supramolecular Gas-Sensing Ensemble

Nau and co-worker have established a highly sensitive fluorescence-based method for the quantification of volatile hydrocarbons binding with cucurbituril [53]. The working principle for gas sensing is depicted in Figure 5. Starting from the pre-assembled highly fluorescent host–dye complex by using a microenvironmentally sensitive 1-naphtylamine-5-sulfonic acid chromophore dye and cucurbit[6]uril (CB6) host, the addition of gas results (with an immediate onset signaling fast exchange on the time scale of the experiment) in a continuous displacement of the dye until the saturation limit has been achieved [53]. Volatile hydrocarbons bind very tightly and selectively to cucurbituril in water. From the final plateau of the fluorescence intensity and the accurately known aqueous solubility of the volatile hydrocarbons, the binding constants were directly calculated by assuming a 1:1 complexation stoichiometry. They also reported a set of binding constants of hydrocarbons with CB6, which is the most extensive one so far obtained for the binding of nonpolar neutral guests with cucurbiturils [53]. This is a convenient method to monitor volatile hydrocarbon binding to CB6 by employing indicator displacement strategy.

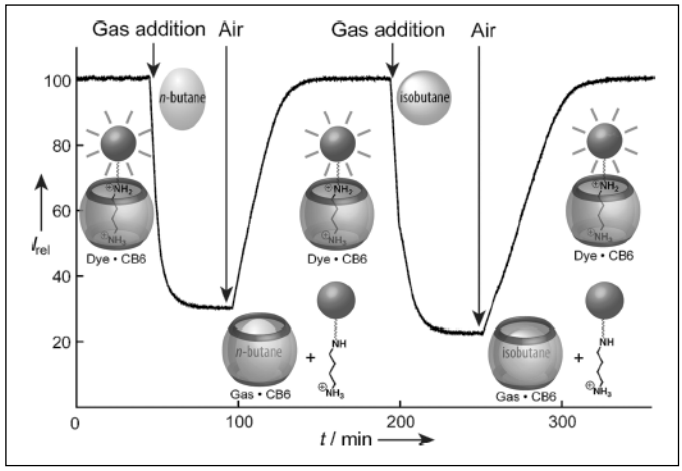

Fig.5: Fluorescence-based approach for gas sensing in aqueous solution. The trace refers to actual experiments with sequential uptake and release of n-butane and isobutane.

4.5. Supramolecular Velcro for Reversible Underwater Adhesion

Underwater adhesion is a challenging task for most synthetic adhesives. Kim et al reported the synthesis of supramolecular "velcro" – a new approach for achieving strong, mechanically reversible and chemically switchable macroscale underwater adhesion based on the ultrahigh-affinity host–guest binding pair [46]. The host- and guest-molecule anchored loop and hook surfaces of the

supramolecular velcro were synthesized by conjugating the CB7 and aminomethylferrocene (Fc) moieties, respectively, to the polymer grafted silicon surface. The strategy, using a velcro or "hook-and-loop fastener" type mechanism, involves functionalizing two separate silicon surfaces ([Si]): a "loop" surface functionalized with CB7 hosts and a "hook" surface with ferrocene (Fc guests) (Fig. 6) [46]. The CB7 loops and Fc hooks form a supramolecular velcro, which adheres in water without any need of curing agents. The velcro exhibits excellent holding power and lap shear adhesion strength, which can be tuned by controlling the density of Fc hooks. This strategy offers both mechanical reversibility and chemical switchability at the macroscopic level. The noncytotoxic nature of CB7 and Fc permits potential biological applications. In addition, the redox-active nature of the Fc moiety is promising for the development of controlled electroactive adhesive materials in aqueous environment.

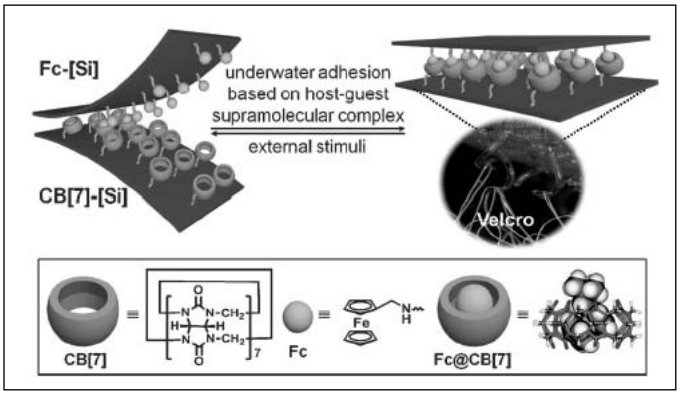

Fig. 6: *Supramolecular velcro or hook-and-loop strategy for underwater adhesion based on CB7- and Fc-modified surfaces. In an aqueous environment, the surfaces strongly adhere with each other through ultra-high affinity host–guest interactions, which is similar to commercial Velcro or hook-and-loop fastener (optical microscope image of commercial Velcro). The supramolecular velcro can be unfastened by mechanical and chemical means and fastened again.*

4.6. Multistimuli-responsive Supramolecular Hydrogels

Hydrogels are three-dimensional networked materials that are similar to soft biological tissues and have highly variable mechanical properties, making them increasingly important in a variety of biomedical and industrial applications. Appel *et al*. reported the preparation of extremely high water content hydrogels (up to 99.7% water by weight) driven by strong host−guest complexation with cucurbit[8]uril (CB8) [47]. Cellulosic derivatives and commodity polymers such as poly(vinyl alcohol) were modified with strongly binding guests for CB8 ternary complex formation (K_{eq} = 10^{12} M^{-2}). When these polymers were mixed in the presence of CB8, whereby the overall solid content was 90% cellulosic, a lightly colored, transparent hydrogel was formed instantaneously (Fig. 7A) and the schematic representation of the hydrogel formation is given in Fig. 7B [47]. The supramolecular nature of these hydrogels afforded the material with highly tunable mechanical properties, and the dynamics of the CB8 ternary complex cross-links provided rapid self-healing of the damage caused by any deformation. Moreover, these hydrogels display responsivity to a multitude of external stimuli, including temperature, chemical potential, and competing guests [47]. These materials can be easily processed, and the simplicity of their preparation, their availability from inexpensive renewable resources, and the tunability of their properties are encouraging features for many important water-based applications.

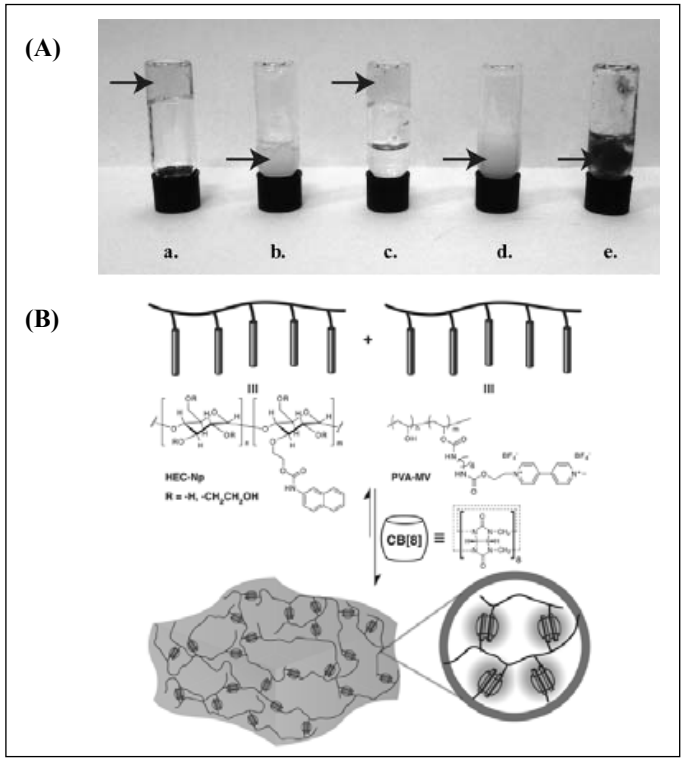

Fig. 7: *(A) Hydrogels formed from (a) HEC-Np (0.5 wt %)/PVA-MV (0.1 wt %)/CB[8] (1 equiv) have variable responsiveness to perturbation in the presence of (b) toluene, (c) hexane, and (d) a competitive second guest (2,6-dihydroxynaphthalene) and also demonstrates responsiveness to (e) sodium dithionite reducing agent. In the case of (c) the intact hydrogel (indicated by the arrow) can be seen with its original color, while the hexane layer has flowed to the bottom of the vial. (B) Schematic representation of a supramolecular hydrogel prepared through addition of cucurbit[8]uril to a mixture of multivalent first- and second-guest-functionalized polymers in water.*

4.7. Transition-Metal-Promoted Chemoselective Photoreactions

In a recent report, Nau et al. have demonstrated a chemoselective transformation of included guests promoted by transition-metal ions coordinated to the

cucurbituril rim [48]. They have considered a two-phase system (Fig. 8), in which the host CB7 acts as an inverse phase-transfer catalyst to bind a photoreactive substrate i.e. bicyclic azoalkanes 2,3-diazabicylo[2.2.2]oct-2-ene (DBO) and 2,3- diazabicylo[2.2.1]hept-2-ene (DBH) by hydrophobic interactions in the aqueous phase and allows the subsequent docking of transition metal ions to the carbonyl rim through ion–dipole interactions. The resulting ternary self-assembly is synergistically reinforced by weak metal–ligand bonding interactions, which affect the chemoselectivity in the spatially resolved laser photolysis of the aqueous phase. A new photoproduct i.e. cyclopentene (41%) was obtained from the DBH·CB7·Ag^+ ternary complex on photoirradiation [48]. The presence of the macrocycle is, indeed, essential to produce cyclopentene, since even the photolysis of DBH in the presence of 1M $AgNO_3$ did not lead to this unexpected cyclopentene (CP) product. It is evident that Ag^+ ions promote the photochemical formation of CP inside CB7. This reveals the potential for metal catalysis at the cucurbituril rim and the concomitant exploitation of the same macrocycles as inverse phase-transfer catalysts [48].

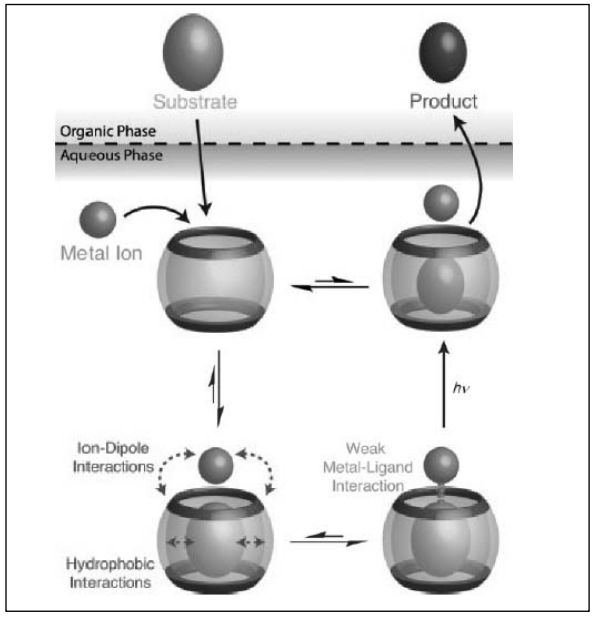

Fig. 8: Dynamic self-assembly of a ternary guest/host/metal-ion complex and the transition-metal-promoted photoreaction.

4.8. Cucurbit[7]uril-Regulated Biological Catalysis

Isaacs et al. have used the high binding affinity of CB7 towards its guest to control the catalytic activity of bovine carbonic anhydrase (BCA) [49]. They have synthesized a two-faced inhibitor (**1**; Fig. 9) that contains a benzenesulfonamide unit that binds to the Zn co-factor of BCA and inhibits catalytic activity and an ammonium ion unit that binds to CB7 [54]. Addition of CB7 to BCA•**1** results in the transient formation of the BCA•**1**•CB7 ternary complex that undergoes rapid dissociation to form free catalytically active BCA along with CB7•**1** complex (Fig. 9). The on-off cycle can be performed repetitively by the sequential addition of competitive guest and CB7. The detailed origin of this on-off switching of the catalytic activity of BCA is delineated by the combined inference of UV/vis catalytic assays, fluorescence displacement assays and ^{1}H NMR. In this manner CB7 can be used to control the biological catalytic activity.

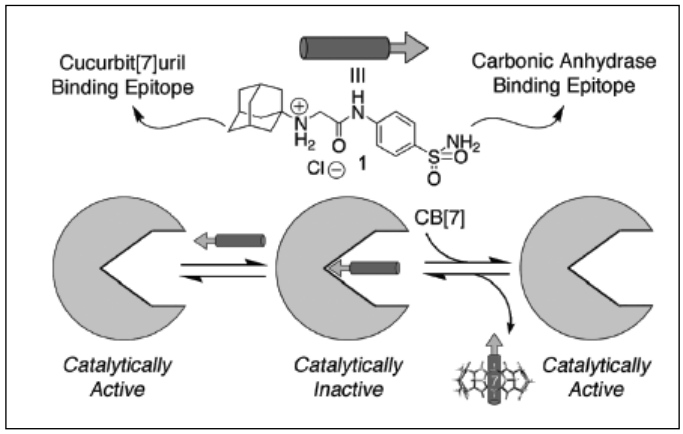

Fig. 9: Regulation of bovine carbonic anhydrase catalytic activity.

4.9. Cucurbiturl-based Photosensitizers with Enhanced Antibacterial Efficiency

Liu et al. fabricated a novel supramolecular photosensitizer by utilizing the strong host–guest interaction between cucurbit[7]uril (CB7) and naphthalene–methylpyridinium moiety of porphyrin (TPOR) which shows a greatly improved antibacterial efficiency [55]. The fabrication of the supramolecular photosensitizer is facile, highly efficient, environmentally friendly and has greatly decreased the number of required synthetic steps. In addition, it also allows for an adaptive system with switchable photophysical properties. The bulky CB7 "noncovalent substituents" in the supramolecular photosensitizers have ensured a dramatically increased efficiency for the $^1O_2$ generation of the porphyrins, regardless of aggregation at high concentrations. These photosensitizers can attain an elevated concentration of local $^1O_2$ when irradiated by white light (Fig. 10), leading to an improved photocytotoxicity for application in photodynamic therapy. The antibacterial activities of TPOR and TPOR/$(CB7)_4$ toward Escherichia coli (E. coli), a Gram-negative bacteria have been investigated by a traditional surface plating method. The E. coli was incubated with TPOR and TPOR/$(CB7)_4$, respectively, in the dark at a fixed concentration of porphyrin sensitizer, after which

the bacteria were illuminated with a white light at a flux rate of 25 mW cm^{-2} for the duration of 40 s (corresponding to fluences of 1 J cm^{-2}). Colony counting shows that the inhibition ratio towards E. coli is about 17% for TPOR, whereas the value increases to 97% for the TPOR/$(CB7)_4$ supramolecular photosensitizers (Fig. 11) [55]. Thus, the antibacterial efficiency is greatly enhanced after the porphyrins have been incorporated into the supramolecular photosensitizers. The result is consistent with the enhanced $^1O_2$ generation of the supramolecular photosensitizers, indicating that the improved antibacterial efficiency should be ascribed to the enhanced ability of porphyrins to sensitize oxygen. The TPOR/$(CB7)_4$ supramolecular photosensitizer is amongst the most efficient porphyrin-based antibacterial photodynamic therapy (PDT) systems reported to date, in terms of the low porphyrin concentration and low fluences of light energy required [55]. It is predicted that such supramolecular photosensitizer might also be effective for improving the anticancer properties of porphyrins or other photosensitizers in photodynamic therapy systems.

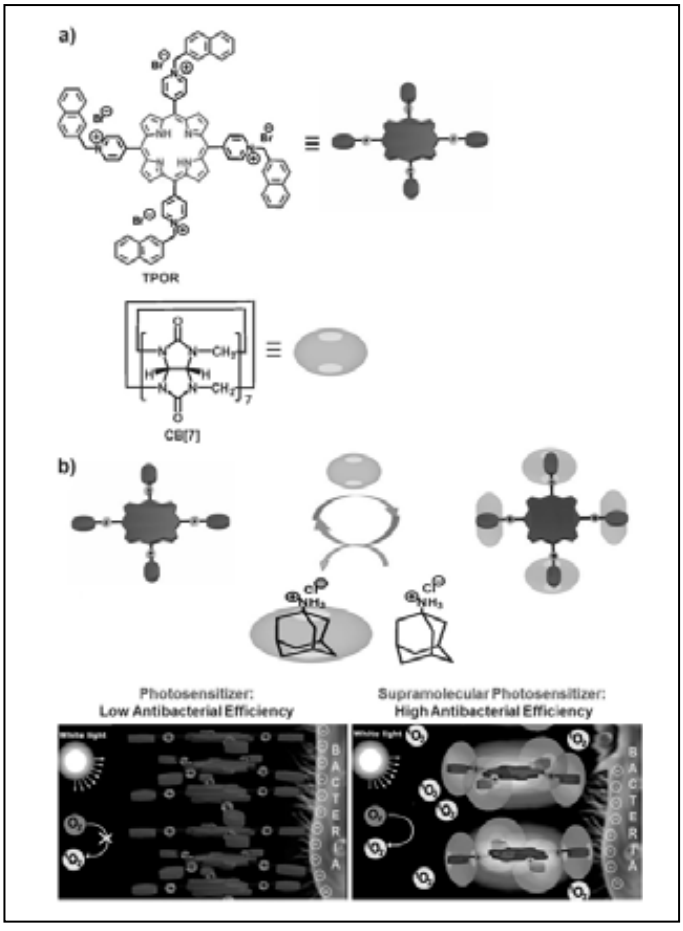

Fig. 10: *a) Chemical structures of the TPOR (photosensitizers) and CB7. b) The construction of TPOR/$(CB7)_4$ supramolecular photosensitizers and the mechanism for the enhanced antibacterial efficiency of TPOR/$(CB7)_4$ compared with that of TPOR.*

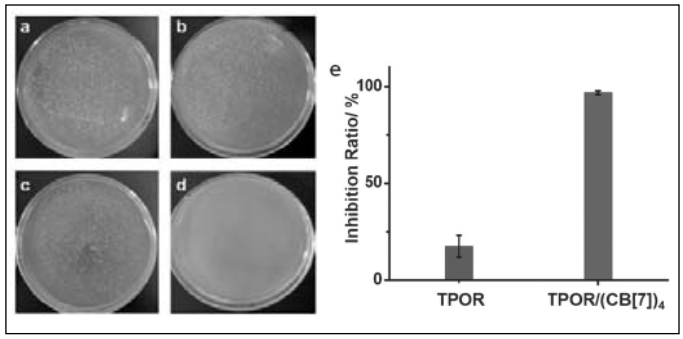

Fig. 11: *Plate photographs for E. coli on YTD agar plate treated with a) TPOR in the dark, b) TPOR under photo-irradiation, c) TPOR/$(CB7)_4$ in the dark, d) TPOR/$(CB7)_4$ under photoirradiation, and e) biocidal activities of TPOR and TPOR/$(CB7)_4$ toward E. coli. The values represent the mean standard deviation of three separate experiments. The error bars represent standard deviations of data from three separate measurements. The concentration of TPOR is fixed at 7.2×10^{-7} M for killing E. coli.*

4.10. Surface Functionalized Silver Nanoparticle Conjugates

Surface modification of metal or metal oxide nanoparticles is an actively pursued protocol to gain control over their size, shape and stability as well as for modulation of surface plasmonic features which are inherently related to the potential applications based on these nanomaterials. A facile supramolecular approach to prepare size controlled and stable surface functionalized silver nanoparticle (CB7-AgNPs) conjugates (down to ~5 nm) in the presence of CB7 has been established, where portal features of CB7 provide control on the nanoparticle size [29]. Due to the presence of several surface attached CB7 receptors, these CB7-AgNPs have been explored to demonstrate the uptake and stimulus responsive release (Fig. 12) of a phototherapeutic porphyrin dye, 5,10,15,20-tetrakis(4-N-methylpyridyl) porphyrin (TMPyP) [29], which find enormous biomedical applications in drug delivery and therapeutics.

5. Perspectives and Outlook

Development of new applications of noncovalent molecular assemblies constructed through host-guest

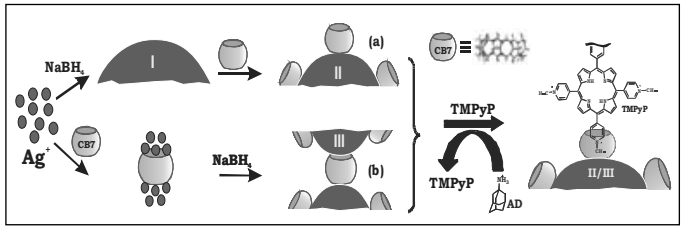

Fig. 12: *Schematic representation of the silver nanoparticles proposed in post (**a**) and pre (**b**) addition of CB7 and the recognition and release mechanism for TMPyP. I, II and III represents the Type I, Type II and Type III particles, respectively.*

interaction has received much attention in the area of supramolecular chemistry. The modulation of the physico-chemical properties of small organic guest molecules achieved through the encapsulation using cucurbituril homologues have been exploited to demonstrate fluorescence based sensors, water-based supramolecular dye lasers, molecular capsule, drug delivery systems, catalysis, etc. The variation of cavity dimensions in the homologues of cucurbituril has revealed many intriguing supramolecular structural forms and their chemistry. There is ample scope to introduce substituted/functionalized CB*n*, which will have different/controlled guest binding behaviour and may offer new opportunities for targeted applications. The association complexes between the pharmacologically relevant guests and functionalized CB*n* are of particular interest in relation to the improvements of drug stability and its *on demand* delivery. The non-covalent nature of the binding interactions makes it quite convenient to tune the molecular properties of the guest species through a wide range of stimuli, such as, competitive binders, temperature, light, redox control, etc. [41, 45, 56]. This has attracted immense research interest due to its tremendous potential in constructing sensors, on-off switches [35, 57, 58], substrate selective tandem assays [59, 60], controlled uptake and release actions for drug delivery, especially considering the low toxicity of cucurbituril hosts [14, 24, 41, 45]. All these features have tremendous prospects in the development of custom-made photofunctional materials. The interactions between metal ions and cucurbituril host–guest complexes hold promise for nanoreactors and metalloenzyme models, when inert metal ions are replaced by transition metal ions with redox activity or catalytic properties [45, 61]. In addition, host-functionalized metal nanoparticles provide the opportunity to modulate their electronic and optical properties, and can largely affect their catalytic, molecular recognition and sensing behaviors. These nanocomposite systems will find applications for cellular activation or therapeutics, and have great challenges in the field of supramolecular chemistry.

Acknowledgements

We sincerely acknowledge the contributions of all the co-authors and collaborators of our published works. We also thank the colleagues in RPCD and Chemistry Group, BARC for their constant encouragement and support.

References

1. J.-M. Lehn, *Supramolecular Chemistry: Concepts and Perspectives*, VCH Verlagsgesellschaft mbH D-69451, Weinheim, Germany, 1995.
2. J.-M. Lehn, *Science* **227**, (1985), 849-856.
3. J. W. Steed, J. L. Atwood, *Supramolecular Chemistry*, John Wiley & Sons Ltd., Chichester, U.K., 2009.
4. C. Wang, S. Yin, S. Chen, H. Xu, Z. Wang, X. Zhang, *Angew. Chem., Int. Ed.* **47**, (2008), 9049-9052.
5. E. R. Johnson, S. Keinan, P. Mori-Sa´nchez, J. Contreras-Garcı´, A. J. Cohen, W. Yang, *J. Am. Chem. Soc.* **132**, (2010), 6498-6506.
6. F. Versluis, I. Tomatsu, S. Kehr, C. Fregonese, A. W. J. W. Tepper, M. C. A. Stuart, B. J. Ravoo, R. I. Koning, A. Kros, *J. Am. Chem. Soc.* **131**, (2009), 13186-13187.
7. M. J. Frampton, H. L. Anderson, *Angew. Chem. Int. Ed.* **46**, (2007), 1028-1064.
8. Y. H. Ko, E. Kim, I. Hwang, K. Kim, *Chem. Commun.*, (2007), 1305-1315.
9. A. V. Davis, R. M. Yeh, K. N. Raymond, *Proc. Natl. Acad. Sci.* **99**, (2002), 4793-4796.
10. J. Mohanty, S. Dutta Choudhury, N. Barooah, H. Pal, A. C. Bhasikuttan, in *Elsevier Reference Module in Chemistry, Molecular Sciences and Chemical Engineering* (Ed.: J. Reedjik), Elsevier, Waltham, MA, 2014, DOI: 10.1016/B978-0-12-409547-2.11028-5.
11. P. Comba, B. Martin, *Macrocyclic Chemistry: Current Trends and Future Perspectives*, Springer, Netherlands, 2005.
12. W. M. Nau, O. A. Scherman, *Isr. J. Chem.* **51**, (2011), 492 - 494.
13. J. W. Lee, S. Samal, N. Selvapalam, H.-J. Kim, K. Kim, *Acc. Chem. Res.* **36**, (2003), 621-630.
14. R. N. Dsouza, U. Pischel, W. M. Nau, *Chem. Rev.* **111**, (2011), 7941-7980.
15. A. C. Bhasikuttan, H. Pal, J. Mohanty, *Chem. Commun.* **47**, (2011), 9959-9971.
16. E. Masson, X. Ling, R. Joseph, L. Kyeremeh-Mensah, X. Lu, *RSC Advances* **2**, (2012), 1213-1247.
17. J. Lagona, P. Mukhopadhyay, S. Chakrabarti, L. Isaacs, *Angew. Chem. Int. Ed.* **44**, (2005), 4844-4870.
18. C. Marquez, F. Huang, W. M. Nau, *IEEE Trans. Nanobiosci.* **3**, (2004), 39-45.
19. A. Day, A. P. Arnold, R. J. Blanch, B. Snushall, *J. Org. Chem.* **66**, (2001), 8094-8100.
20. J. Kim, I. S. Jung, S. Y. Kim, E. Lee, J. K. Kang, S. Sakamoto, K. Yamaguchi, K. Kim, *J. Am. Chem. Soc.* **122**, (2000), 540-541.
21. S. Liu, C. Ruspic, P. Mukhopadhyay, S. Chakrabarti, P. Y. Zavalij, L. Isaacs, *J. Am. Chem. Soc.* **127**, (2005), 15959-15967.
22. V. D. Uzunova, C. Cullinane, K. Brix, W. M. Nau, A. I. Day, *Org. Biomol. Chem.* **8**, (2010), 2037-2042.
23. G. Hettiarachchi, D. Nguyen, J. Wu, D. Lucas, D. Ma, L. Isaacs, V. Briken, *PLoS One* **5**, (2010), e10514.
24. I. Ghosh, W. M. Nau, *Adv. Drug Deliv. Rev.* **64**, (2012), 764-783.
25. F. Biedermann, V. D. Uzunova, O. A. Scherman, W. M. Nau, A. D. Simone, *J. Am. Chem. Soc.* **134**, (2012), 15318−15323.
26. K. I. Assaf, W. M. Nau, *Chem. Soc. Rev.*, 44, (2015), 394-418.
27. A. C. Bhasikuttan, S. Dutta Choudhury, H. Pal, J. Mohanty, *Isr. J. Chem.* **51**, (2011), 634-645.
28. N. Barooah, J. Mohanty, H. Pal, A. C. Bhasikuttan, *Phys. Chem. Chem. Phys* **13**, (2011), 13117-13126.

29. N. Barooah, A. C. Bhasikuttan, V. Sudarsan, S. Dutta Choudhury, H. Pal, J. Mohanty, *Chem. Commun.* **47**, (2011), 9182-9184.
30. N. Barooah, J. Mohanty, H. Pal, A. C. Bhasikuttan, *Org. Biomol. Chem.* **10,** (2012), 5055-5062.
31. J. Mohanty, A. C. Bhasikuttan, W. M. Nau, H. Pal, *J. Phys. Chem. B* **110**, (2006), 5132-5138.
32. M. Shaikh, J. Mohanty, P. K. Singh, W. M. Nau, H. Pal, *Photochem. Photobiol. Sci.* **7**, (2008), 408-414.
33. J. Mohanty, K. Jagtap, A. K. Ray, W. M. Nau, H. Pal, *ChemPhysChem* **11**, (2010), 3333-3338.
34. S. Dutta Choudhury, N. Barooah, V. K. Aswal, H. Pal, A. C. Bhasikuttan, J. Mohanty, *Soft Matter* **10**, (2014), 3485-3493.
35. J. Mohanty, S. Dutta Choudhury, H. P. Upadhyaya, A. C. Bhasikuttan, H. Pal, *Chem. Eur. J.* **15**, (2009), 5215-5219.
36. M. Shaikh, S. Dutta Choudhury, J. Mohanty, A. C. Bhasikuttan, H. Pal, *Phys. Chem. Chem. Phys.* **12**, (2010), 7050-7055.
37. M. Sayed, F. Biedermann, V. D. Uzunova, K. I. Assaf, A. C. Bhasikuttan, H. Pal, W. M. Nau, J. Mohanty, *Chem. Eur. J.* **21, (2015), 691-696.**
38. A. I. Day, R. J. Blanch, A. P. Arnpld, S. Lorenzo, G. R. Lewis, I. Dance, *Angew. Chem. Int. Ed.* **41**, (2002), 275-277.
39. S. Liu, A. D. Shukla, S. Gadde, B. D. Wagner, A. E. Kaifer, L. Isaacs, *Angew. Chem. Int. Ed.* **47**, (2008), 2657-2660.
40. X. Fang, P. Kogerler, L. Isaacs, S. Uchida, N. Mizuno, *J. Am. Chem. Soc.* **131**, (2009), 432-433.
41. M. Shaikh, J. Mohanty, A. C. Bhasikuttan, V. D. Uzunova, W. M. Nau, H. Pal, *Chem. Commun.*, (2008), 3681-3683.
42. C. P. Carvalho, V. D. Uzunova, J. P. D. Silva, W. M. Nau, U. Pischel, *Chem. Commun.* **47**, (2011), 8793-8795.
43. N. Saleh, A. L. Koner, W. M. Nau, *Angew. Chem. Int. Ed.* **47**, (2008), 5398-5401.
44. J. Mohanty, A. C. Bhasikuttan, S. Dutta Choudhury, H. Pal, *J. Phys. Chem. B (Letts.)* **112**, (2008), 10782-10785.
45. S. Dutta Choudhury, J. Mohanty, H. Pal, A. C. Bhasikuttan, *J. Am. Chem. Soc.* **132**, (2010), 1395-1401.
46. Y. Ahn, Y. Jang, N. Selvapalam, G. Yun, K. Kim, *Angew. Chem. Int. Ed.* **52**, (2013), 3140-3144.
47. E. A. Appel, X. J. Loh, S. T. Jones, F. Biedermann, C. A. Dreiss, O. A. Scherman, *J. Am. Chem. Soc.* **134**, (2012), 11767−11773.
48. A. L. Koner, C. Marquez, M. H. Dickman, W. M. Nau, *Angew. Chem. Int. Ed.* **50**, (2011), 545-548.
49. S. Ghosh, L. Isaacs, *J. Am. Chem. Soc.* **132**, (2010), 4445-4454.
50. C. Eggeling, J. Widengren, R. Rigler, C. A. M. Seidel, *Anal. Chem.* **70**, (1998), 2651-2659.
51. A. L. Koner, W. M. Nau, *Supramol. Chem.* **19**, (2007), 55-66.
52. J. Mohanty, H. Pal, A. K. Ray, S. Kumar, W. M. Nau, *ChemPhysChem* **8**, (2007), 54-56.
53. M. Florea, W. M. Nau, *Angew. Chem. Int. Ed.* **50**, (2011), 9338 -9342.
54. L. Isaacs, *Isr. J. Chem.*, (2011), 578-591.
55. K. Liu, Y. Liu, Y. Yao, H. Yuan, S. Wang, Z. Wang, X. Zhang, *Angew. Chem. Int. Ed.* **52**, (2013), 8285 –8289.
56. A. C. Bhasikuttan, J. Mohanty, W. M. Nau, H. Pal, *Angew. Chem. Int. Ed.* **46**, (2007), 4120-4122.
57. R. Wang, L. Yuan, H. Ihmels, D. H. Macartney, *Chem. Eur. J.* **13**, (2007), 6468-6473.
58. R. Wang, L. Yuan, D. H. Macartney, *Chem. Commun.*, (2005), 5867-5869.
59. A. Hennig, H. Bakirci, W. M. Nau, *Nature Methods* **4**, (2007), 629-632.
60. W. M. Nau, G. Ghale, A. Henning, H. Bakirci, D. M. Bailey, *J. Am. Chem. Soc.* **131**, (2009), 11558-11570.
61. W. M. Nau, *Nature Chemistry* **2**, (2010), 248-250.

Dr. (Mrs.) Jyotirmayee Mohanty obtained her M. Sc. in Chemistry from Utkal University, Odisha in 1992 and joined Bhabha Atomic Research Centre, Mumbai, India, in 1994 after one year advanced orientation course conducted by the institute. After her Ph.D. from the University of Mumbai in 2002, she carried out her postdoctoral research at MPIBPC, Göttingen and JUB, Bremen, Germany, 2002-2004. Her current research interests focus on the dynamics of noncovalent supra-biomolecular assemblies, tuning their molecular properties and exploring their photofunctional activities towards various applications. In fact, she has initiated the research activities on the fascinating chemistry of cucurbiturils in India and a number of her recent publications in high impact international journals including patents and reviews are the testimony to her contribution in this area. She is a recipient of the Distinguished Lectureship Award-2009 from the Chemical Society of Japan, APA-Prize for Young Scientist-2010, Samanta Chandra Sekhar Award-2011, Scientific & Technical Excellence Award-2011 from DAE, and the fellow of Maharashtra Academy of Sciences and National Academy of sciences, India. She has also received the prestigious Humboldt Fellowship for Experienced Researchers from Alexander von Humboldt Foundation.

Dr. Achikanath C. Bhasikuttan obtained his M.Sc. in Chemistry from Calicut University, Kerala in 1989 and joined Bhabha Atomic Research Centre, Mumbai, India, in 1991 after one year advanced orientation course conducted by the institute. After his Ph.D. from the University of Mumbai in 1998 he joined as a JSPS postdoctoral fellow at Osaka University, Japan, 1999-2001. His research interests include the excited state molecular dynamics and to probe the intricacies of non-covalent interactions in supra-biomolecular systems. He is a recipient of Scientific & Technical Excellence Award -2009 from DAE, CRSI Bronze medal-2014 and the fellow of Maharashtra Academy of Sciences & National Academy of sciences, India.

Self-Assembled Supramolecular Materials: Prospects in Biocatalysis to Biomedicine

Prasanta Kumar Das
Department of Biological Chemistry, Indian Association for the Cultivation of Science, Jadavpur, Kolkata-700032, India
E-mail: bcpkd@iacs.res.in

Introduction:

The spontaneous and reversible orientation of molecular units into ordered structures by non-covalent interactions is known as self-assembly.[1] This interesting phenomenon is an outcome of the orchestration of molecules and results in the formation of diversified self organized systems together which form an intriguing stream of chemistry, commonly known as 'Supramolecular Chemistry'. The broad interest in supramolecular science also stems from the perspectives offered by this highly interdisciplinary field of science which weaves the chemical, physical and biological sciences. When we look at the unit of life, the cell membrane is a manifestation of the process of self-assembly where the amphiphilic molecules like lipid arrange themselves to form the bilayer structures. Additionally, these structures also harbor the proteins and enzymes which are absolutely vital for many functions of the living systems. In this regard, model systems mimicking the complicated structures of biomembrane can help us to understand their mode of operation and structure-function relationships. Additionally, the mimicking structures can also host proteins and enzymes in a similar fashion as done by the biomembrane of living systems. Self organized assemblies like micelles, reverse micelles, vesicles and liposomes are few examples of the beautiful manifestation of self-assembly primarily by amphiphilic molecules which can be an excellent mimic to the compartmentalized systems like the biomembrane.[2] Another beautiful choreography of self assembly includes gelation which is a result of the balance between crystallization and solubilization.[3] A molecule competent of gelation must have the necessary features like the optimum balance of the hydrophilicity and lipophilicity and also functional groups capable of indulging into various non-covalent interactions.[4] Most supramolecular gels are composed of amphiphilic nanofibers (supramolecular polymers) which entangle among each other to form a network where the solvent is entrapped in the nano-spaces. Coming to another domain, nanomaterials are a fascinating class of material, where almost everything ranges around one billionth of a meter. For the stabilization of these nanoparticle a variety of chemical templates like micelles, reverse micelle, silicate templates, block polymers, dendrimers etc are commonly known. Among them, supramolecular aggregates are widely used for the stabilization of nanoparticles as the features of nanoparticle can easily be regulated by altering the nature of non-covalent interactions involved in self-assembly. The integration of nanoparticle into these self-assembled structures provides them amazing features, which can be utilized in the field of nanotechnology to biomedicines. Apart from the metal nanoparticles, carbon nanomaterials are finding significant importance across the disciplines. Interestingly they exist in widely different shapes, geometry and exhibit interesting properties.

Our research group has the expertise of working in the interdisciplinary domain of bio-organic chemistry including the design and development of rich variety of self-assembled aggregate structures like micelle, reverse micelle, low molecular weight gels and so on with variety of structural motifs. We have successfully utilized these soft materials in diversified fields ranging from biocatalysis, synthesis of nanoparticles, development of soft-nanocomposites, antimicrobial agents and cellular transporters. Specifically designed amino acid based amphiphiles have been used for the said purposes and subsequent variations in the molecular architecture have been carried out to investigate their influence on activity of enzymes, gelation and other physicochemical properties.[5-7] These supramolecular soft materials have been applied towards various applications, particularly as potent antimicrobial agents and synthesis of silver (Ag), gold nanoparticles (Au-NPs).[8] We have also rationally designed and developed functional amphiphiles for efficient dispersion of nanodimensional allotropes of carbon. These dispersed nanomaterials have shown considerable viability towards eukaryotic cells and are used as intracellular cargo carriers. Functional amphiphilic molecules are designed to make these delivery agents task specific.

Reverse Micellar Enzymology:

A living system controls its activity through enzymes. An enzyme is a protein molecule that acts as a biological catalyst. In this perspective, controlling the effectiveness of enzymes (also known as biocatalyst) is extremely important. To simulate in vitro the conditions of enzyme action in vivo, enzymatic reactions are often performed

in water or in mixtures of water and organic solvents. However, such homogeneous media are far from ideal. The primary uniqueness of the reverse micelles due to which a variety of biomolecules get entrapped is that they have a large number of solubilization sites. For example, a hydrophilic protein (trypsin) most likely locates itself inside the water-pool to avoid direct contact with the organic medium; interfacially localized enzymes (such as lipase) can interact with the surface layer of the micelle, while typical membrane enzymes may come into contact with the organic solvent.[9] On the other hand, increasing the stability and reactivity of enzymes are primary concern to use it as an industrial catalyst.[10] Enzymes are sensitive to environmental factors like pH, temperature, ionic strength of the solvent and under stressed conditions they get denatured.[11] Nanotechnology offered the most promising opportunity to get a grip on our desired purpose. Our group has been successful in devising novel water-in-oil microemulsion primarily on the basis of rational designing of surfactants where the efficiency of biocatalyst has dramatically improved. Amphiphiles with judicious variations in their structure were utilized to prepare reverse micelles, which acted as remarkable hosts for various enzymes.[12] In this regard, the most important outcome of these studies in reverse micellar enzymology is that the 'space' or surface area in vicinity of the enzyme plays the most crucial role in modulating biocatalytic activity of surface-active enzyme. To this end, it is very important to constantly refurbish existing systems that can lead to the development of improved hosts for biocatalyst. Thus new hybrid systems of nanosized reverse micelles integrated with materials having similar dimensions i.e. nanomaterials were included within reverse micelles to make it more effective host for various proteins and enzyme (Figure 1).

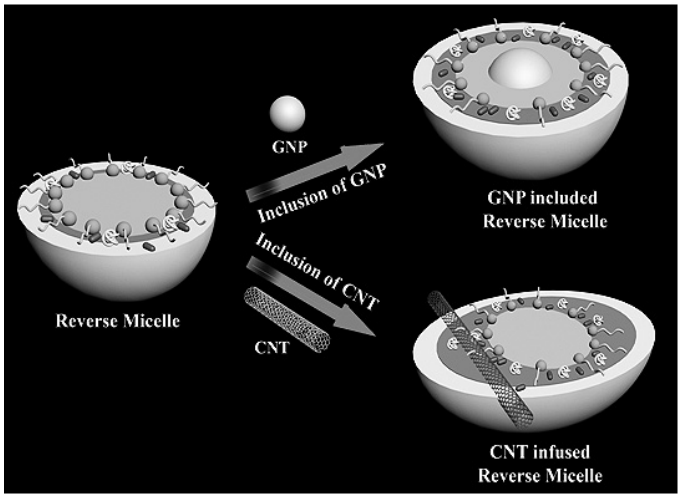

Figure 1. Nanomaterials induced enhanced interfacial area within reverse micelles.

Carbon nanomaterials (such as carbon nanotube (CNT), graphene and carbon dots) and Au nanoparticles and Au-nanorods of suitable dimensions have been extensively used for the purpose of enhancement in space around the entrapped enzyme thereby increasing its activity.[13-16] We have also designed a fluorimetric assay for the sensitive and specific detection of histone protein using quaternized carbon dot-DNA hybrid, a label-free, real time histone sensing simply by monitoring fluorescence quenching (off) and restoration (on) signal, with limit of detection as low as 0.2 ng mL^{-1}. This is the first utilization of luminescence property of carbon dot in histone sensing as well as its effectiveness in developing biosensors.[17] At the same time, surface-functionalized carbon dot-enzyme nanoconjugate was used to detect the region of location of enzyme/protein in the microenvironment of membrane mimetic systems like reverse micelle.[18] Exploiting nanotechnology to boost up enzyme's efficiency in completely hostile medium i.e. organic solvents will surely be an interesting as well as stimulating for further biotechnological advancement.

Self-Assembled Soft Nanocomposite:

Assembly of small organic molecules in aqueous and organic solvents into supramolecular nanostructures brings in interesting scope in the fields of molecular recognition and self-assembly. Low molecular weight gelators are classified in two major categories depending upon the nature of the solvent which they immobilize, i) hydrogelator (gelate water) and ii) organogelator (immobilize organic solvents).[19] There are also few examples of small molecule gelators termed as ambidextrous gelator, can gelate water as well as organic solvents simultaneously. The phenomenon of gelation arises mainly from fibers (nano- to micrometer) that become entangled and trapped the solvent via surface tension and capillary forces. Self-aggregation is primarily driven by non-covalent interactions such as hydrogen bonding, π– π stacking, van der Waals and electrostatic interactions, hydrophilic lipophilic balance (HLB) and other supramolecular weak forces.[20] The beauty of a low molecular weight gels lies in its "discipline" to create well-defined molecular array directed by hierarchical self-assembly processes forming fibrous, tubular or helical structures and others.

Over the last few years our group have continuously indulged in the synthesis of new functional small molecule gelators with the objective of task-specific applications. The supramolecular gel matrix has been used as a scaffold for the *in situ* synthesis and stabilization of metal nanoparticles (MNPs like Au, Ag-NPs) by modulating the gel structure with suitable functionality. Cholesterol- and naphthalene-based amino acid containing hydrogelators, coupled

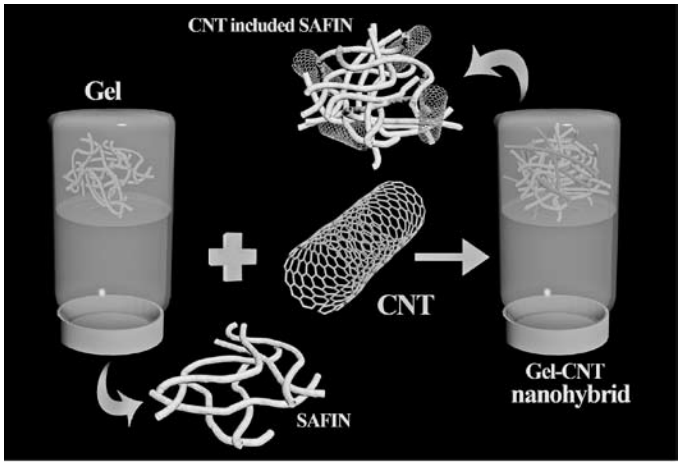

Figure 2. Nanomaterial incorporated self-assembled fibrillar network.

with *in situ* synthesized Ag-nano particle exhibits notable bactericidal property against both Gram-positive and Gram-negative bacteria.[21,22] Along with rapid structural modification, attempts have been made to improve the mechanical rigidity of the physical gel by developing novel soft-nanocomposites. The interstitial space present in a self-assembled fibrillar network (SAFIN) provides sufficient room for inclusion of exogenous material that can modulate the viscoelastic properties of gels. Nanomaterials, such as CNTs, graphene oxide, Ag and Au-NP, could be suitable contenders for preparing such nanocomposites. Hydrogel-*in situ* synthesized Au-NP composites also possess improved viscoelastic property than the native hydrogel. The efficient inclusion of CNTs to peptide based ammonium/imidazolium tethered hydrogels assist manifold enhancement (~85-fold) in their mechanical strength (Figure 2).[23] Moreover, the inclusion of functionalized CNTs (single walled carbon nanotube (SWNT–COOH)) plays a pivotal role in the networking of self-assembled fibrillar network (SAFIN) by reducing minimum gelation concentration (MGC) compared to only amphiphiles.[24] Successful inclusion of CNT in the pyrene containing ambidextrous gel helped to improve the mechanical rigidity of both organo- and hydrogel up to ~4 fold.[25] Importantly, the fitting fusion of dispersed CNTs within the SAFIN of hydrogels was exploited to improve the peroxidase activity of immobilized cytochrome c (cyt c) in toluene (120 times greater than that in water). Cyt c entrapped within SWNT–hydrogel exhibited superior activity (1.7-fold higher) compared to that of the native hydrogel.[26] The optoelectronic and mechanical properties of the composites can also be easily tuned by varying the amount of doped naomaterials, the capping/stabilizing agents, temperature and so forth. Newly developed CNT-gel composite are coming up as new age hybrid materials needed for advanced tissue engineering. With all these applications, nanocomposites have seemed to be a great boon, which have added a new vision to modern science.

Self-Assembly-Carbon Nanotube Hybrid as Cellular Transporter:

There has been a surge in the research for the development of new generation drug delivery system which can simultaneously improve the bioavailability and reduce the cytotoxic effect of a drug. In pursuit of developing such cutting edge delivery modalities, factors like specific delivery of cargo to a particular site with minimal side effects, smart release with maximum effect of the drug and complete removal of the delivering unit from the system are the dream goals, which are still eluding us. In this regard, the use of nano dimensional materials is showing huge promise and consequently conventional drug design protocols are being refreshed with the option to include these nanomaterials. A substantial portion of the research in the frontiers of cellular delivery of cargo is involving the use of carbon nanomaterials like fullerene, graphene, carbon nanotube etc. Carbon nanotube (CNT), a cylindrical allotrope of carbon has emerged with huge promise in this area of research.[27] However, the major problem of using CNTs in the biomedicinal arena is its inherent insolubility. To counter the problem of insolubility, CNTs are capped with exogenous capping agents either by covalently or non-covalently. In fact, it is possible to induct functionality into the CNTs either by proper designing of dispersing agents or by manipulation of the covalent functionalization. More specifically side-chains or dispersing agents can be designed according to the purposes to make the systems applicable for task specific objectives. For example, features like biocompatibility, target specificity, pH responsiveness can be installed into the nanoconstruct by way of tuning the structure of the side-wall functionalization or the dispersing agent. This barrier was overcome by complementary fusion between self-assembled amphiphiles and nanotubes. In this regard amino acid based cationic, anionic and neutral (polyethylene glycol, PEG containing) amphiphiles were designed for effective dissolution of single walled carbon nanotubes (SWNTs) in water which successfully internalized fluorophore-tagged proteins into mammalian cells (Figure 3).[28] Also incorporation of biotin into the architecture of the CNT dispersing agent developed a multifaceted delivery vehicle having target specificity towards cancer cells.[25] Cholesterol based dipeptide carboxylates were designed which exhibited effective nanotube dispersing ability.[29] Importantly, these solution showed pH-responsive reversibility of dispersion on successive acid-base treatments which could be used for target specific release of cargo.[30] These highly dispersed

nanotubes were used (i) to act as a platform for the loading of the otherwise sparingly soluble drug molecule and (ii) to increase the local concentration of the drug in the vicinity of the cancer cells compared to that of normal cells by release of the drug specifically in the cancer cell microenvironment (having pH range of 6.0-6.5), ensuing maximum therapeutic activity and minimum side effects of the drug. Most importantly these drug loaded nanohybrids were highly efficient in selective killing of cancer cells with compared to that of normal cells.

In summary, fabrication of self assembled supramolecular materials with task specific functionalities are emerging with lots of scope in the various research

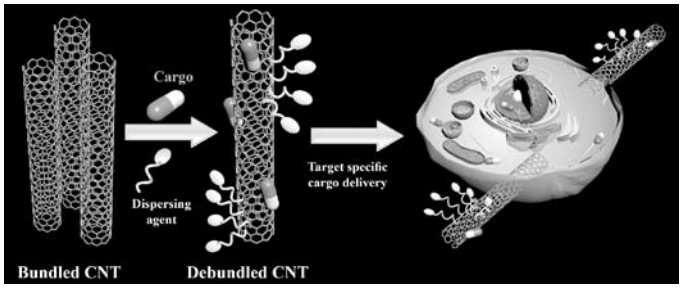

Figure 3. Target specific cargo delivery to cancer cells by non-covalently dispersed carbon nanotubes.

arenas like advanced materials, biocatalysis, biomedicine, drug delivery and others. The designed nanohybrids would surely help in the evolution of newer modalities for diverse applications and therefore will significantly contribute across the discipline of sciences.

Acknowledgement:

PKD is thankful to DST, India, CSIR, India and IACS for financial assistance and research facilities.

References:

1. A. Blanazs, S. P. Armes, A. J. Ryan, *Macromol. Rapid Commun.*, **2009**, *30*, 267.
2. J. H. Fendler, *Membrane Mimetic Chemistry*, Wiley: New York, 1982.
3. P. Terech, R. G. Weiss, *Chem. Rev.* **1997**, *97*, 3133.
4. L. A. Estroff, A. D. Hamilton, *Chem. Rev.*, **2004**, *104*, 1201.
5. D. Das, P. K. Das, *Langmuir* **2003**, *19*, 9114.
6. R. N. Mitra, A. Dasgupta, D. Das, S. Roy, S. Debnath, P. K. Das, *Langmuir* **2005**, *21*, 12115.
7. S. Debnath, A. Dasgupta, R. N. Mitra, P, K, Das. *Langmuir* **2006**, *22*, 8732.
8. S. Roy, A. Dasgupta, P. K. Das. *Langmuir* **2007**, *23*, 11769.
9. S. Krauser, P. Kiefer, E. Heinzle, *ChemCatChem*, **2012**, *4*, 786.
10. S. C. Barton, Handbook of Fuel Cells, John Wiley and Sons., **2010**.
11. E. D. Koshland, *Sci. Am.*, **1973**, *229*, 52.
12. D. Das, S. Roy, R. N. Mitra, A. Dasgupta, P. K. Das, *Chem. Eur. J.*, **2005**, *11*, 4881.
13. M. Ghosh, S. Maiti, S. Brahmachari P. K. Das, *RSC Adv.*, **2012**, *2*, 9042.
14. S. Maiti, M. Ghosh, P. K. Das, *Chem. Commun.*, **2011**, *47*, 9864.
15. K. Das, S. Maiti, M. Ghosh, D. Mandal, P. K. Das, *J. Colloid Interface Sci.*, **2013**, *395*, 111.
16. D. Mandal, M. Ghosh, S. Maiti, K. Das, P. K. Das, *Colloids Surf. B: Biointerfaces*, **2014**, *113*, 442.
17. S. Maiti, K. Das, P. K. Das, *Chem. Commun.*, **2013**,*49*, 8851.
18. K. Das, S. Maiti, P. K. Das *Langmuir*, **2014**, *30*, 2448-2459.
19. N. M. Sangeetha, U. Maitra, *Chem. Soc. Rev.*, **2005**, *34*, 821.
20. N. Mohmeyer, H. W. Schmidt, *Chem. Eur. J.*, **2005**, *11*, 863.
21. S. Dutta, T. Kar, D. Mandal, P. K. Das, *Langmuir*, **2013**, *29*, 316.
22. S. K. Mandal, S. Brahmachari, P. K. Das, *ChemPlusChem*, **2014**, *79*, 1733-1746.
23. S. K. Mandal, T. Kar, P. K. Das; *Chem. Eur. J.*, **2013**, *19*, 12486-12496.
24. S. K. Mandal, T. Kar, D. Das, P. K. Das, *Chem. Commun.*, **2012**, *48*, 1814.
25. D. Mandal, T. Kar, P. K. Das, *Chem. Eur. J.*, **2014**, *20*, 1349.
26. T. Kar, S. K. Mandal, P. K. Das, *Chem. Commun.*, **2012**, *48*, 8389-8391.
27. A. P. Goodwin, S. M. Tabakman, K. Welsher, S. P. Sherlock, G. Prencipe, H. Dai, *J. Am. Chem. Soc.*, **2009**, *131*, 289.
28. S. Brahmachari, D. Das, A. Shome, and P. K. Das, *Angew. Chem. Int. Ed.*, **2011**, *50*, 11243.
29. S. Brahmachari, M. Ghosh, S. Dutta, P. K. Das., *J. Mater. Chem. B*, **2014**, *2*, 1160.
30. M. Ghosh, S. Brahmachari, P. K. Das, *Macromol. Biosci.*, DOI: 10.1002/mabi.201400290.

Prasanta K Das *received BSc and MSc in Chemistry from Jadavpur University, Kolkata. He completed PhD from Indian Institute of Chemical Technology (Osmania University), Hyderabad in 1999. After postdoctoral work at Massachusetts Institute of Technology, USA, he joined Department of Biological Chemistry, Indian Association for the Cultivation of Science, Kolkata in 2002. Presently he is a Professor in the same department. He is recipients of CRSI (Chemical Research Society of India) Bronze Medal, Ramanna Fellowship of DST, India, B. M. Birla Science Prize in Chemistry and also the fellow of West Bengal Academy of Science & Technology. His primary research domain is the design and development of novel supramolecular self-assemblies for exploiting them in diversified range from advanced materials to biomedicine. This includes enzymology in membrane mimetic systems, preparing antimicrobial as well as functional hydrogels, gel-nanocomposite and using amphiphile-carbon nanotube self-assembled hybrids to develop cellular transporters.*

Highly Ordered Supramolecular Hydrogel Electrolyte for Advanced Devices

R. L. Vekariya, K. K. Sonigara, B. G. Solanki, K. B. Fadadu, S. S. Soni*
Department of Chemistry, Sardar Patel University, Vallabh Vidyanagar – 388 120, Gujarat, INDIA
**Corresponding Author: (email: soni_b21@yahoo.co.in)*
Telephone: +91-2692-226857-Ext.216, Tele Fax: +91-2692-236475

Abstract

Supramolecular hydrogel electrolyte is prepared using amphiphilic block copolymer in which polymer micelles are self assembled to form ordered microcrystalline phases. It was found that the ionic diffusion occur through the gel which depends on the micellar phases and independent of viscosity. This supramolecular hydrogel electrolyte is used as redox mediator in dye solar cell with ionic liquid and achieved 1.9 % photovoltaic efficiency with good stability. This ordered gel with $LiClO_4$ salt, exhibited efficient Li ion transport ($t_{Li}^+ > 0.85$) and thus, could be used as an electrolyte or separator in lithium ion battery.

1. Introduction

The supramolecular self-assembly has been considered as one of the most dynamic and interdisciplinary areas of science, with great application potentials for a wide range of fields. Among the self-assembly strategies studied, supramolecular host−guest chemistry that employs well-established non-covalent interactions for achieving stimulus-responsive functional materials which attracted great attention. Because of these unique properties, supramolecular gel has attracted great attention for potential applications in the advanced devices like Li ion batteries, supercapacitors, dye-sensitized solar cells, sensors, electrochromical devices, etc.[1] among all these applications, use of supramolecular gels as an electrolyte in electrochemical devices received enormous attention.[2]

Photo-electrochemistry for solar to electricity conversion has been extensively investigated for a long time by using semiconductor and various organic light harvesting materials. Gratzel's pioneering work on Dye Sensitized Solar Cell (DSSC) has paved way for the efficient, low cost and cleaner energy from sunlight.[3] DSSC is one of the promising alternatives for conventional silicon technology, which contains dye adsorbed nanocrystalline wide band gap semiconductors like TiO_2, ZnO etc. as light responsive material. Highest 11% efficiency has been reported for DSSC using N719 dye and liquid electrolyte.[4] Use of liquid electrolyte creates leaking problem which render them difficult for long term outdoor application. Thus, solid and gel based electrolytes such as *p*-type semiconductors (CuI, CuSCN etc.),[5,6] organic hole conducting materials,[7] plastic crystal electrolyte,[8] solid polymer electrolytes and polymer gel electrolytes[9,10] etc. have been used as an alternative for liquid electrolyte. Overall photovoltaic performance of solid state DSSC is lowered due to the poor carrier mobility and imperfect contact with sensitized titania electrode.

Simultaneously, the energy storage systems are urgently needed to fully utilize renewable energies including their connection with smart grids. Lithium ion batteries have been well acknowledged as an energy storage system of high energy density.[11] However, their safety and superfast charging performance except cost are still challenging issues to be solved for the large-scale energy storage in electric vehicles and smart grids since a large amount of combustible organic electrolytes is used and the ionic conductivity of organic electrolyte is about two orders of magnitudes lower than those of the aqueous ones.[11] As a result, new energy storage systems of high reliability and rapid charging are urgently needed. Scrosati et al. have reported a PEO (PEO swollen in ethyl carbonate/ diethyl carbonate as solvent) based membrane electrolyte having conductivity 2.1×10^{-3} S cm^{-1} at 20 °C.[8] They also used this gel electrolyte membrane in Li ion battery.[12] Looking to these results, PGE are potential substitute for conventional liquid electrolytes.[13] However, use of organic solvent in this electrolyte is not safe and have an environmental impact. To make it safer, any water based solid facility will be needed. In view of all these issues, it is desired to develop supramolecular hydrogel which can self assemble into various micro-liquid crystalline phases and effectively pave the migration of desired ion through it, which is a prime requirement for effective electrolytes.

Here, we report the development of ordered hydrogels via supramolecular host-guest recognization. Lithium salts with iodide/iodine and other anions were selected as the guest, whereas amphiphilic block copolymer was used as the host compound with water as medium. A proper ratio

of Li salt, copolymer and water yielded thermo-reversible ordered gels. The resultant gels show higher co*n*ductivity and selective ion transport. The prepared supramolecular hydrogels were used as the quasi-solid-state electrolytes for DSSCs which show power conversion efficiency ~ 2.0 % with excellent long-term stability.

2. Experimental

2.1 Materials and Methods

The Pluronic F77 ($EO_{52}PO_{35}EO_{52}$, MW = 6600 g/mol) having 70% PEO was obtained as gift samples from BASF, USA. $LiClO_4$ and PEG (Mw, 6,000 gm/mol) were purchaged from Sigma-Aldrich. Unless and otherwise stated all the chemicals were purchased from Sigma-Aldrich and used as received. All solvents and ionic liquid (1-butyl-3-methyl imidazolium iodide) were purchased from Merck, India and purified as per standard procedure. Water used in this study was Milli – Q grade (18 MΩ).

2.2 Preparation of electrolytes

All the ordered supramolecular gel electrolytes (SGEs) were prepared by mixing appropriate amount of either lithium salt or IL in block copolymer in presence of water and the resultant mixtures were kept below 10°C for a week prior to use. The gel electrolytes were prepared according to the literature procedure.[13] Required amount of LiI and Iodine was dissolved in water to make an electrolyte solution. Gel was prepared from this electrolyte by mixing it with block copolymer in appropriate amount. Gels from ionic liquid were prepared in situ by mixing IL, I_2, 4-tert-butyl pyridine(4-TBP), water and polymer in a glass bottle. For lithium ion battery, gels were prepared by same method using $LiClO_4$ salt and polymer with water.

2.3 Fabrication of DSSC

Dye coated TiO_2 electrodes were fabricated as working electrodes for DSSC as follow: A thin layer of non porous TiO_2 was deposited from ethanolic titanium tetra-isopropoxide solution on a cleaned FTO (15Ω/ cm^2, Solaronix, SA, Swiss) conducting glass with >80% transmittance in visible region, by spin coating at 2000 rpm. This thin layer of titania was annealed at 450°C for 20 min. Titania paste consists of TiO_2 (P-25, Degussa), ethyl cellulose and α-Terpineol, was deposited on above pre-treated FTO glass by screen printing technique.[14] The electrodes were fired into the tubular furnace at 500°C for 30 min. and the net thickness of titania film was found to be 12 µm. Working electrodes were soaked into the $TiCl_4$ solution for 20 min. at 60°C and sintered in air at 450°C for 10 min. The electrodes were allowed to cool to 70°C and immersed into the 0.3mM solution of D907 dye (Eversolar, Taiwan)[15] in anhydrous acetonitrile : tert-butyl alcohol (1:1) for 12 hrs.

Electrodes were washed thoroughly with acetonitrile and dried under the stream of nitrogen gas. Counter electrodes were prepared from Platisol solution (Solaronix, SA, Swiss) by spin coating method and rapidly fired into the furnace at 450°C for 20 min. Gel was dropped onto the dye sensitized electrode and kept at below 10°C for 1 hour (in order to get good penetration of gel below its gelation temperature ≈ 27°C). By keeping 25µm spacer, cells were sealed using epoxy adhesive and stored in dark for 12 hrs prior to measurements. It should be noted that cell active area was 0.25 cm^2. For comparison purpose the DSSC was also fabricated with same procedure just by replacing PGE with liquid electrolyte containing 0.5 M LiI, 0.05 M I_2, 0.5 M 4-*tert.*-butyl pyridine (4-TBP) in acetonitrile.

2.4 Characterizations of SGEs, DSSC and Lithium ion tansport numbers

I-V characterizations were carried out using Keithley 2400 sourcemeter and 100 W Xenon lamp as light source equipped with Band Pass filter. Light intensity was set to 100mW/cm^2 (the light intensity was calibrated using standard Si-photodiode). Conductivity of the polymer gel electrolytes were measured using Solartron 1260 (Impedance and Gain Phase analyzer) by sandwiching the sample between two stainless steel electrodes. AC frequency 1MHz to 0.01 Hz was swept onto the test cell with 10 mV AC amplitude. ^{1}H NMR study of gel electrolyte also carried out using Brucker instrument. It should be noted that all the measurements were carried out twice and their mean values are reported here. For lithium salt based gel electrolyte, characterization has done using same instrument with transference number measurement.

3. Results and Discussion

3.1 Supramolecular Gel Electrolyte in DSSC:

Pluronic F77 contains alternate polyethylene oxide (PEO) and polypropylene oxide (PPO) units with 70% PEO respectively. In water, these block copolymers form micelles in which a hydrophobic core consisting of PPO blocks which are surrounded by an outer shell or corona of hydrophilic PEO (hydrated) blocks. With increasing concentration of amphiphilic block copolymer, micelles self assembles themselves into various lyotropic liquid crystalline phases viz. Cubic, 2D-Hexagonal, Lamellar etc. From our recent study, we have found that the ionic conduction through such higher ordered structures depend upon the arrangement of micelles and conductivity follows that Cubic > 2D-Hex > Lamellar order.[13] Highest conductivity in the cubic phase (*Im3m*), is due to the

interconnected micellar nanochannels. The latter consists of alternate hydrophilic and hydrophobic domains which pave the way for ionic conduction without hurdle. In view of this, we have selected 50%(w/w) concentration of F77, which is having cubic phase (*Im3m*) in its microstructure.[14,16] For comparison purpose, we have also prepared 50%(w/w) gel electrolytes using polyethylene glycol (PEG, MW 6000 g.mol^{-1}) which is devoid of any micelles or higher ordered structures.

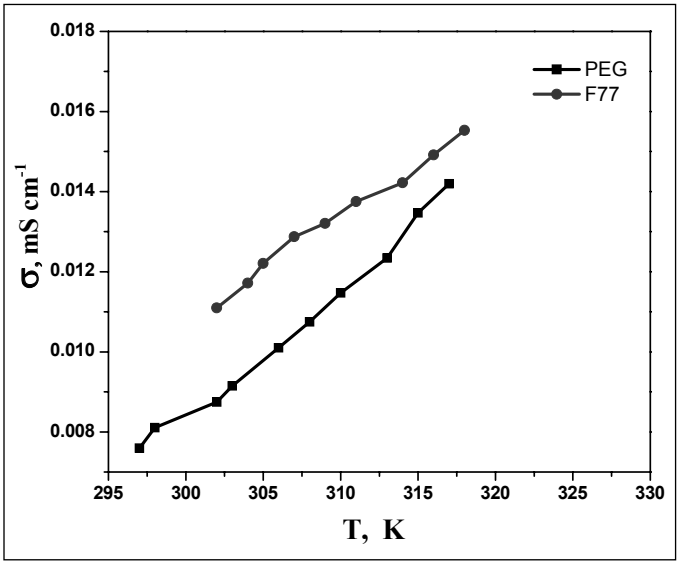

Fig. 1: Variation in conductivity of SGEs as a function of temperature

The ionic conductivities of the gels were recorded using AC impedance method by sandwiching the gels between two stainless steel disk electrodes. The variation in the conductivities as a function of temperature was collected and shown in **Figure 1,** which shows linear behaviour. The data were fitted into the Arrhenius type equation and the extracted activation energies (E_a) and conductivity at 30°C are depicted in **Table 1**.

It is clear from these parameters that the ionic conduction in these gel electrolytes has a little influence on the viscosity of the media since we have observed lowest conductivity in the simple polymer solution, F77 > PEG.

Table 1. Conductivities and Activation energies SGEs

	σ (mS.cm^{-1})	E_a (Kcal. mol^{-1})	R_s	W_s-T	D_{app} (cm^2. sec^{-1})
F77 based SGE	11.1	3.8	19.51	20.35	1.23 × 10^{-6}
PEG based SGE	8.8	6.0	64.52	25.28	9.88 × 10^{-7}

The mixture of IL (C_4MimI) and Iodine will generate triiodide species into the solution having lesser solubility in aqueous phase. Hence triiodide ion would prefer to reside in the hydrophobic domain i.e. PEO-PPO interface or PPO blocks. If this is the case then there must be some interaction of triiodide anion with tertiary carbon atom of PPO chain, since the latter is slight electropositive in nature**.** This fact was further supported by ^{1}H NMR experiment of Pluronic solution in D_2O performed at 25°C as shown in **Figure 2.**

Chemical shift values in NMR spectrum deduce the environment of protons into the molecule i.e. shielded or deshielded. Hence, chemical shift data would suggest whether there is an interaction of added salt with PPO chain or not. This interaction will alter the electron density from the respective hydrogen atom leading to the difference in chemical shift than that of pure solution. **Figure 2** shows the ^{1}H NMR spectra of pure F77 solution (a) as well as F77 in electrolyte solution (b). **Table 2** summarizes the values of chemical shifts obtained from NMR experiment for PO-CH_3 and PO-CH- protons.

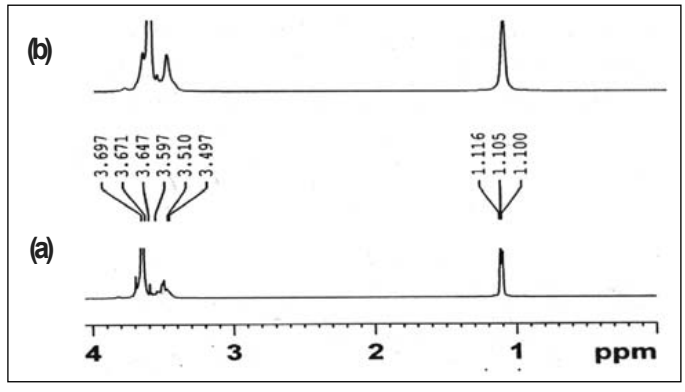

Fig.2 ^{1}H NMR spectrum of (a) Pure F77 solution (b) F77 in electrolyte solutions

Table 2. Chemical shift values for PO-CH_3 and PO-CH- protons in polymer solutions

	δ ppm (PO-CH_3)	δ ppm (PO-CH-)
Pure F77	1.105	3.510
F77 with electrolytes	1.165	3.538

From this table it is obvious that there is remarkable change in the chemical shifts of PPO protons upon addition of salts. Hence we can conclude that there is presence of triiodide species inside the PPO domain.

Ionic diffusion in SGEs by impedance method

Electrochemical Impedance measurements of the polymer SGEs were recorded using a thin layer cell.

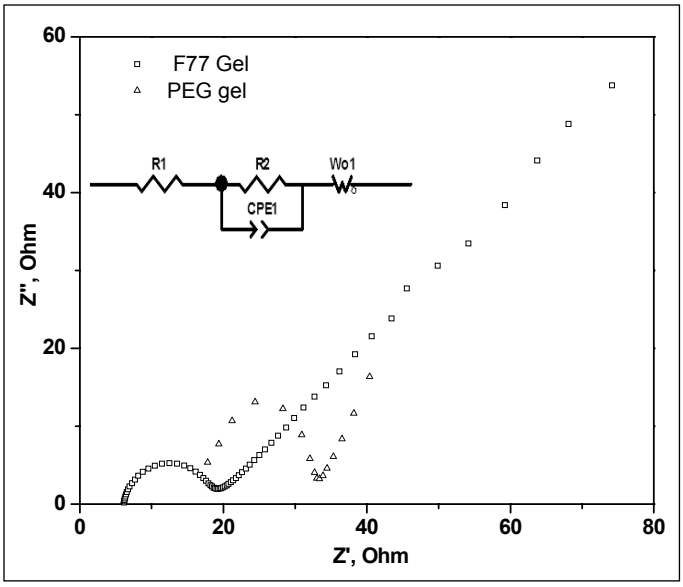

Fig.3: Nyquist plots of various SGEs using thin layer symmetrical cell

High frequency (1E6 Hz to 100 Hz) response can be attributed to the Pt/Electrolyte interface while low frequency response is due to the mass transfer or diffusion of the electroactive species through the polymer matrix. Since the concentration of Iodide is much higher than triiodide, the diffusion limiting processes are approximated due to the diffusion of triodide. First arc in the impedance spectra was fitted using parallel RC circuit in which capacitor was replaced by CPE (Constant Phase Element). This is due to the surface irregularity of the platinum electrode.

While the 45° line which is a characteristic of diffusion limiting processes and can be fitted using finite length Warburg impedance. This method has successfully been employed for the estimation of triiodide diffusion from the Warburg impedance.[17-18] The last three column of **Table 1** show the parameters extracted from the impedance measurements. Diffusion coefficients of gel electrolytes were roughly estimated from the following equation 1.

$$D = \frac{L^2}{W_s - T} \quad (1)$$

L is the distance between the two electrode which was maintained constant using scotch tape as spacer (50 µm) while *Ws-T* is a parameter which was extracted from the Warburg impedance. Diffusion coefficients estimated from the EIS are depicted in last three column of **Table 1.** It shows that diffusion of the triiodide is slower in the PEG gel as compared to ordered supramolecur gel. The magnitude of triodide diffusion is somehow higher in case of F77 based gel. The estimated diffusion coefficients for SGE and PGE are comparable with those reported (~ 1 x 10^{-7} cm^2 s^{-1}) by other groups for pure ionic liquids and polymer gel electrolytes.[19]

Photovoltaic Characterization of DSSC:

Photovoltaic characterizations of the DSSC's fabricated from the hydrogel electrolytes were carried out by applying external bias to the cell and measuring generated photocurrent. **Figure 4** shows *I-V* curves obtained for the DSSC assembled with different gel electrolytes as well as liquid electrolyte and parameters calculated from these, are shown in last column **Table 3**. Devices A, B, and C consists of PEG, liquid, and F77 based electrolytes. These data set forth a clear enhancement in the photocurrent when ordered SPE is used instead of ordered less PEG based electrolytes. SGE containing block copolymers J_{sc} increase from 2.1 to 6.2 mA/cm^2 and overall efficiency reached to 1.9%. Which is quite comparable with those reported by O'Regan et. al. using water based liquid electrolytes.[20]

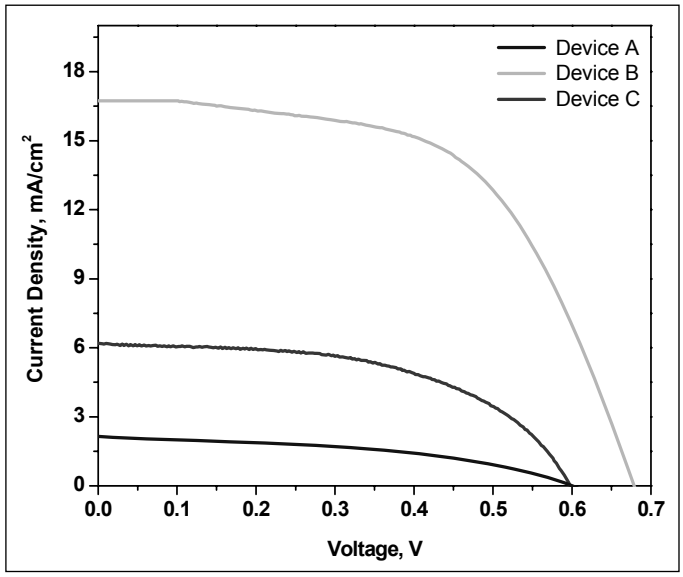

Fig. 4: Photovoltaic characteristics of DSSC based on different gel electrolytes

The trend of photovoltaic performance was unexpected considering the enhanced ionic conductivity and higher triiodide diffusion in case of F77 gel as discussed before. But this anomalous behaviour can be explained by considering the physical state of the so formed gel electrolytes. F77 based gel shows remarkable structural polymorphism i.e. thermoreversible sol to gel transition. By lowering the temperature of F77 based gel converts it into liquid state having reduced viscosity which enhances the pore filling properties of F77 based gel is pretty higher.

Table 3. Photovoltaic parameters of DSSC

Device	Electrolyte Composition	J_{sc} (mA/cm^2)	V_{oc} (V)	FF (%)	η (%)
Device A	2M IL, 50 mM I_2, 0.5 M TBP and water in PEG	2.1	0.603	44	0.6
Device B	2M IL, 50 mM I_2, 0.5 M TBP in Acetonitrile	16.8	0.676	54	6.5
Device C	2M IL, 50 mM I_2,0.5 M TBP and water in F77	6.2	0.595	53	1.9

Stability test for the efficient DSSC was carried out over 500 hour time period **(Figure 5)** which shows that there is ≈ 3% reduction in the overall performance of DSSC based on F77. In case of PEG based gel electrolyte, dye desorption was observed since water molecules are free.

3.2 Lithium ion Battery

In lithium ion batteries, the electrolyte should be have good lithium ion transference number (~ 1.0) along with conductivity. In view of this, the lithium ion transference number was evaluated using SGE with $LiClO_4$ as a guest and ordered F77 as host. The ionic conductivity of the polymer gels has been probed using AC impedance method by sandwiching them between two stainless steel disk electrodes. Bulk resistance from the impedance measurement was recorded for all samples for a set of four numbers of gel electrolytes and derived ionic conductivity. Plot of Z′ vs Z″ (**Figure 6**) shows the bulk resistance as 50% (w/w) F77 polymer in water with 50mM > 100mM > 300mM > 500mM $LiClO_4$ and based on this trend 500mM concentration shows highest conductivity at 30° C (**Table 4**).

Lithium ion transport number also measured by potentiostatic polarization (Wagner's polarization technique) in Ag/electrolyte/Ag cell in which Ag electrode working as blocking electrode for cations.

Table. 4: Lithium ion transport number, and conductivity of SGE with various concentration of guest $LiClO_4$

Conc. of $LiClO_4$ mM	I_{Ini} µA	I_S µA	t_{Li+}	σ mS cm^{-1}
50	1.0796	0.14616	0.86	5.8
100	8.5471	0.76636	0.85	6.9
300	2.1104	0.53625	0.74	17.9
500	8.9582	1.2982	0.91	23.86

A 10 mV fixed voltage applied to the cell and obtaining current was measured as a function of time up to 12000 sec **(Figure 7)**. It was found that initial current (I_i) which is composed of ionic current and electronic current and final residual current (I_f) it is come after time t, which mainly contain electronic current. Lithium transference number was calculated by putting value of this current in equation 2;

$$t_+ = \frac{I_i - I_f}{I_i} \quad (2)$$

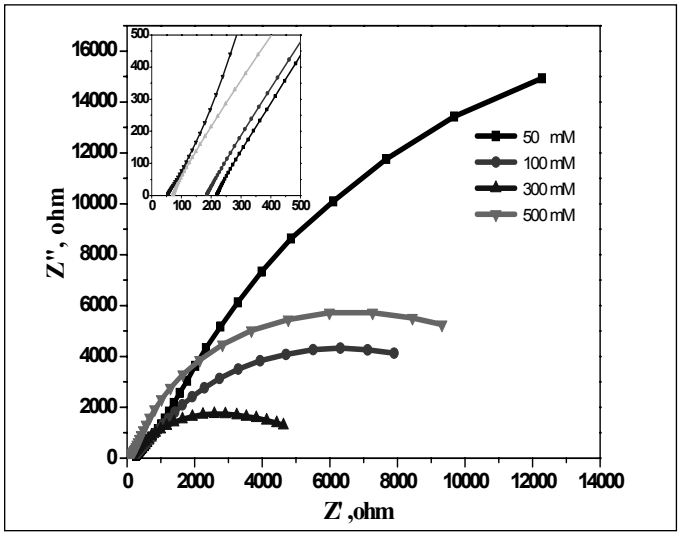

Fig. 6 : Nyquist plots of 50% F77 + Diff. conc. of $LiClO_4$ (50mM, 100mM, 300mM, 500mM)

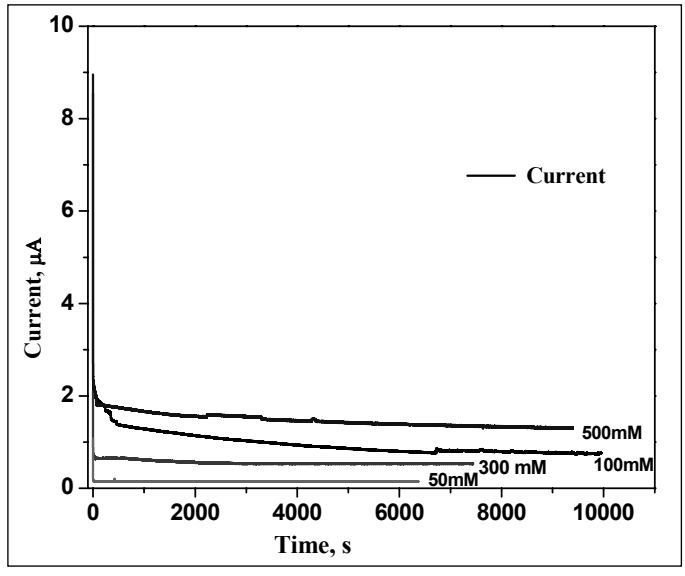

Fig. 7: Plot of current as a function of time for various concentration of $LiClO_4$ in SGE at 30° C

Lithium transport numbers obtained from the curve are 0.86, 0.85, 0.74, and 0.91 for 50mM, 100mM, 300mM, 500mM $LiClO_4$ with 50% (w/w) SGE respectively. These data shows that as concentration of salt increases conductivity and transport number increase linearly.

From the basic study of all sets of electrolyte, system with highest amount of $LiClO_4$ (50% F77 + Water + 500 mM $LiClO_4$) shows the better conductivity and reliable transference number. The result suggests that, this SGE could be used as an electrolyte or separator in lithium ion battery. Lithium ion cell fabrication and their characterizations are under progress.

4. Conclusion

We have demonstrated an ordered supramolecular hygrogel based DSSC using D907 hydrophobic dye. We have prepared SGEs from F77 based amphiphilic block copolymer using ionic liquid and iodine as guest. Gels are having good ionic conductivity even at room temperature and shows good properties for triiodide diffusion. The conductivity and the ionic diffusion of these ordered SGE was compared with that of PEG based gel and results suggests that there is remarkable effect of microcrystalline phases in the F77 based supramolecular gels. Triiodide diffusion through such SGE depends upon the ratio of hydrophilic and hydrophobic domain. This fact was experimentally supported by Impedance spectroscopy. These SGE's were successfully employed as a redox mediator in the dye solar cell. F77 based DSSC shows highest performance as compared to PEG; the former achieved 1.9% solar to electricity conversion efficiency with good stability, which quite comparable with water based polymer gel electrolytes. Thus we have developed a strategy to reduce the contact of water with photoelectrode by incorporating it into the amphiphilic block copolymer matrix. Hence the dye desorption from the photoelectrode in presence of water can be retarded to greater extent.

The SGEs were prepared with various concentrations & $LiClO_4$ and t_{Li+} was evaluated which are above 0.85 with good ionic conductivity. Thus, it could be utilized as an electrolyte in Li-ion battery.

Acknowledgement:

Authors are thankful to the Department of Science and Technology (DST), New Delhi, India for their financial support through the projects DST/TSG/PT/2009/23, and SB/FT/CT-173/2011.

References:

1. (a) J. B. Goodenough, Y. Kim, *Chem. Mater.* **2010**, *22*, 587. (b) F. M. Grey, Solid Polymer Electrolytes; *VCH Publishers*: New York, **1991**. (c) B. Scrosati, *Application of Electroactive Polymers; Chapman & Hall: London*, **1993**. (d) F. S. Freitas, J.N.; Ito, B. I. de Freitas, M. A. de Paoli, A. F. Nogueira, *ACS Appl. Mater. Interfaces*, **2009**, *1*, 2870.
2. (a) W. Zhang, C. Yuan, J. Guo, L. Qiu, F. Yan, *Applied Materials & Interfaces,***2014**, *6*,8723-8728. (b) Y. J. Lee, J. H. Kim, M. S. Kaung, M. J. Lee, J. Won, J. C. Lee, Y. S. Kang, *Advance Materials*, **2004**, *16*, 19.
3. B. O'Regan, M. Gratzel, *Nature* **1991**, *353*, 737.
4. B. O'Regan, D. T. Schwartz, S. M. Zakeeruddin, M.Gratzel, *Adv. Mater.* **2000**, *12*, 1263.
5. Q. B. Meng, K. Takahashi, X. T. Zhang, I. Sutanto, T. N. Rao, O. Sato, A. Fujishima, *Langmui*r **2003**, *19*, 3572.
6. B. O'Regan, F. Lenzmann, R. Muis, J. Wienke, *Chem. Mater.* **2002**, *14,* 5023.
7. U. Bach, D. Lupo, J. E. Moser, F. Weissortel, J. Salbeck, H. Speritzer, M. Gratzel, *Nature (London)*, **1998**, *395*, 583.
8. (a) B. Lee, D. B. Buchholz, D. -K. Hwang, R. P. H. Chang, *J. Phys. Chem. C* **2011**, *115*, 9787, (b) Q. Dai, D. R. MacFarlane, P. C. Howlette, M. Forsyth, *Angew. Chem. Int. Ed.* **2005**, *44*, 313.
9. B. Li, L. Wang, B. Kang, P. Wang, Y. Qui, *Sol. Energy Mate. Sol. Cells* **2006**, *90*, 549.
10. J. Shi, S. Peng, J. Pei, Y. Liang, F. Cheng, J. Chen, *Appl. Mater. & Interfaces,* **2009**, *1*, 944.
11. Y.P. Wu, X.B. Dai, J.Q. Ma, Y.J. Cheng, *Lithium Ion Batteries: Practice and Applications, Chemical Industry Press,* Beijing, **2004**.
12. (a) G. B. Appetecchi, Y. Aihara, B. Scrosati, *Solid State Ionics*, **2004**, *170,* 63.

    (b),G. B. Appetecchi, Y. Aihara, B. Scrosati, *J. Electrochem. Soc.* **2003**, *150*, A301.
13. S. S. Soni, K. B. Fadadu, A. Gibaud, *Langmuir* **2012**, *28*, 751.
14. S. Ito, T. N. Murakami, P. Comte, P. Liska, C. Grätzel, M. K. Nazeeruddin, M. Grätzel, *Thin Solid Films* **2006**, *516*, 4613.
15. For details and specifications please visit http://www.everenergy.com.tw, Taiwan.
16. P. N. Hurter, J. M. H. M. Scheutjens, T. A. Hatton, *Macromolecules* **1993**, *26*, 5592.
17. C. Longo, A. F. Nogueira, M. –A. De Paoli, H. Cachet, *J. Phys. Chem. B* **2002**, *106*, 5925.

180 G. Nazmutdinova, S. Sensfuss, M. Schodner, A. Hinsch, R. Sastrawan, D. Gerhard, S. Himmler, P. Wasserscheid, *Solid State Ionics* **2006**, *177*, 3141.

19. P. Wang, S. M. Zakeeruddin, J. E. Moser, M. K. Nazeeruddin, T. Sekiguchi, *Nat. Mater.* **2003**, *2*, 402,
20. C. H. Law, S. C. Pathirana, X. Li, A. Y. Anderson, P. R. F. Barno, A. Lisorti, T. H. Ghaddar, B. C. O' Regan, *Adv. Mater.* **2010**, *22*, 4505.

	***Dr. Rohit L. Vekariya*** *completed his M.sc and Ph.D in Chemistry from Sardar Patel University He works in the area of polymer gel electrolyte for advance devices. His thesis studies were supported by UGC funded RFSMS (Research Fellowship in Science for Meritorious Students) fellowship from 2010 to 2012 and he work as a project fellow in UGC-DAE, BARC funded major research project from 2012 to till date.*
	***Kishan B. Fadadu*** *received his M.Sc. in Chemistry from Sardar Patel University in 2009. He currently is pursuing his Ph.D under the guidance of Dr. Saurabh S. Soni. His research area is the synthesis dyes and applications of dyes in advance devices like solar cell (DSSC). His thesis studies were supported by DST (Department of Science and Technology, New Delhi) from 2009 to 2012.*
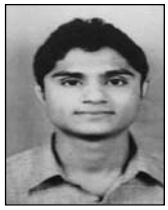	***Keval K. Sonigara*** *received his M.Sc. in Chemistry from Sardar Patel University in 2012. He currently is pursuing his Ph.D under the guidance of Dr. Saurabh S. Soni. His research area is the synthesis dyes and applications of dyes in DSSCs. He also works in the area of polymer gel electrolyte for advance lithium ion batteries. His research work is supported by DST (Department of Science and Technology, New Delhi).*
	***Bharat G. Solanki*** *received his M.Sc. in Chemistry from Sardar Patel University in 2012. He currently is pursuing his Ph.D under the guidance of Dr. Saurabh S. Soni. His research area is Design and synthesis of organic molecules and materials, its application in advanced devices like DSSC. He also works as a project fellow in UGC major research project.*
	***Dr. Saurabh S. Soni*** *is working as Assistant Professor at Department of Chemistry, Sardar Patel University, Vallabh Vidyanagar. He received his B. Sc., M. Sc. (Physical Chemistry) and Ph. D. from Sardar Patel University. He did post doctorate at University Du Maine, France and also received CNRS fellowship during his stay. His area of research are dye sensitized solar cell, ionic liquids and their applications as catalyst, development of mesoporous materials, and surface activity of block copolymers in aqueous solutions. His research work is funded by various funding agencies like DST, UGC, UGC-DAE etc. He also awarded with "Young Scientist Award" under DST-Fast Tract scheme. He visited countries like France, Australia, Italy for research purpose.*

Organization of colloidal particles in surfactant mesophases

Guruswamy Kumaraswamy
J-101, Polymers and Advanced Materials Laboratory, CSIR-National Chemical Laboratory
Dr. HomiBhabha Road, Pune 411008, Maharashtra.
Email: g.kumaraswamy@ncl.res.in
Phone: +91-20-2590-2182 / Fax: +91-20-2590-2618

Abstract

Here, I review recent advances in the organization of large colloidal particles into macroscopic, porous assemblies. I begin by describing the organization of particles in ordered surfactant mesophases. Work from our group has demonstrated that phase separation of particles from growing surfactant hexagonal mesophase domains can result in their organization into macroporousscaffolds. This approach appears to be largely independent of the chemistry of the particles and depends only on the particle size. Such materials hold promise for optical metamaterials, as catalyst scaffolds and in separation technologies. More recently, we have demonstrated that an interplay between the bending rigidity of lamellar surfactant phases and particle size determines the structures that form when nanoparticles are dispersed within a lamellar surfactant mesophase. This work has implications for the emerging field of nanoparticle based therapeutics.

The organization of surfactants into dilute micellar dispersions is well known, and forms the basis of detergency and cleaning action of soaps. At higher concentrations (compared to that in typical cleaning solutions), surfactants can self-assemble into a myriad of equilibrium ordered supramolecular structures called *mesophases*.[1] Remarkably, simple geometric packing considerations guide the local organization of the surfactants. Israelachvili[1] proposed the critical packing parameter, P = v/al, as a determinant of the shape of the micellar assemblies (where, v is the effective volume of the hydrophobic tail, a is the effective surface area of a surfactant molecule and l is the effective length of the surfactant tail). When P < 1/3, the micelles organize as spherical aggregates, and on increasing P, one-dimensional string-like assemblies form and as P approaches 1, the surfactants organize into lamellar structures. These *micro* phase-separated assemblies allow partitioning of space into hydrophilic and hydrophobic regions,the size of which are characterized by a length scale that is, typically, a few nanometers. These surfactant assemblies are, therefore, templates for nanostructures – organized surfactant mesophases have been exploited to spatially modulate materials synthesis to produce locally lamellar, cylindrical or bicontinuous nanomaterials architectures.[2]

Apart from directing the localization of chemical reactions, self-assembled surfactant mesophases have also been employed to guide the spatial organization of preformed particles. When particles smaller than the length scale that characterizes mesophase dimensions are incorporated into surfactant assemblies, these particles directly template the mesophase geometry. The chemistry of the particle surface determines its interactions with the matrix and, therefore, determines particle localization in either the hydrophilic, hydrophobic or (interfacial) palisade regions of the surfactant mesophase. For example, the French group of Fabre et. al. prepared composites of ferromagnetic particles in lamellar mesophases, and demonstrated that these particles were confined within the lamellar domains.[3] Subsequently, the same group demonstrated that such templated lamellar assemblies can also be prepared using non-magnetic nanoparticles.[4]Similar behaviour has been reported for nanoparticles in hexagonal mesophases.[5] Particles that "fit" within the hexagonal channels (or in the spaces between the channels) of the mesophase are confined within these regions. Recently, metal nanoparticles have been organized in hexagonal mesophases to produce ordered "soft" metallo-organic composites.[6] Such materials might have importance as precursor templates for the formation of inorganic mesoporous materialsdoped with catalytically important metal nanoparticles.[7]

Our group has investigated[8-14] the effect of particle size on nanoparticle organization in lamellar and hexagonal surfactant mesophases. In our work, we have used nonionic surfactants of the type, CnEm, where Cn represents a hydrophobic n-carbon aliphatic chain coupled to a hydrophilic segment comprised on m units of ethylene oxide. The use of nonionic surfactants has several advantages. The phase behaviour of non-ionic surfactants is relatively insensitive to ionic strength and pH, unlike the case for common anionic or cationic surfactants. Therefore, the surfactant assembly is robust to the introduction of moieties that might change the pH or ionic strength. We use preformed silica particles as model systems for the

particle phase, since these particles are commercially available in a variety of particle sizes ranging from a few nanometers to microns. The silica particles are water dispersible and have a negatively charged surface. The ethylene oxide units of the nonionic surfactants used in our work have an attractive interaction with the silanols on the surface of the silica particles. This results in an interesting interplay between the surfactant assemblies and the particles, as will be exemplified below.

We first describe a composite system comprising silica nanoparticles, ranging in size from 8 nm to 22 nm, that are dispersed in a $C_{12}E_4$/water (3:1, by weight) system, that forms a lamellar phase. This lamellar phase is characterized by a lamellar repeat spacing of d_1 = 47.5Å at room temperature. We anticipate that, when silica nanoparticles that are larger than d_1 are dispersed in the lamellar mesophase, they will phase separate from the mesophase and aggregate. Indeed, this is observed and we have reported[12] that the silica nanoparticles between 8 and 22 nm in size, aggregate in the lamellar phase. The phase separation of particles in surfactant mesophases is driven by the elasticity of the organized phases. Ordered surfactant mesophases represent lyotropic liquid crystalline smecticsystems, that are characterized by elasticity. Introduction of particles that locally disrupt the long range orientational order of these liquid crystalline systems increase the free energy of the system by κR, where, κ is the elastic constant that characterizes the mesophase and R is the particle size. Surfactant mesophases have κ ~ O(pN), viz. they are about ten-fold "softer" than nematic liquid crystal. For R in the range of 8 to 22 nm, κR exceeds k_BT, and therefore, the phase separation of the particles and their aggregation is anticipated.

On heating the composite to temperatures exceeding the order-disorder transition, the lamellar phase transforms to a disordered micellar phase. Here, we observe behaviour that exhibits an unusual particle-size dependence. For small particles, for example, for the 8 and 11 nm silica particles, we observe that the particles stay aggregated even once the lamellar phase disorders. In contrast, larger particles, such as, for example the 15 and 22 nm particles exhibit reversible aggregation. They stay aggregated in the lamellar surfactant mesophase, but disperse when the lamellar phase transitions to the disordered state. We have reported that the origin of this behaviour can be traced to the strong attractive interaction between the silica particle surface and the surfactants, and to the bending rigidity of the lamellar surfactant sheet. Investigations on systems containing a low concentration of particles and surfactant reveal that lamellar surfactant sheets are unable to bend around 8 and 11 nm particles, but readily coat larger, 15 and 22 nm particles. Neutron scattering studies of particle/surfactant composites in D_2O/H_2O mixtures, where the silica is constrast matched, clearly indicate a characteristic dip for the 15 nm particles (termed S15, see Figure 1 A), and no corresponding feature for the 11 nm particles. Thus, the picture that emerges is that "small" nanoparticles, smaller than about 15 nm in size aggregate irreversibly in the surfactant phase, even in the disordered state (Figure 1 C), while particles larger than about 15 nm are sterically stabilized by a bilayer coating of the lamellar surfactant. In the lamellar mesophase, exclusion of these particles from the ordered mesophase drives their aggregation – however, on reheating to the disordered surfactant phase, the particles readily redisperse (Figure 1 B). Surfactant bilayers that comprise the lamellar phase represent models for biological membranes. Therefore, these results have important implications for nanoparticle-based therapeutics. Our results reinforce recent observations in the literature[15,16] that nanoparticles smaller than a certain critical size "puncture" the bilayer membranes of cells, while larger particles are coated by the same membranes. Further, our work provides a physical basis for the understanding of the size dependence of nanoparticle-cell wall interactions. The critical size observed in these investigations is determined by the interplay of nanoparticle/membrane bilayer attractive interactions, and by the bending rigidity of the membrane cell walls.

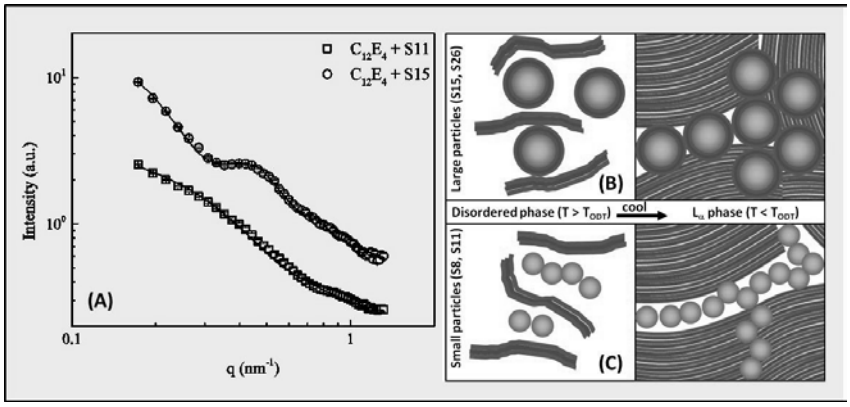

Figure 1: (A) SANS data from 11 nm (S11) and 15 nm (S15) silica nanoparticles dispersed in $C_{12}E_4$/water. The silica is contrast matched by adjusting the D_2O/H_2O ratio of the water. (B) and (C) Schematic of the assembly of large (S15) and small (S11) particles in $C_{12}E_4$/water above and below the lamellar disordering temperature.

(Figure adapted and reprinted with permission from V. Edakkal. et. al., Langmuir, 29 (2013), 9643. Copyright 2013 American Chemical Society.)

The $C_{12}E_4$/water system does not admit a spherical micellar phase, even at dilute

concentrations. However, nonionic surfactant, $C_{12}E_9$ forms a spherical micellar phase at low surfactant concentrations in water. This has important implications for the structures formed when $C_{12}E_9$ interacts with silica particles. We have reported that, even at dilute concentrations (above the critical micelle concentration) of surfactant and dispersed silica particles, $C_{12}E_9$ micelles adsorb on the surfaces of silica particles. Micellar adsorption on nanoparticle surfaces happens even for nanoparticles as small as 8 nm in size. A detailed SANS investigation revealed[9] that, about 14 to 15 surfactant micelles (about 3 nm in size) adsorbed, on average, on the surface of a 15 nm silica particle (Figure 2).

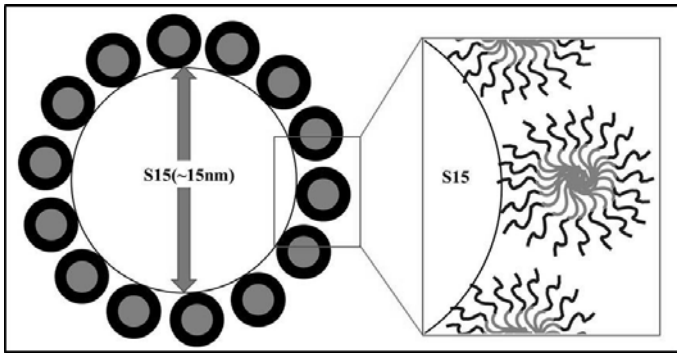

Figure 2: Schematic of surfactant micelle organization around 15 nm silica nanoparticles (S11).

(Reprinted with permission from K. P. Sharma et. al., J. Phys. Chem. B, 114 (2010), 10986. Copyright 2010 American Chemical Society.)

At a concentration of 1:1 in water, $C_{12}E_9$ forms a hexagonal (H_1) phase, with hydrophobic cylinders organized in a hexagonal geometry in a hydrophilic matrix. At room temperature, the H1 phase formed by 1:1 $C_{12}E_9$/ water is characterized by a spacing, $a \approx 5$ nm (represented schematically in Figure 3, top). We reported,[8] for the first time, a systematic investigation of the effect of particle size on the organization in silica particle/H_1 phase composites. We prepared composites of the H_1 phase with particles starting with sisesquioxane cages (size ≈1.5 nm) that lie at the border of molecular complexes and particles, up to 500 nm colloidal silica. We observed that, for molecular silsesquioxane cages, whose size was smaller than *a*, there is an increase in the H_1 lattice spacing. These ultra-small "particles" behave similar to a solvent and swell the surfactant mesophase. A combination of SAXS, optical microscopy and freeze-fracture TEM (FFTEM) reveals that the larger silica particles aggregate at the boundaries of the H_1 phase domains, forming a network structure. For particles with a size comparable to *a*, for example, the 8 nm silica particles,a small fraction of particles is incorporated within the mesophase domains while the majority aggregate at the domain boundaries. Even larger particles, for example, the 15 nm particles entirely aggregate into a percolated network of string-like linear assemblies that decorate the boundaries of the H_1 domains. This is schematically represented in Figure 3, bottom.

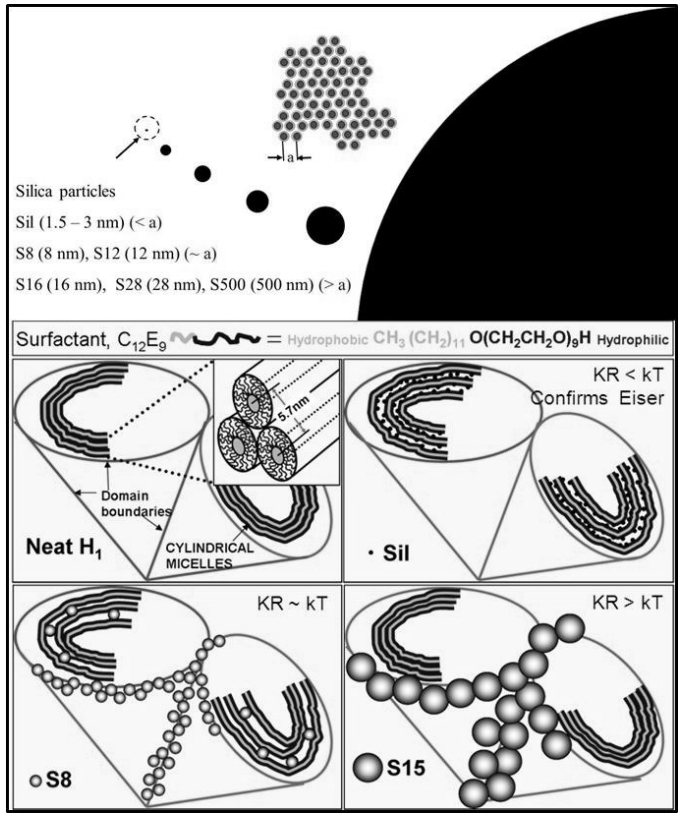

Figure 3: (Top) Schematic of the hexagonal phase viewed down the axis and the silica nanoparticles used to prepare the composite. The relative sizes of the hexagonal phase lattice distance and the particle sizes is maintained. (Bottom) Phase behaviour of the silica nanoparticle/H_1 composite, as a function of particle size from 1.5 nm (Sil), 8 nm (S8) and 15 nm (S15).

(Reprinted with permission from K. P. Sharma et. al., J. Phys. Chem. B, 113 (2009), 3423. Copyright 2009 American Chemical Society.)

Two remarkable features characterize the network assembly of particles in the H_1 phase. Firstly, independent of particle size, the particle aggregation is thermo-reversible. Thus, on heating the composites above the order-disorder transition for the H_1 phase, the particles disperse and they re-aggregate only on cooling the composite below the H_1 ordering transition. The particles do not aggregate irreversibly even with dramatic change in pH or increase in ionic strength of the composite. We have demonstrated[9] that the origin of this unique behaviour can be traced to the formation of the adsorbed layer of surfactant micelles on the particle surface, driven by surfactant/silica attraction. This changes the screened Coulombic repulsions that characterize inter-silica particle interactions in aqueous dispersions to a hard-sphere like

interaction, due to the steric interactions of the adsorbed micellar layer. Those who have worked with nanoparticle dispersions can appreciate the difficulties in maintaining a stable dispersion with change in pH and salt concentration. The opportunities presented by this system that can aggregate thermoreversibly in a controlled manner are several. These represent model colloidal systems with hard-sphere interparticle interactions for fundamental studies.

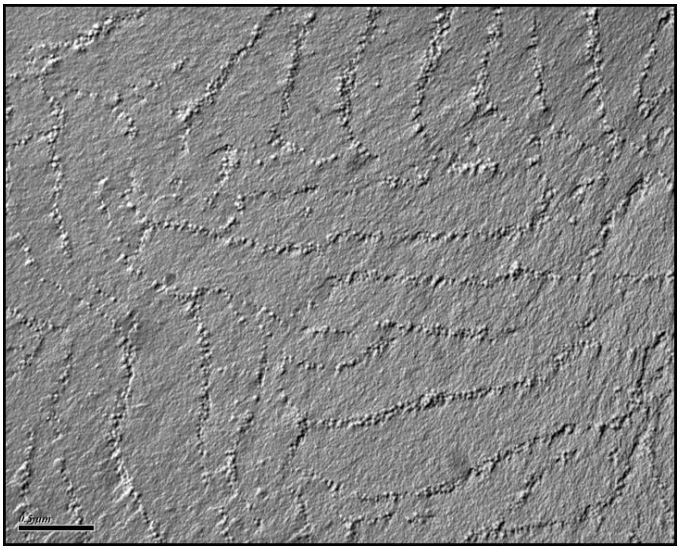

Figure 4: Freeze fracture TEM replica of a composite of 15 nm silica nanoparticles and the H_1 phase. The scale bar represents 500 nm. (Reprinted with permission from K. P. Sharma et. al., J. Phys. Chem. B, 113 (2009), 3423. Copyright 2009 American Chemical Society.)

Secondly, the enchainment of particles, driven by their exclusion from the H_1 domains is primarily a *size*-effect,[10] viz. it is independent of the chemistry of the particles (see, for example, in Figure 4, a FF-TEM of 15 nm silica particles organized as a network in $C_{12}E_9$/water). Therefore, if this network assembly of nanoparticles can be frozen, then this would represent a powerful new templating technique for the preparation of macroporous nanoparticle assemblies, that would work for any nanoparticle that can be dispersed in a $C_{12}E_9$/water system, independent of the chemistry of the nanoparticle. We have demonstrated that coating the particles with a crosslinkable polymer, polyethylene imine (PEI) allows us to crosslink the particle network *in-situ*, in the surfactant mesophase. Thus, a self-standing macroporous nanoparticle scaffold can be obtained by simply washing out the surfactant after completion of crosslinking. This is a versatile method that we have employed to create macroporous materials,[10] staring from a variety of nanoparticles, ranging from metal and inorganic particles, glassy polymer latices, and even soft bio-nanoparticles such as the protein, ferritin. Control over the cooling rate into the H_1 phase allows systematic variation of the macropore size over two orders of magnitude (from 0.5 to 50 microns) while application of stress on the H_1 gel during particle crosslinking allows the formation of oriented scaffolds. Thus, our understanding of the fundamental interactions between surfactant mesophases and particles has resulted in a practical, facile recipe for the generation of useful macroporous materials, with the possibility of systematic variation of the scaffold microstructure.

We have employed this technique to generate networks of catalyst-embedded mesoporous particles and have demonstrated the use of such scaffolds as monolithic cartridges for water purification.[14] An exciting new advance has been a recent demonstration of highly porous, low-pressure drop ferritin scaffolds where the iron nanoparticle contained in the ferritin has been used for catalytic chemical transformations, without any leaching out of the embedded metal nanoparticles.[13]Thus, fundamental investigations of nanoparticle-surfactant interactions have implications beyond the traditional areas of dispersion stability and can yield novel techniques for nanoparticle assembly.

References:

1. J. Israelachvili, Intermolecular and Surface Forces, third ed., Academic Press, 2011.
2. C. T. Kresge, M. E. Leonowicz, W. J. Roth, J. C. Vartuli, J. S. Beck, Nature 359 (1992) 710; P. V. Braun, P. Osenar, V. Tohver, S. B. Kennedy, S. I. Stupp, J. Amer. Chem. Soc. 121 (1999) 7302; G. S. Attard, J. C. Glyde, C. G. Goeltner, Nature 378 (1995) 366; M. Templin, A. Franck, A. DuChesne, H. Leist, Y. Zhang, R. Ulrich, V. Schaedler, U. Wiesner, Science 278 (1997) 1795; C. J. Brinker, Y. Lu, A. Sellinger, H. Fan, Adv. Mater. 11 (1999) 579.
3. P. Fabre, C. Casagrande, M. Veyssie, V. Cabuil, R. Massart, Phys. Rev. Lett. 64 (1990) 539-542.
4. C. Quilliet, P. Fabre, V. Cabuil, J. Phys. Chem. 97 (1993) 287-289.
5. C. Quilliet, V. Ponsinet, V. Cabuil, J. Phys. Chem. 98 (1994) 3566-3569.
6. E. Eiser, F. Bouchama, M. B. Thathagar, G. Rothenberg, Chem. Phys. Chem. 4 (2003) 526; F. Bouchama, M. B. Thathagar, G. Rothenberg, D. H. Turkenburg, E. Eiser, E. Langmuir 20 (2004)477.
7. A. K. Prasher, R. P. Hodgkins, R. Kumar, R. N. Devi, Chem. Mater. 18 (2008), 1765.
8. K.P. Sharma, G. Kumaraswamy, I. Ly, O. Mondain-Monval, J. Phys. Chem. B 113 (2009) 3423-3430.
9. K. P. Sharma, V. K. Aswal, G. Kumaraswamy, J. Phys. Chem. B 114 (2010) 10986.
10. K.P. Sharma, A.K. Ganai, S.S. Gupta, G. Kumaraswamy, Chem. Mater. 23 (2011) 1448-1455.
11. K. P. Sharma, A. K. Ganai, D. Sen, B. L. V. Prasad, G. Kumaraswamy, J. Phys. Chem. B 117 (2013) 12661.

12. E. Venugopal, V. K. Aswal, G. Kumaraswamy, Langmuir 29 (2013) 9643.
13. S. Kumari, A. Kulkarni, G. Kumaraswamy, S. Sengupta, Chem. Mater. 25 (2013) 4813.
14. G. Kumaraswamy, K. P. Sharma, Polymer and colloidal inclusions in lyotropic lamellar and hexagonal surfactant mesophases. In Advances in Planar Lipid Bilayers and Liposomes. v18, Eds: Iglic, A.; Kulkarni, C. V. (Elsevier, 2013)
15. Y. Roiter, M. Ornatska, A. Rammohan, J. Balakrishnan, D. Heine, S. Minko, Nano Lett. 8 (2008) 941.
16. S. Zhang, A. Nelson, P.A. Beales, Langmuir 28 (2012) 12831-12837.

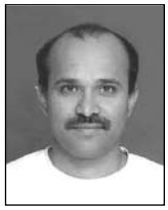

Guruswamy Kumaraswamy *received a B.Tech.(1994) from IIT-Bombay and, an M.S. (1996) and Ph.D. (2000) from CalTech, USA (all in chemical engineering). After postdoctoral research at the Max Planck Institute for Colloids and Interfaces, Germany, Guruswamy joined CSIR-NCL in 2001. Guruswamy is part of the Complex Fluids and Polymer Engineering group and uses a variety of experimental tools (rheology, microscopy, scattering) to investigate structure-property relations in polymers (especially semicrystalline polymers); self-assembly in colloidal dispersions and in surfactant mesophases.*

Achievements, Honours and Awards received by the SMC members

Name of the member and Affiliation	Name of the award/honour	Conferred by
Prof. Vivek Polshettiwar TIFR, Mumbai	Fellow of the Royal Society of Chemistry (FRSC)	RSC, UK
Dr. Tapan K Ghanty TCS, BARC	Homi Bhabha science & Technology Award	Department of Atomic Energy
	Fellow, Maharshtra Academy of Sciences	Maharashtra Academy of Sciences
	Fellow, National Academy of Sciences, India	National Academy of Sciences, India
Dr. Sriparna Chatterjee CSIR, Bhubaneswar	Ganesh Mishra Memorial Award	The Institution of Engineers (Odisha State Centre)
Prof. Amitava Patra IACS, Kolkata	Fellow of Royal Society of Chemistry	Royal Society of Chemistry
	C.N.R. Rao National Prize for Chemical Research award	Chemical Research Society of India
Miss Indrani Thakur CSIR, Bhubaneswar	Ganesh Mishra memorial Award	The Institution of Engineers (Odisha State Centre)
Dr. Sebastian C. Peter JNCASR,Bangalore	Emerging Scientist in the field of solid state chemistry	American Chemical Society
Prof. B. M. Bhanage ICT, Mumbai	M.M. Sharma Science and Technology Award	Marathi Vidhyan Parishad
Dr. Dilip Maity HBNI, Mumbai	CRSI Bronze medal	Chemical Research Society of India
Dr. A. K. Tyagi Chemistry Division, BARC	CCRS Award for Excellence in Chemical Sciences	Coastal Chemical Research Society, Andhra University, Visakhapatnam
Dr. G. Kedarnath Chemistry Division, BARC	Science and Technology Excellence Award	Department of Atomic Energy
Dr. C. Majumder Chemistry Division, BARC	Science and Technology Excellence Award	Department of Atomic Energy

Printed by:
Ebenezer Printing House
Unit No. 5 & 11, 2nd Floor, Hind Service Industries
Veer Savarkar Marg, Shivaji Park Sea-Face, Dadar (W), Mumbai - 400 028
Tel.: 2446 2632 / 2446 3872 Tel Fax: 2444 9765 E-mail: outworkeph@gmail.com

In this issue

Published by

Society for Materials Chemistry

C/o. Chemistry Division Bhabha Atomic Research Centre, Trombay, Mumbai, 400 085 (India)

Tel: +91-22-25592001, E-mail: socmatchem@gmail.com